Don’t Mess with Texas

Getting the Lone Star State to Net-Zero by 2050

Appendix F

Full WIS:dom-P Results

April 2022

Appendix F: Full WIS:dom-P Results

The following Appendix was prepared by Vibrant Clean Energy, LLC by Christopher T M Clack, Aditya Choukulkar, Brianna Coté, and Sarah A Mckee as "Economy-wide Decarbonization Pathways for Texas."

Contents

1 Study Description

1.1 Modeled Scenarios

In this study, University of Texas, Austin (UT Austin), University of Colorado Boulder (CU Boulder) and Vibrant Clean Energy (VCE®) model various pathways for the state of Texas to achieve economy-wide decarbonization by 2050. To study the various scenarios, ERCOT, along with the rest of the state of Texas and its interconnections to the rest of the continental United States (CONUS) is modeled. As part of the economy-wide decarbonization efforts, the scenarios model electrification of energy related activities in the rest of the economy as well as hard to electrify sectors such as industry and agriculture. All scenarios are modeled using WIS:dom®-P, VCE's flagship energy system modeling software.

The scenarios modeled in this study are:

1. **Business as Usual ("BAU"):** This scenario is the counterfactual against which other scenarios are compared. In this scenario, the state of Texas undergoes optimal capacity expansion to meet load growth out to 2050. This scenario has no emission constraints. Transmission within the state of Texas is allowed to expand subject to historical growth constraints, while the interconnections with the rest of the CONUS remain static over the years. WIS:dom-P co-optimizes the distribution system with the utility-scale generation to find a cost-optimal solution.

2. **Business as Usual with Carbon Capture ("Extensive Capture"):** This scenario models complete decarbonization of the state of Texas with the least end-user impact. This is done by allowing the rest of the economy to continue business-as-usual, with the carbon emissions being removed through use of carbon capture and sequestration (CCS) and direct air capture (DAC) to ensure net zero net-carbon emissions by 2050. The CCS and DACs need to capture carbon emissions from all sectors of the economy that do not choose to electrify or decarbonize. Transmission is allowed to grow subject to historical constraints while the interconnection to the rest of the CONUS remains static. WIS:dom-P co-optimizes the distribution system along with the utility-scale generation.

3. **Electrify rest of the economy with zero carbon electricity sector by 2050 ("Electrification"):** In this scenario the rest of the economy including industry (heating, fuels and feedstocks) and agriculture (ammonia and ammonium nitrate production, agricultural equipment) undergo electrification and are fully electrified by 2050 with any remaining emissions removed using DACs or CCS to reach net zero carbon emissions for the state of Texas by 2050. Some hard to electrify industry and agriculture activities are run using Hydrogen as fuel. The electricity sector is decarbonized and deploys advanced clean energy technologies such as Natural Gas with CCS, Enhanced Geothermal Systems (EGS) and Small Modular Reactors (SMR). Transmission is allowed to grow subject to historical growth constraints

while the interconnections with the rest of the CONUS remain static. WIS:dom-P co-optimizes the distribution grid along with the utility-scale generation.

4. **Electrify most of the economy and use Hydrogen for hard to electrify sectors ("Hydrogen and Carriers"):** In this scenario, similar to the "Electrification" scenario, economy-wide electrification is pursued. However more sectors of the economy switch to using Hydrogen as fuel rather than electrification. In addition, Green Ammonia and Renewable Natural Gas (RNG) are allowed to compete with conventional ammonia and natural gas production. The electricity sector decarbonizes completely by 2050 and CCS and DACs are deployed to remove any remaining carbon emissions to achieve net zero carbon emissions by 2050. Advanced clean energy technologies such as Natural Gas with CCS, EGS and SMR are deployed in the electricity sector. Transmission is allowed to grow subject to historical growth constraints while interconnections with the rest of the CONUS remain static. WIS:dom-P co-optimizes the distribution grid along with the utility-scale generation.

5. **Electrify the rest of the economy with the electricity sector decarbonizing by 2035 ("Electrification: Accelerated Clean Power"):** This scenario is similar to the "Electrification" scenario, but with the electricity sector setting a more ambitious goal to decarbonize completely by 2035. This scenario will investigate the tradeoff between additional cost to decarbonize against the additional emission savings. Transmission is allowed to grow subject to historical constraints and interconnections with the rest of the CONUS remain static. WIS:dom-P co-optimizes the distribution grid along with the utility scale generation.

To model the above scenarios, VCE customized its grid planning modeling software WIS:dom-P. A state-of-the-art combined capacity expansion and production cost model, WIS:dom-P performs detailed capacity expansion and production cost while co-optimizing utility-scale generation, storage, transmission, and distributed energy resources (DERs). The scenarios were initialized and calibrated with 2018 generator, generation, and transmission topology datasets.

For all the scenarios, WIS:dom-P determines a pathway from 2020 through 2050 with results outputted every 5 years. Detailed technical documentation describes the mathematics and formulation of the WIS:dom-P software along with input datasets and assumptions.[1] Discussion of the generator input datasets is also included in Section 3.1. A description of the wind and solar siting potential is contained in Section 3.2. Economic and policy inputs are presented in Section 3.3. Finally, Section 3.4 overviews the wind and solar resources in Texas.

The results of the scenarios are discussed in Section 2. The change in system costs, retail rates and jobs are provided in Section 2.1. The changes to generating capacity, installation rates of utility and distributed generation are detailed in Section 2.2. Section 2.3 discusses changes to the generation mix along with a description of how WIS:dom-P uses variable renewable energy resourc-

[1] https://vibrantcleanenergy.com/wp-content/uploads/2020/08/WISdomP-Model_Description(August2020).pdf

es (VREs) to meet demand without fail. The impact on pollution and emissions is discussed in Section 2.4. Section 2.5 describes the transmission buildout selected by WIS:dom-P for the various scenarios.

As part of the optimal capacity expansion, WIS:dom-P must ensure each grid meets reliability constraints through enforcing the planning reserve margins specified by the North American Electric Reliability Corporation (NERC) and having a 7% load following reserve available at all times. Section 2.6 discusses the details around how capacity value of both thermal and VRE generation is estimated. Finally, Section 2.7 shows the detailed siting, at 3-km resolution, of the capacity expansion performed for the scenarios modeled.

1.2 WIS:dom-P Model Setup

To accurately study the evolution of the electricity grid over Texas, WIS:dom-P models the entire Texas grid (along with its interconnections to the rest of the CONUS). The state of Texas is divided into 12 economic regions[2] to get higher resolution on the load and bulk transmission within the state. The entire state is simulated with all its generators, demands, and transmission pathways within the state and interconnections to the rest of the CONUS at a 3-km resolution. The model domain with the economic regions modeled is shown in Fig. 1.1 (left panel) and with existing generators on the grid along with the transmission pathways are shown in Fig. 1.1 (right panel). The rest of this section discusses the loads and transmission topology used to initialize WIS:dom-P.

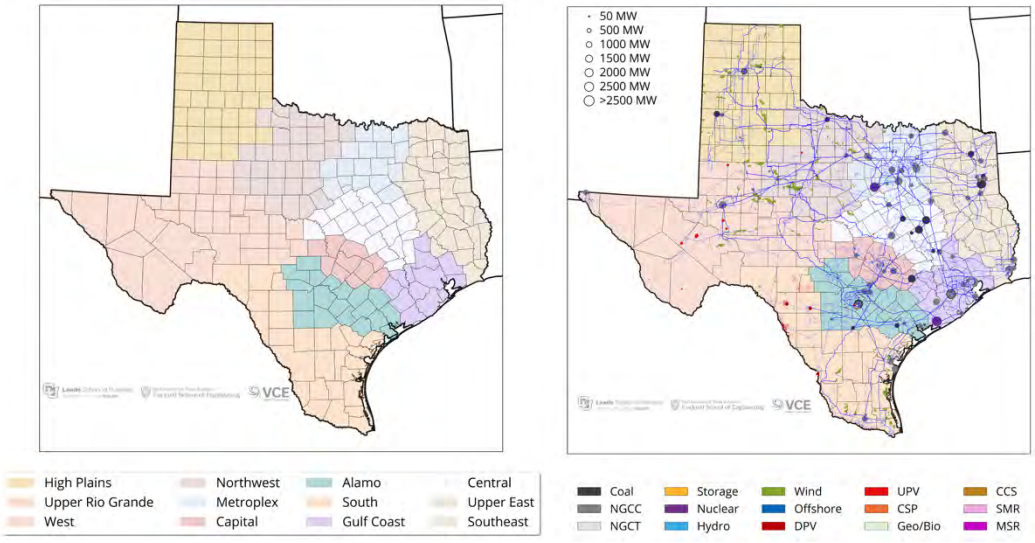

Figure 1.1: WIS:dom-P model domain (left) and existing generators with transmission (right).

[2] https://comptroller.texas.gov/economy/economic-data/regions/2018/snap-texas.php

The initialized generator dataset is created by aligning the Energy Information Administration Form 860 (EIA-860) dataset[3] with the High-Resolution Rapid Refresh (HRRR)[4] model grid. More details on creation of the generator dataset can be found in Section 3.1.

Three sets of forecasted annual demand totals for Texas were provided out to 2050 by UT. The "BAU" and "Extensive Capture" scenarios share the same input demands. The "Electrification" and "Electrification: Accelerated Clean Power" also share the same demands. These demands were broken down into five main components: (1) Space heating demand, (2) water heating demand, (3) transportation demand, (4) conventional demand (including industrial demands, residential cooling demands, lighting demands, and so on) and (5) hydrogen demand. These demands are used in alignment with the temporal demand profiles created by VCE for Texas and discussed in detail below. Figure 1.2 shows the annual demands ingested into WIS:dom-P for the present study.

Annual demand data through 2050 was also provided for the novel chemical technologies used in the "Hydrogen and Carriers" scenario including Ammonia (NH3), Ammonium Nitrate (NH4NO3) and Natural Gas/Methane (CH4). These loads are shown in Fig. 1.3. The Methane demand is for use in buildings. The novel technologies are simulated in WIS:dom-P simultaneously with the electricity system and the formulation of the model is described in the technical documentation Section 1.12.[5] The WIS:dom-P model determines the capacity, location, dispatch and costs for these novel technologies (including Direct Air Capture).

[3] https://www.eia.gov/electricity/data/eia860/
[4] https://rapidrefresh.noaa.gov/hrrr/
[5] https://vibrantcleanenergy.com/wp-content/uploads/2020/08/WISdomP-Model_Description(August2020).pdf

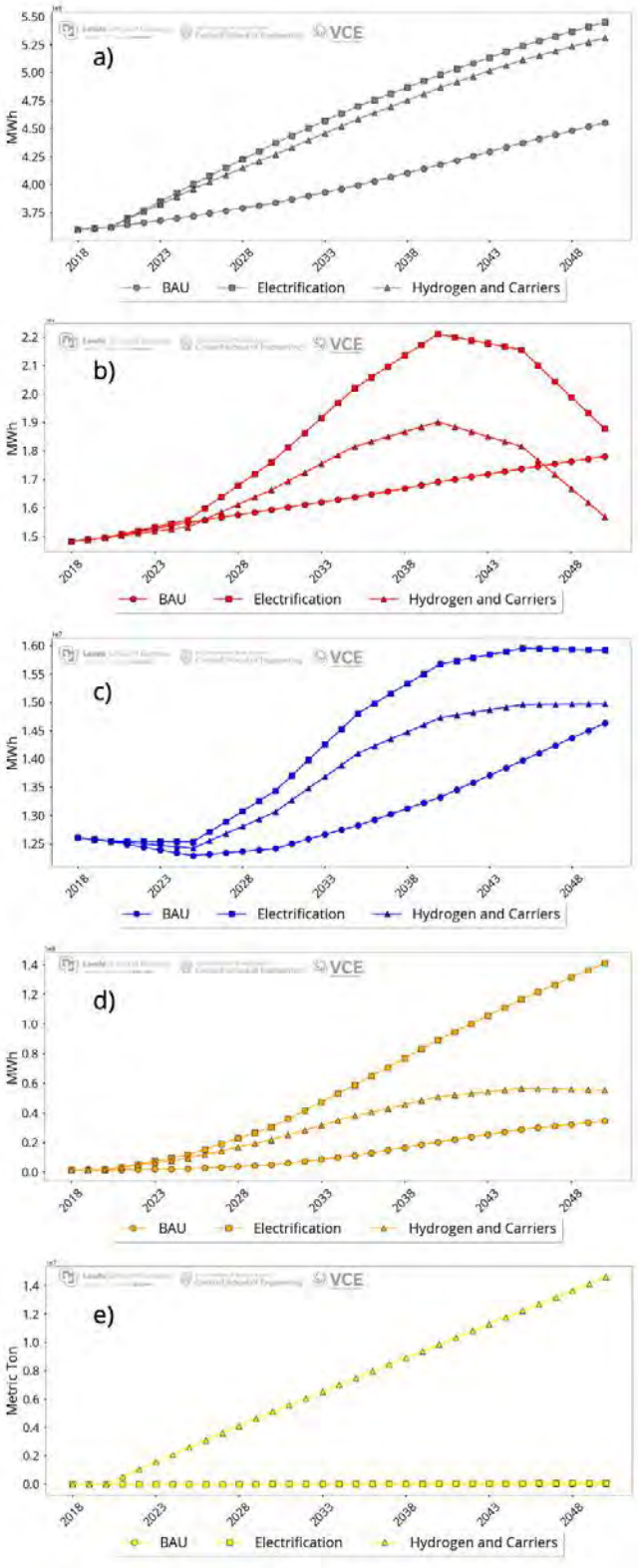

Figure 1.2: Annual demand values provided by UT to ingest into WIS:dom-P for a) conventional, b) space heating, c) water heating, d) transportation and e) hydrogen demands. All values are in MWh except the hydrogen demand, which is in metric tons. Two scenarios run for UT use the "BAU"

demands. Two scenarios for UT use the "Electrification" demands. One scenario for UT uses the "Hydrogen and Carriers" demands.

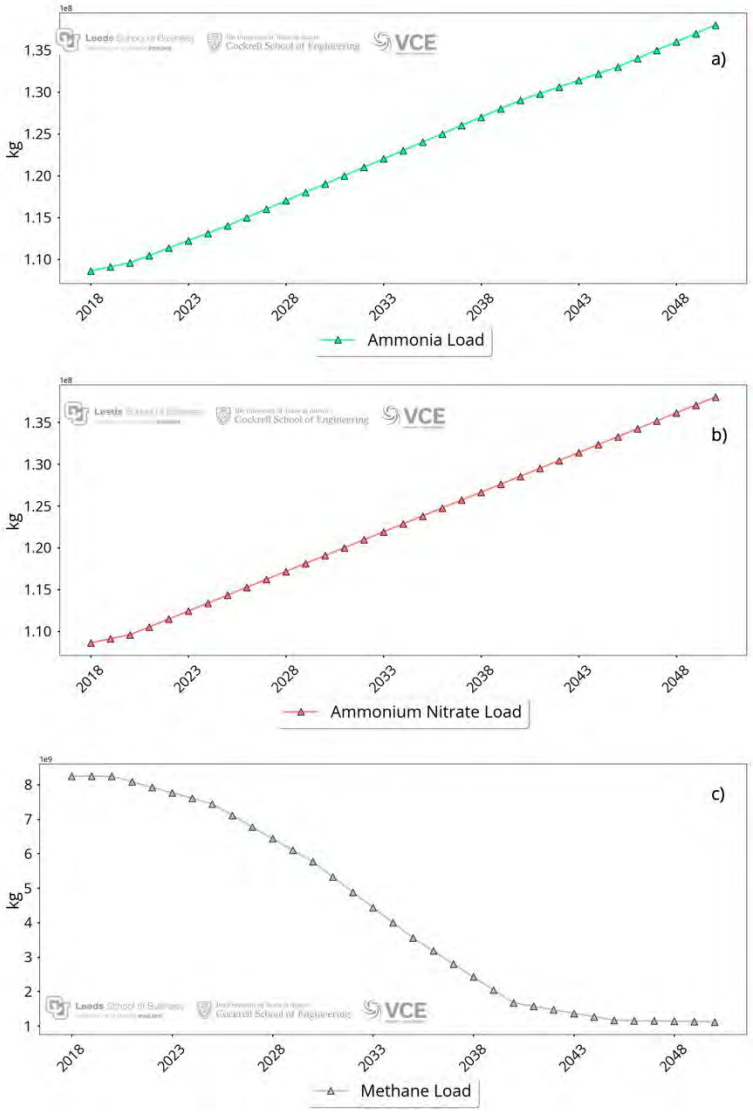

Figure 1.3: Annual demand values (kg) provided by UT to ingest into WIS:dom-P for the novel chemicals a) Ammonia (NH_3), b) Ammonium Nitrate (NH_4NO_3) and c) Methane (CH_4) which were used in the "Hydrogen and Carriers scenario.

The demand profiles are computed using a combination of weather data and Federal Energy Regulatory Commission form 714 (FERC-714) data.[6] The FERC-714 data provides total demand by reporting agencies over the Continental United States (CONUS) at an hourly time resolution. The created demand dataset is split into four components: (1) Space heating demand, (2) water heating demand, (3) transportation demand, and (4) conventional demand (including industrial

[6] https://www.ferc.gov/industries-data/electric/general-information/electric-industry-forms/form-no-714-annual-electric/data

demands, residential cooling demands, lighting demands, and so on). Using the weather data, profiles for space heating, water heating, and transportation are created for the required temporal and spatial resolution.

The 2018 demand components aggregated to state level are shown in Fig. 1.4. The conventional load makes up the largest fraction of the total load with a peak demand of 73 GW occurring in summer. The space and water heating are smaller components of the total load with peaks in the winter periods. Transportation is a negligible part of the electricity demand in 2018 as most of the vehicles run on gasoline and diesel.

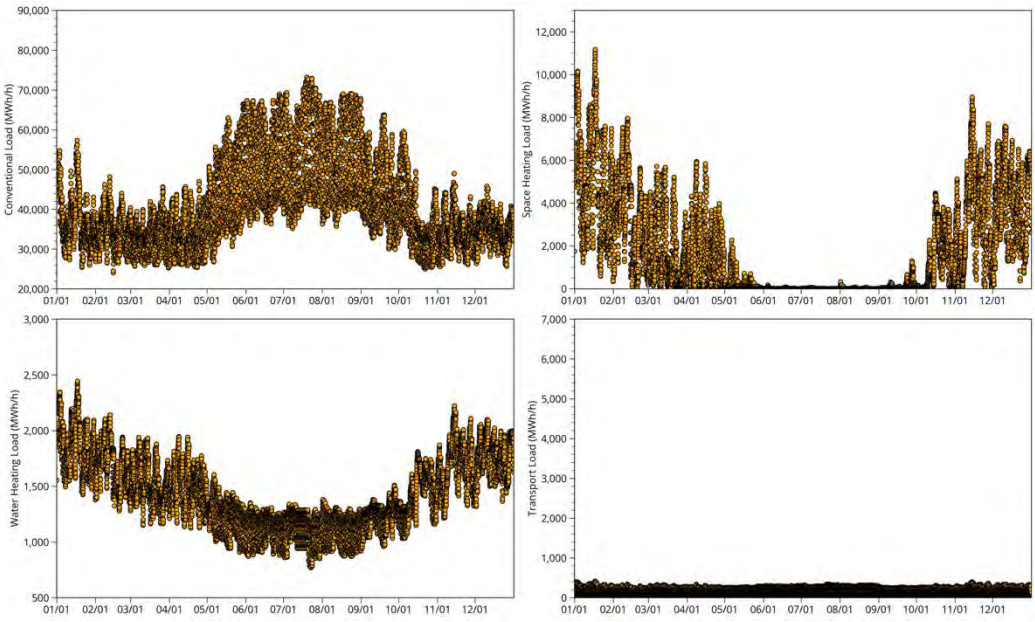

Figure 1.4: Aggregated demand profiles for Texas in 2018. Conventional (top left), space heating (top right), water heating (bottom left) and transport (bottom right).

The historical demand curves derived from the FERC-714 data are adjusted to remove the weather-derived profiles of space heating, water heating, and transport to produce weather-aligned conventional demand profiles. The aggregated demand profiles (obtained by summation of the four components of the demands) are shown in Fig. 1.5. As seen from Fig. 1.5, Texas has a bimodal demand shape in 2018 with the summer peak higher than the winter peak. Further details on the procedure to create the demand dataset is discussed in Sections 2.5 and 2.6 of the WIS:dom-P technical documentation.[7]

[7] https://vibrantcleanenergy.com/wp-content/uploads/2020/08/WISdomP-Model_Description(August2020).pdf

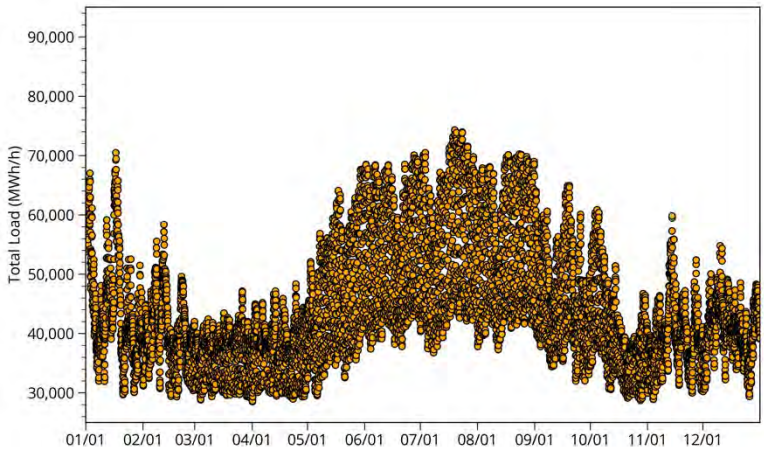

Figure 1.5: Aggregated total demand profile for Texas in 2018.

The change in components of the electricity demand by 2050 as a result of business-as-usual load growth is shown in Fig. 1.6. The conventional load increases by almost 11 GW from 2018 with a new peak load of 85 GW. The space heating load is also increased slightly as some part of the population switches gas heating to heat pumps. Water heating load remains almost static as any increases in electricity load due to switching from gas to electric heating are offset by updating the current stock of water heater to newer electric water heaters. The transportation load grows the most with a new peak load of 6.5 GW during the winter period.

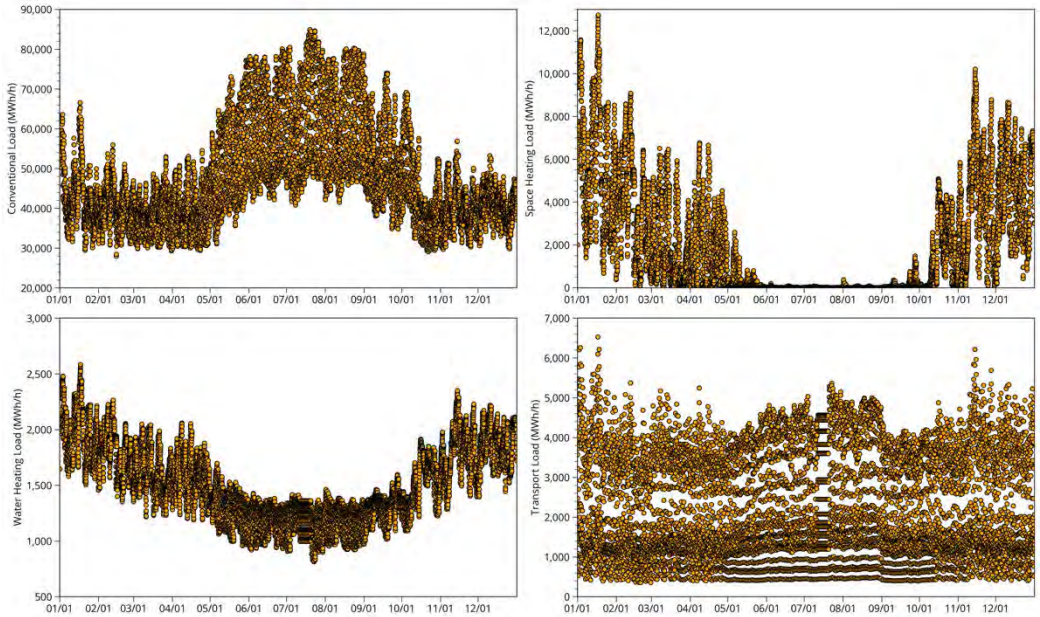

Figure 1.6: Aggregated demand profiles for Texas in 2050 taking into account electrification and climate change. Conventional load (top left), space heating (top right), water heating (bottom left), transport (bottom right).

The combined demand profile in 2050 as a result of the changes in the various components of the load are shown in Fig. 1.7. The total demand profile in Texas retains its bimodal shape, but the winter peak is now almost equal to the summer peak as a result of the growth in space heating and transportation load in the electricity sector.

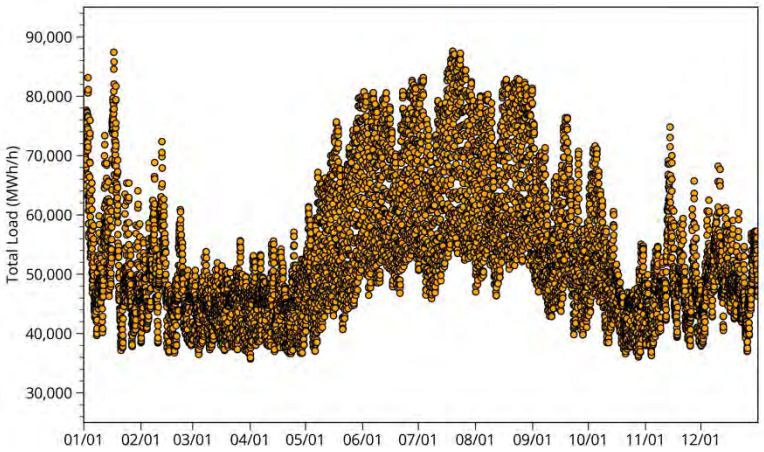

Figure 1.7: Aggregated total demand profile for Texas in 2040.

WIS:dom-P also incorporates demand flexibility, which is tied to the weather data as discussed in detail in Section 2.5 of the WIS:dom-P technical documentation. The total demand flexibility available in the years 2020, 2030, 2040 and 2050 is shown in Fig. 1.8. The demand flexibility available is greater in the winter periods as there is more space and water heating demand (and transportation demand in the later years) to flex. Industrial demand is assumed to be less flexible and, hence, in summer a smaller portion of the conventional load is available for demand flexibility. The peak demand flexibility available in 2020 is 2,176 MW in winter and about 1,592 MW in summer. The demand flexibility increases gradually to 7,862 MW in winter and about 5,139 MW in summer by 2050.

It is critical to model the temporal availability of flexibility to ensure a reliable operation of the simulated grid. The demand flexibility is bound by the capacity of the demands themselves as well as the physics of the weather that drives some of the flexibility. For instance, the non-coincident peak demand flexibility available in 2050 is 13,583 MW. However, due to physical limitations such as weather conditions and coincident availability, the actual demand flexibility that can be called upon changes at every timestep. Figure 1.8 shows the actual demand flexibility that can be called upon in Texas at each timestep over the investment periods.

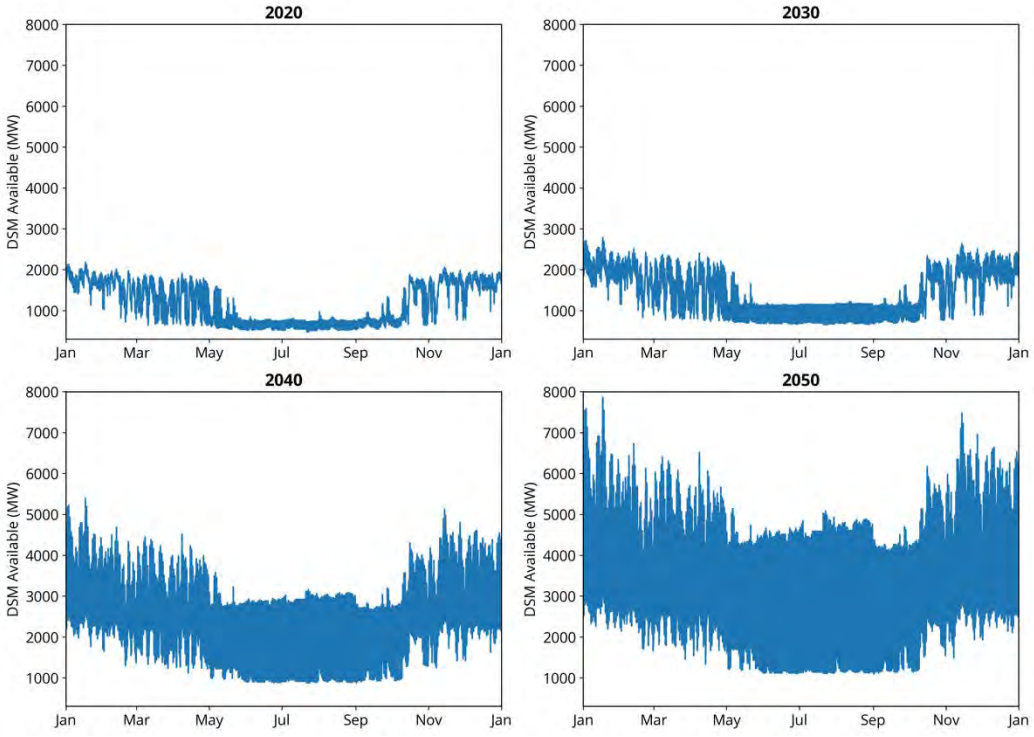

Figure 1.8: Available demand flexibility during each time period of the year over the investment periods.

WIS:dom-P resolves the transmission topology of the modeled grid down to each 69-kV substation resolution as shown in Fig. 1.9 (left panel). The transmission topology can be aggregated to create a reduced-form (county- or economic region- level) as required for each model simulation. The transmission topology aggregated to county-level resolution is shown in Fig. 1.9 (middle panel). The outer simulation utilizes the economic region- and county- level reduced-form transmission systems (middle and right panels). The county-level is for the spur line connections, while the economic region-level is for the bulk transmission. The inner simulation uses the results from the outer simulation reduced-form transmission as boundary conditions upon the full 69-kV resolution transmission system.

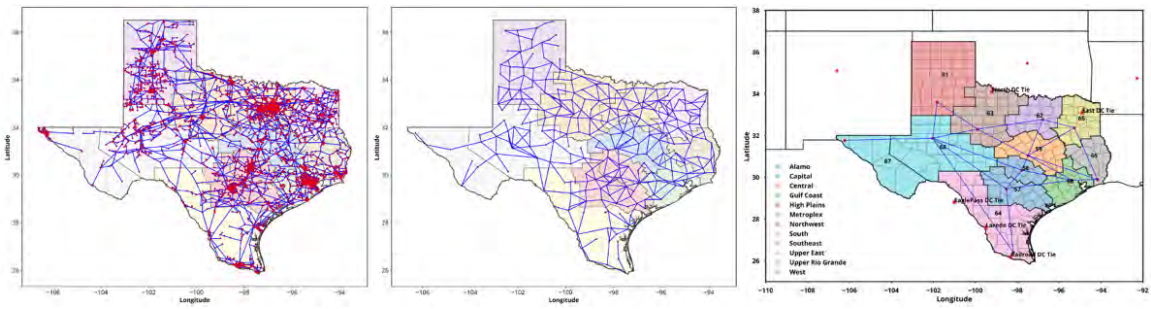

Figure 1.9: Transmission topology of the utility scale electricity system across Texas down to 69-kV substation (left), aggregated to county level resolution (middle), and aggregated to economic region-level (right).

A unique feature of WIS:dom-P is its ability to resolve the utility-scale electricity grid with detailed granularity over large spatial domains. This unique feature has recently been expanded to allow for the model to co-optimize and coordinate the utility grid with the distribution grid. The tractability of such a co-optimization requires parameterization of all the distribution-level grid topology and infrastructure. Therefore, WIS:dom-P disaggregates the DER technologies, but aggregates the distribution lines and other infrastructure as an interface (or "grid edge") that electricity must pass across. The model does assign costs and can compute inferred capacities and distances from the solutions, but cannot (with current computation power) resolve explicitly all the infrastructure in a disaggregated manner.

The main components of deriving the utility-distribution (U-D) interface are:

a. Utility-observed peak distribution demand;

b. Utility-observed peak distribution generation;

c. Utility-observed distribution electricity consumption.

The definition of "Utility-observed" is the appearance of the metric at 69-kV transmission substation or above. Below the 69-kV, the model is implicitly solved with combinations of DERs, and what remains is exposed to the utility-scale grid at the substation. Figure 1.10 is a schematic of how WIS:dom-P represents the U-D interface and Fig. 1.11 displays an illustration of how the distribution co-optimization results in two distinct concerts playing out: DERs coordinating to reshape the demand exposed to the utility-scale (load shifting to supply) and utility-scale generation and transmission coordinating to serve the demand that appears at the 69-kV substation (supply shifting to load).

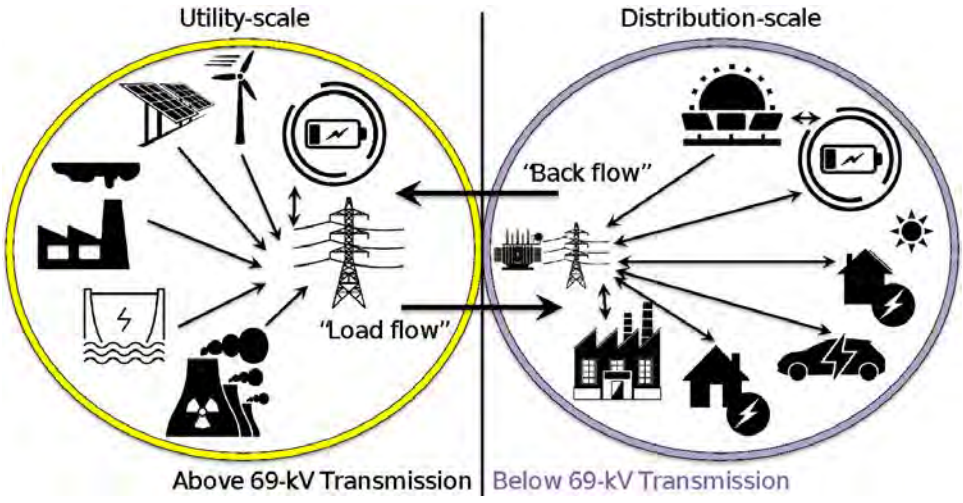

Figure 1.10: A schematic picture of the U-D interface within the WIS:dom-P modeling platform.

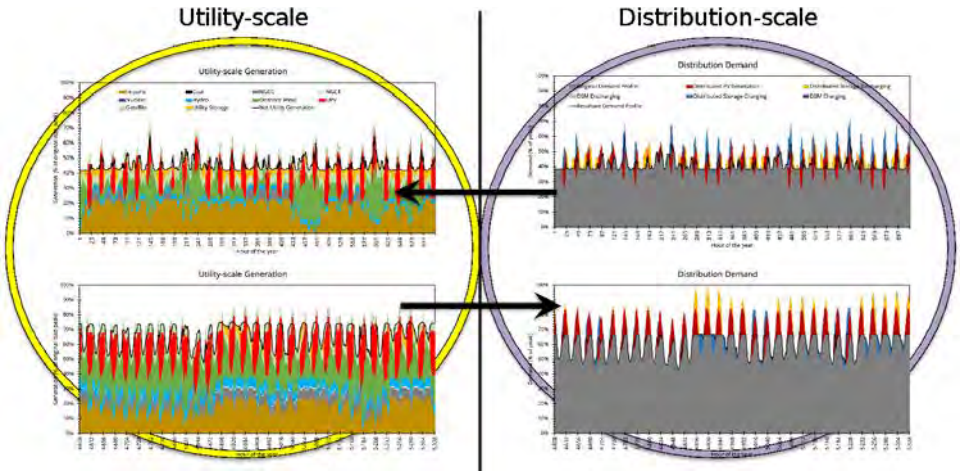

Figure 1.11: Example coordination at the utility- and distribution-scale within the WIS:dom-P model.

To generate an interface for the modeling requires the parameterization of the three components enumerated above. The equations that define the U-D interface directly link to the objective function via the term

$$\Lambda \bullet \left\{ C_L^{dp} \bullet \left[E_L^p + \lambda_a \bullet \left(E_L^b + E_L^m \right) \right] + \; h \cdot C_L^{de} \bullet \sum_t \left(E_{Lt} - \lambda_b \bullet J_{Lt} \right) \right\}. \tag{1}$$

This direct link provides more cost details to the objective function with respect to the distribution infrastructure requirements that results in changes in model logic to find the least-cost system. The U-D interface equations are relatively simple, but have a direct influence on a substantial number of variables and can result in a completely different solution space being accessible to WIS:dom-P compared with other models that do not solve for the co-optimization of the distribution grid.

The U-D interface equations are written as:

$$E_L^p - E_{Lt} + \Lambda \cdot \sum_{L \in L} \left[p_{\{DPV\}Lt} + \sum_D \left(r_{DLt}^- - r_{DLt}^+ \right) + \left(D_{\{dist\}Lt} - C_{\{dist\}Lt} \right) \right] \geq 0, \quad \forall \, L, \, t \tag{2}$$

$$E_L^b + E_{Lt} + \Lambda \cdot \sum_{L \in L} \left[\sum_D \left(r_{DLt}^+ - r_{DLt}^- \right) + \left(C_{\{dist\}Lt} - D_{\{dist\}Lt} \right) - p_{\{DPV\}Lt} \right] \geq 0, \quad \forall \, L, \, t \tag{3}$$

$$\sum_{L \in L} \left\{ J_{Lt} - \Lambda \cdot \left[p_{\{DPV\}Lt} + \sum_D \left(r_{DLt}^- - r_{DLt}^+ \right) + \left(D_{\{dist\}Lt} - C_{\{dist\}Lt} \right) \right] \right\} = 0, \quad \forall \, L, \, t. \tag{4}$$

Equations (1) – (4) and the terms within them are described in detail within the WIS:dom-P technical documentation Section 1.9.[8] Simply, Eq. (2) defines the peak distribution electricity demand observed by the utility-scale grid. Equation (3) defines the peak back flow from the distribution grid to the utility-scale grid. Equation (4) defines the total distributed generation for each time step. Additional documentation on the U-D interface can be found in the explainer documentation on the VCE website.[9]

The Eqs (2) – (4) provide the values to the cost term in the objective function. The exogenous parameters control the relative value of each of the terms. For , there is only a binary option (activate or deactivate). For and , we take values from the report "Trends in Transmission, Distribution and Administration Costs for US Investor-Owned Electric Utilities"[10] by the University of Texas at Austin. These values are national averages, and VCE applies a regionalization by States and counties using internal datasets for locational cost multipliers. The coefficients within Texas take values between $38.74 and $59.25 / kW-peak provided and the coefficients within Texas take values between 0.46 and 1.25 ¢ / kWh provided. Finally, and influence the relative importance of the back flow and distributed generation on the co-optimization of the U-D interface. Here these values are both set to unity.

Lastly, unique to the UT model, greenhouse gas (GHG) emissions information was provided for the rest of the economy, "ROE". All scenarios, apart from "BAU", were set to decarbonize not just the electricity sector, but the economy as a whole. The forecasted amounts of GHG emissions outside of the electricity sector were provided by UT through 2050. This allows WIS:dom-P to know the amount of GHG emissions that need to be removed from the atmosphere while building and optimizing in the electricity sector. Similar to the annual demand data provided, three sets of GHG emissions were provided. ROE GHG emissions were provided for the "Extensive Capture", "Electrification", "Electrification: Accelerated Clean Power" and "Hydrogen and Carriers" scenarios. These GHG emissions are shown in Fig. 2.12.

[8] https://vibrantcleanenergy.com/wp-content/uploads/2020/08/WISdomP-Model_Description(August2020).pdf
[9] https://www.vibrantcleanenergy.com/wp-content/uploads/2021/07/WISdomP_DistnCoOpt.pdf
[10] https://energy.utexas.edu/sites/default/files/UTAustin_FCe_TDA_2016.pdf

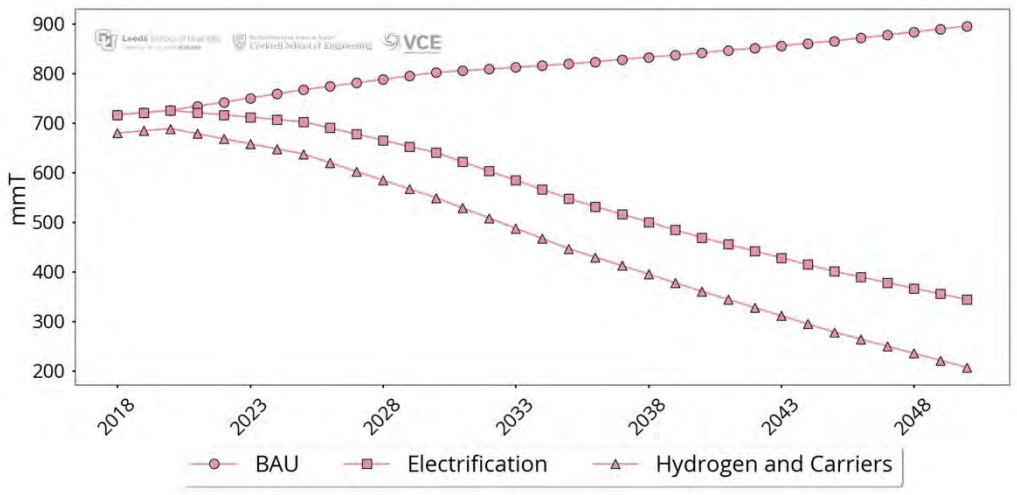

Figure 1.12: The rest of economy emissions (mmT) provided by UT for use in various scenarios. This is the forecasted total emissions from all sectors outside of electricity out to 2050.

The "Hydrogen and Carriers" scenario introduces the use of novel chemical fuels and increased hydrogen demand. The production of Hydrogen occurs through electrolysis or purchase from steam methane reforming (SMR) with CCS plants outside the model. Almost exclusively, the model selects electrolysis. Hydrogen can also be used to produce electricity. It can also blend with the natural gas supply up to 10%. The creation of fertilizer (NH4NO3) and renewable natural gas (RNG) generates electricity in the final stages along with the final chemical product. Additionally, the ammonia (NH3) and RNG can be used in power plants to replace other fuels (coal and natural gas, respectively). Figure 1.13 shows the relationships among the novel chemical technologies. A more detailed discussion of the novel chemical technologies can be referenced in the technical documentation Section 1.12.[11] It is also noted that to create RNG (and CH3OH), CO_2 must be captured either from the atmosphere or via CCS. The WIS:dom-P model endogenously tracks the "cycle" and "deep" storage of CO_2 and where it enters and leaves the infrastructure. The "deep" storage cannot be extracted from, whereas "cycle" storage is for use in chemical production. The pipelines and storage facilities are also endogenously modeled. There is currently no limit on the amount of CO_2 that can be stored in these facilities. Finally, the WIS:dom-P tracks the inputs, byproducts and outputs of the novel chemical production. The novel chemical production, consumption and byproducts are all endogenously modeled at the same temporal and spatial granularity as the electricity grid to ensure that the coupled systems are interacting at a fidelity such that reliability and scarcity are accurately represented.

[11] https://vibrantcleanenergy.com/wp-content/uploads/2020/08/WISdomP-Model_Description(August2020).pdf

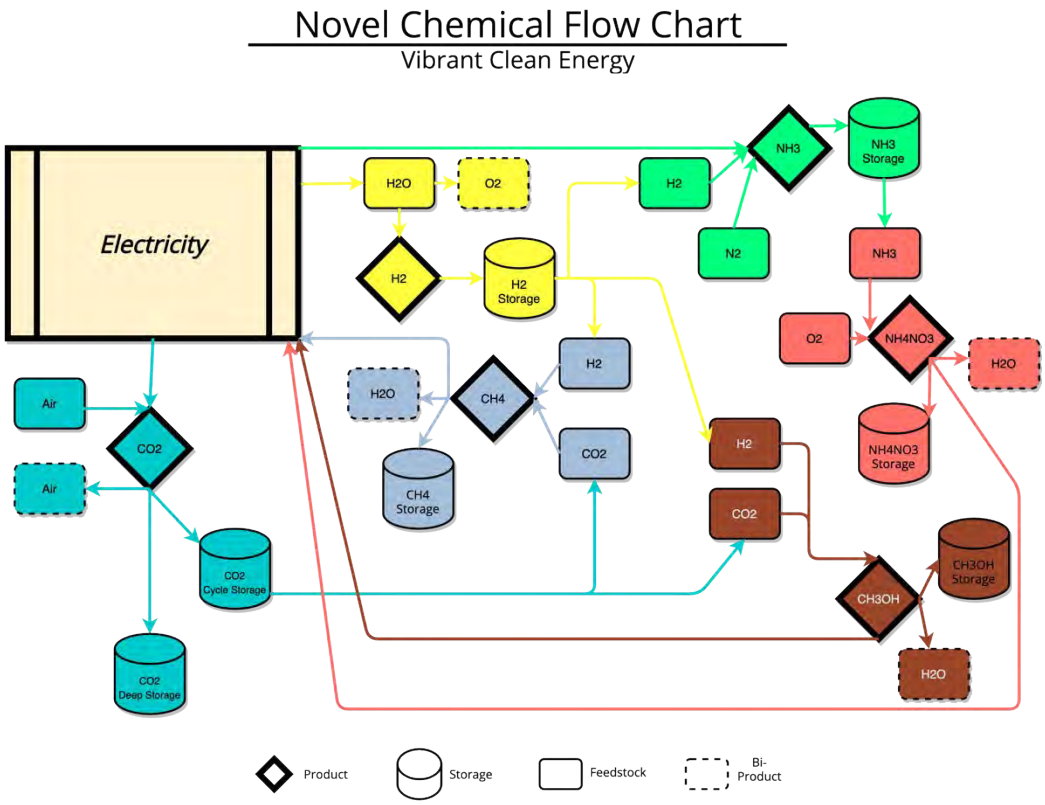

Figure 1.13: The WIS:dom-P Novel Chemical Technology Flowchart showing inputs for creation needed and production results.

2 Modeling Results

2.1 System Costs, Energy Prices, and Retail Rates

The change in total electricity system costs in Texas over the investment periods is shown in Fig. 2.1. In the "BAU" scenario, the system costs change only slightly over the investment periods as the Texas grid undergoes a capacity turnover with older fossil generation replaced with new variable renewable (VRE) generation. The total system cost in 2020 is $30 billion and drops to its minimum value of $29 billion in 2030 as most of the coal generation is retired along with some of the older natural gas combined cycle (NGCC), natural gas combustion turbine (NGCT) and nuclear generation. The total system costs rise again after 2030, reaching $32.6 billion in 2050. All the other scenarios see a rapid rise in total electricity sector costs as these scenarios ensure Texas has net zero carbon emissions by 2050 (since more of the economy becomes dependent on the electricity system), while the "BAU" scenario does not. The "Extensive Capture" scenario has the highest total system cost by 2050 of all scenarios as a result of the large deployment of Direct Air Capture (DAC) to remove the carbon emissions from the electricity sector and the rest of the economy.

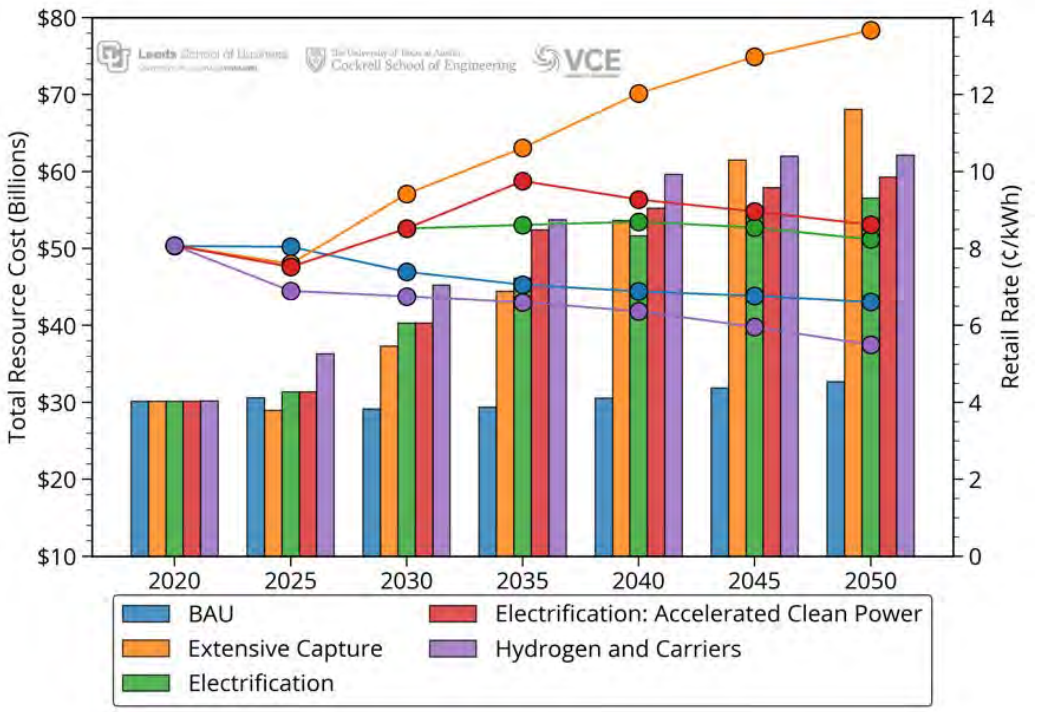

Figure 2.1: Total system cost (bars) and retail rates (solid lines) for Texas.

The "Electrification" scenario results in the lowest system cost of all the decarbonization scenarios, while the "Hydrogen and Carriers" scenario, which initially (2025) has the highest system costs as it builds out the infrastructure needed for producing hydrogen and other synthetic fuels, ends up costing less than the "Extensive Capture" scenario. Therefore, the "Hydrogen and

Carriers" scenario is able to decarbonize the Texas economy with lower disruption, similar to the "Extensive Capture" scenario, but at a lower cost.

Figure 2.1 also shows the estimated retail rates in all the scenarios modeled. The retail rates are calculated assuming the cost of installing and powering the DAC and sequestration of carbon into deep storage (if applicable) is spread out over all electric customers. In the "BAU" scenario, the retail rates reduce from 8 ¢/kWh in 2020 to 6.6 ¢/kWh in 2050. The largest increase in retail rates is observed in the "Extensive Capture" scenario where the retail rates increase to 13.6 ¢/kWh in 2050 as a result of the large DAC deployment whose costs are passed on to customers. The "Electrification" scenario has only a modest increase in retail rates, with retail rates reaching 8.2 ¢/kWh in 2050 compared with 8 ¢/kWh in 2020, as electrification and decarbonization of the electricity sector reduces the need for DAC deployment and the excess generation needed to power them. The "Electrification: Accelerated Clean Power" scenario results in a short-term spike in retail rates in 2035 as a result of the 100% decarbonization by 2035 goal for the electricity sector, but the retail rates reduce again after 2035 reaching 8.6 ¢/kWh in 2050. This also shows that earlier decarbonization goals in Texas do not have a drastic increase in cost to the customer in the longer term. The "Hydrogen and Carriers" scenario results in the largest reduction in retail rates of all scenarios modeled at 5.5 ¢/kWh in 2050. The reason for the lowest retail rates in the "Hydrogen and Carriers" scenario is that it minimizes the need for DAC and spreads investments in all sectors of the economy that it aims to decarbonize resulting in lower burden for electricity sector customers.

The various components of the electrical system that contribute to the retail rates are shown in Fig. 2.2. In 2020, the largest contributors to retail rates are the coal power plants and costs associated with the distribution system at 1.97 ¢/kWh. Over the investment periods, the coal generation is retired and replaced with wind, solar and storage in all scenarios. The retirement of the coal generation is seen to be the largest contributor to reducing costs from 2020 to 2035 in the "BAU" scenario and to 2025 in the decarbonization scenarios. Contributions to cost from the NGCC generation also reduces as the older generation is retired and the existing fleet is used to a lesser extent in all scenarios.

In the decarbonization scenarios, the largest contributor to system cost is the wind generation as it is the largest deployed generator type due to the excellent wind resource in Texas. In the "Extensive Capture" scenario, which has the largest deployment of DAC, the contribution of the actual cost of DAC is found to be a small component of the total system cost. However, the additional generation installed to power the DAC (mostly wind generation in this scenario) has a much larger impact on the system costs. As a result, the "Extensive Capture" scenario ends up having the highest cost of energy from the additional generation installed to power the DAC. The "Electrification: Accelerated Clean Power" scenario shows a different grid layout compared with the "Electrification" scenario having a higher share of cost coming from Enhanced Geothermal and advanced nuclear technologies to meet a more stringent decarbonization timeline. The "Hydrogen and Carriers" scenario has the least amount of additional generation as it is relying on creating synthetic fuels to power portions of the economy which are not electrified and hence re-

sults in the least burden on the electricity sector. Finally, although all scenarios install significant transmission, it contributes a very small portion to the total cost of electricity.

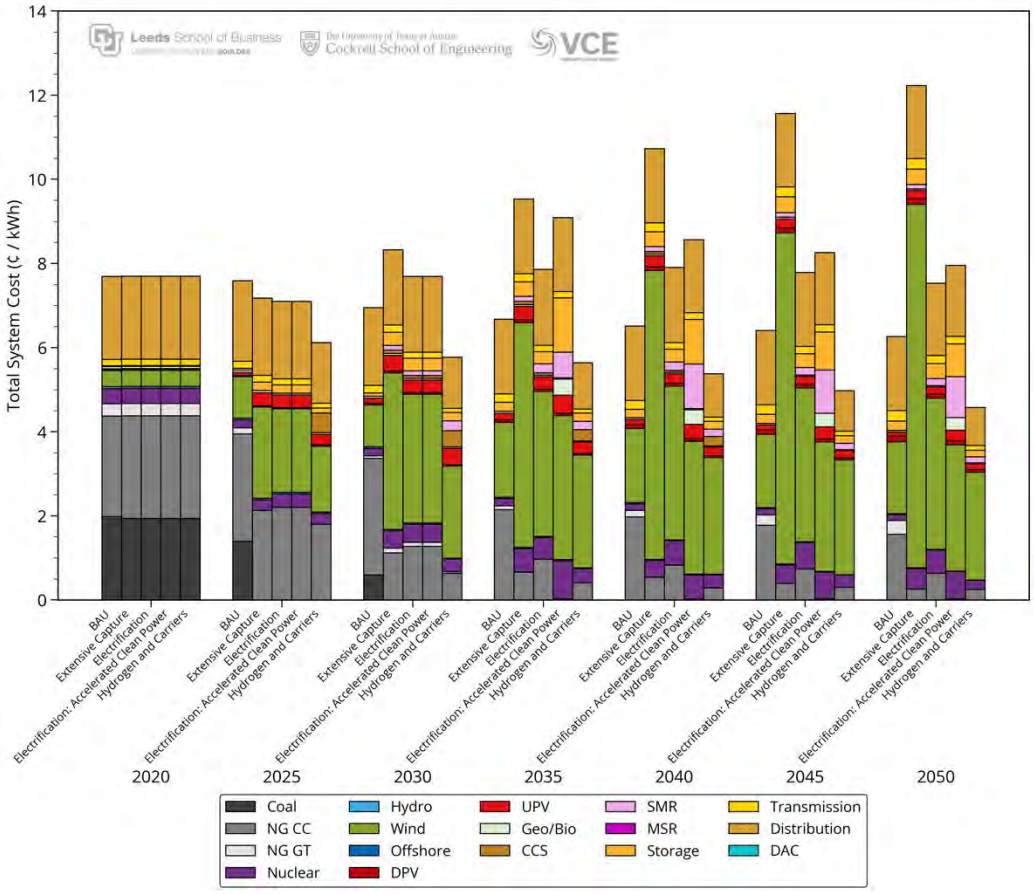

Figure 2.2: System cost per kWh load for each technology in the scenarios modeled.

The total full-time equivalent (FTE) jobs supported by the electricity sector over the investment periods is shown in Fig. 2.3. In 2020, the transmission sector supported the largest number of jobs in the electricity sector in Texas. The jobs in the electricity sector increase from 245,000 in 2020 over the years as new generation and transmission is added and by 2050, the "BAU" scenario supports 741,000 jobs while the decarbonization scenarios support roughly double the number of jobs due to the larger deployment of generation.

Wind and solar industries combined are the largest job creators in Texas in all scenarios modeled. In the decarbonization scenarios, the wind industry creates more jobs compared with the solar industry, while in the "BAU" scenario, the solar industry creates more jobs compared with the wind industry. The largest job creation occurs in the "Extensive Capture" and the "Electrification: Accelerated Clean Power" scenarios due to large buildout of wind generation and storage, respectively. Thermal generation makes only a minor contribution to the total jobs in the electricity sector by 2050. Therefore, the VRE generation, apart from providing clean energy, also brings about economic growth through increased job creation.

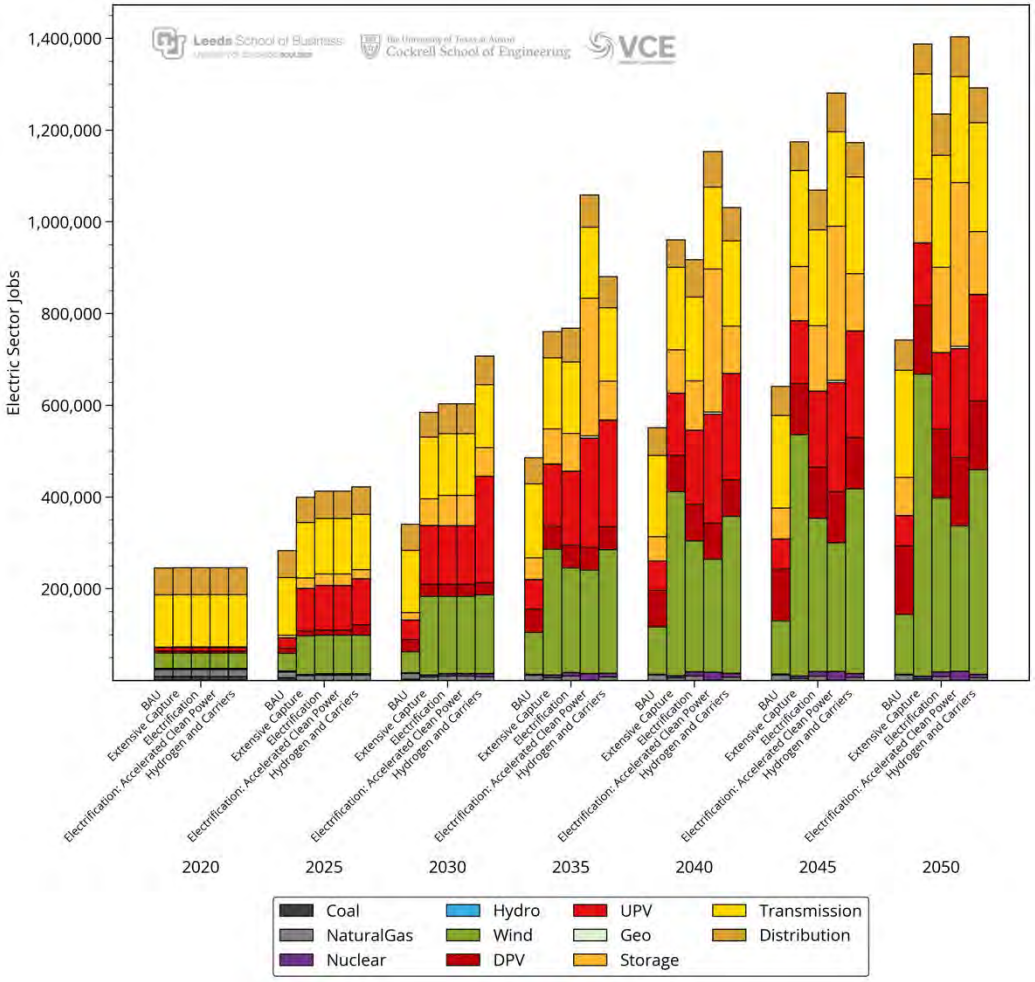

Figure 2.3: Direct full-time equivalent jobs created in the electricity sector by industry.

2.2 Generating Capacity

The evolution of the installed capacity on the Texas grid in the scenarios modeled is shown in Fig. 2.4. The electricity grid in 2020 is largely made up of fossil fuel generation with 75% of the total installed capacity on the grid being either coal or gas generation. In the "BAU" scenario, all the coal generation is retired by 2035, while in the decarbonization scenarios it is fully retired by 2025. The retired fossil generation capacity is mostly replaced by wind and to a lesser extent solar and storage in the "BAU" scenario. The largest installed capacity on the grid occurs in the "Extensive Capture" scenario as this scenario deploys large amounts of wind generation to power the DAC units. The "Electrification: Accelerated Clean Energy" scenario is the only scenario to install significant novel clean technologies such as Molten Salt Reactors (MSR) and Small Modular Reactors (SMR) as it rapidly decarbonizes the grid by 100% by 2035. In addition, in the "Hydrogen and Carriers" scenario there is build out of natural gas with CCS to help reduce GHG emissions faster in the electricity sector and for the production of ammonia and fertilizer. In the later years, as the 45Q tax credit expires, the model deploys DACs to replace the CCS.

Figure 2.5 shows the utility-scale and distribution-scale storage installed in Texas over the investment periods for the scenarios modeled. As seen from Fig. 2.5, by 2025 almost all the new storage is installed on the distribution network. The reason for this is that storage behind the 69-kV substation works along with other distributed energy resources (DER), such as distributed photovoltaic (DPV) and demand-side management (DSM), to not only reduce the peak power passing through the utility-scale and distribution-system interface, but also reduces the total energy crossing the interface. As a result, upgrades to the distribution system from increasing demand can be deferred or are completely eliminated. In addition, due to lower energy crossing the utility-distribution interface, the wear and tear on the distribution infrastructure is reduced, thereby further reducing costs. This co-optimization helps reduce electricity system costs as well as retail rates.

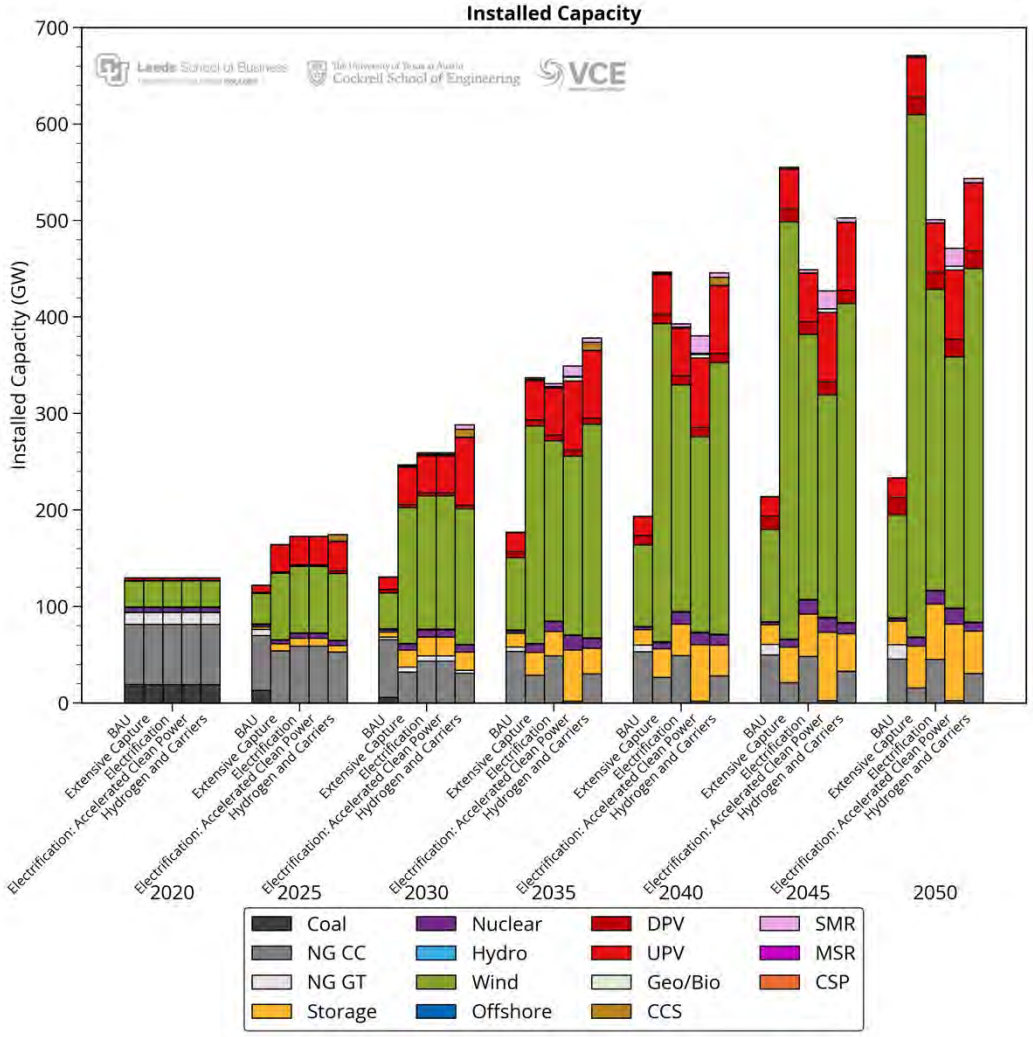

Figure 2.4: WIS:dom-P installed capacities in Texas for the scenarios modeled.

In the "BAU" scenario, about 75% of the storage is installed on the distribution grid in order to optimize the distribution grid with utility-scale generation. In the decarbonization scenarios, however, storage power and energy capacities are almost equally divided on the distribution system and the utility-grid. The largest deployment of storage is in the "Electrification: Accelerated

Clean Power" scenario where WIS:dom-P deploys long duration storage on both the utility and distribution grids between 2030 and 2035 in order to meet the 100% decarbonization goal for the electricity sector. The long duration storage is needed to meet demand during periods of low wind generation, which can last multiple days. No new storage (energy capacity) is added after 2035 in the "Electrification: Accelerated Clean Power" scenario as electrification, in addition to deployment of DAC, provides plenty of flexible demand to work with the existing storage on the grid to ensure the installed generation can meet load during periods of high system strain.

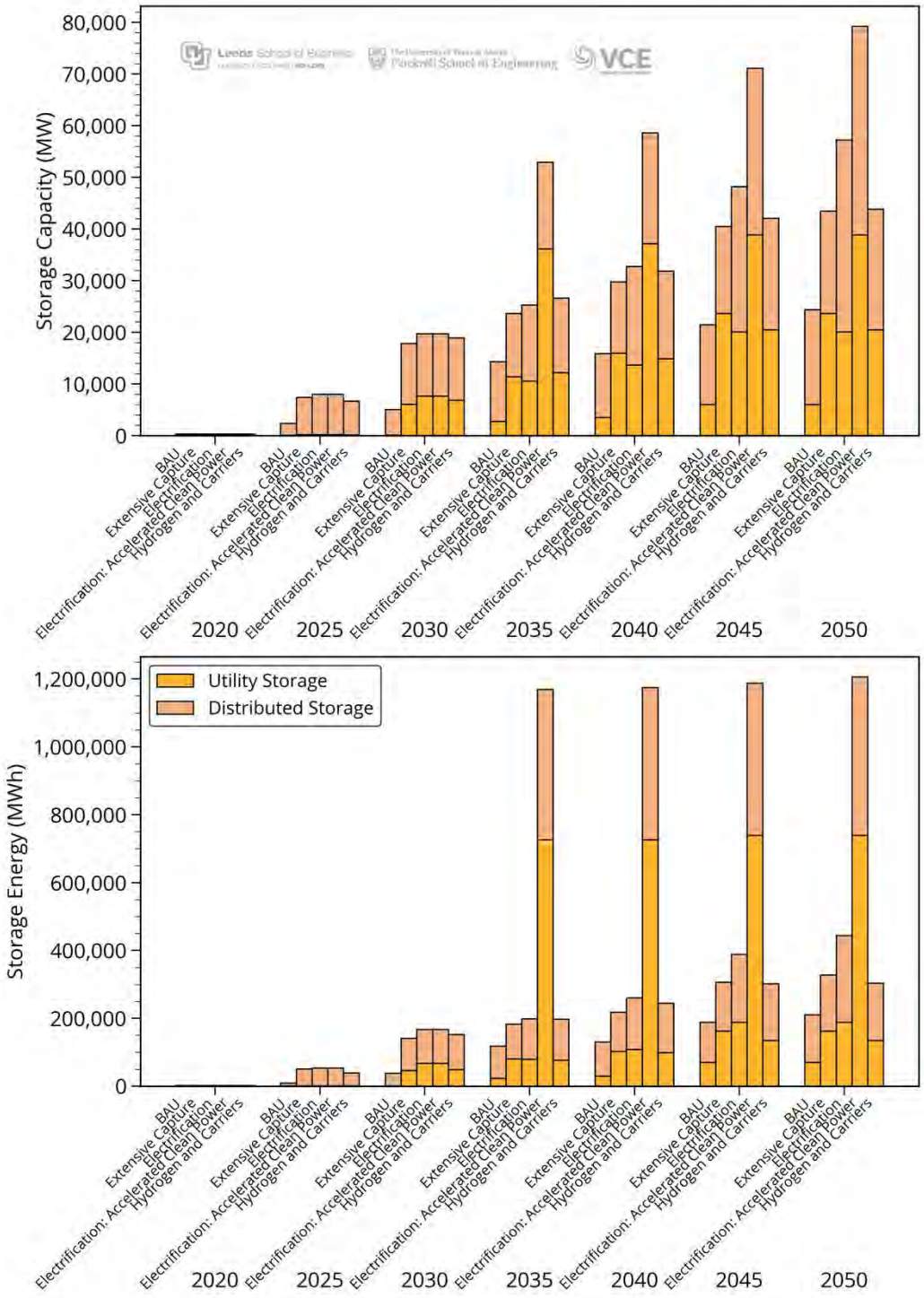

Figure 2.5: Utility storage and distributed storage installed in each investment period in Texas for the scenarios modeled.

The installed utility-scale PV and distributed PV in the scenarios modeled is shown in Fig. 2.6. In the "Hydrogen and Carriers" scenario WIS:dom-P deploys significantly more solar in 2030 compared with the other scenarios to help meet demand for not only the DAC units, but also

ammonia and ammonium nitrate manufacturing. The "Electrification: Accelerated Clean Power" scenario catches up to the "Hydrogen and Carriers" scenario by 2035 as it aims to decarbonize the grid by 2035. The "Electrification: Accelerated Clean Energy" and "Hydrogen and Carriers" scenarios install the most solar on the grid of all the scenarios modeled. In all the scenarios, the additional load due to DACs and hydrogen production (which appear on the utility grid) is significantly larger compared to the increase in load due to electrification on the distribution grid. As a result, the model builds significantly more utility-scale solar generation in order to help meet this load. As a result, it is cheaper for the model to use this large utility-scale generation along with distributed storage to meet the load rather than build additional distributed solar.

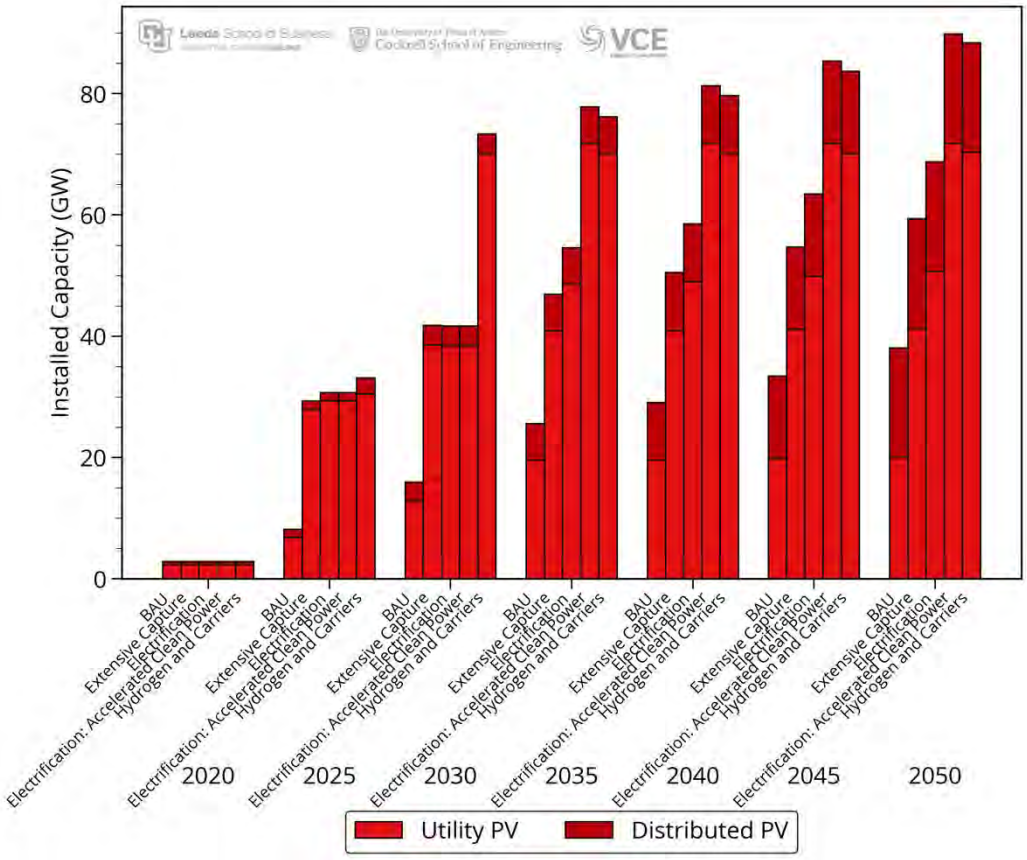

Figure 2.6: Utility PV and Distributed PV installed over the investment periods over Texas for the scenarios modeled.

2.3 Electricity Generation

The evolution of the generation in Texas over the investment periods for the scenarios modeled is shown in Fig. 2.7. As discussed in Section 2.2, all the coal generation is retired by 2035 in the "BAU" scenario and replaced by mostly wind generation. In the "BAU" scenario, the NGCC generation used initially increases from 2020 to 2030 as the coal generation is steadily retired. However, after 2030, wind generation ramps up and is the largest contributor to generation by 2035 and continues to be the largest contributor into 2050. In the decarbonization scenarios, all

the coal generation is retired by 2025, gas generation is ramped down considerably by 2030 and wind generation ramps up to replace it. The "Electrification: Accelerated Clean Power" is the only scenario where a significant amount of generation comes from novel clean technologies.

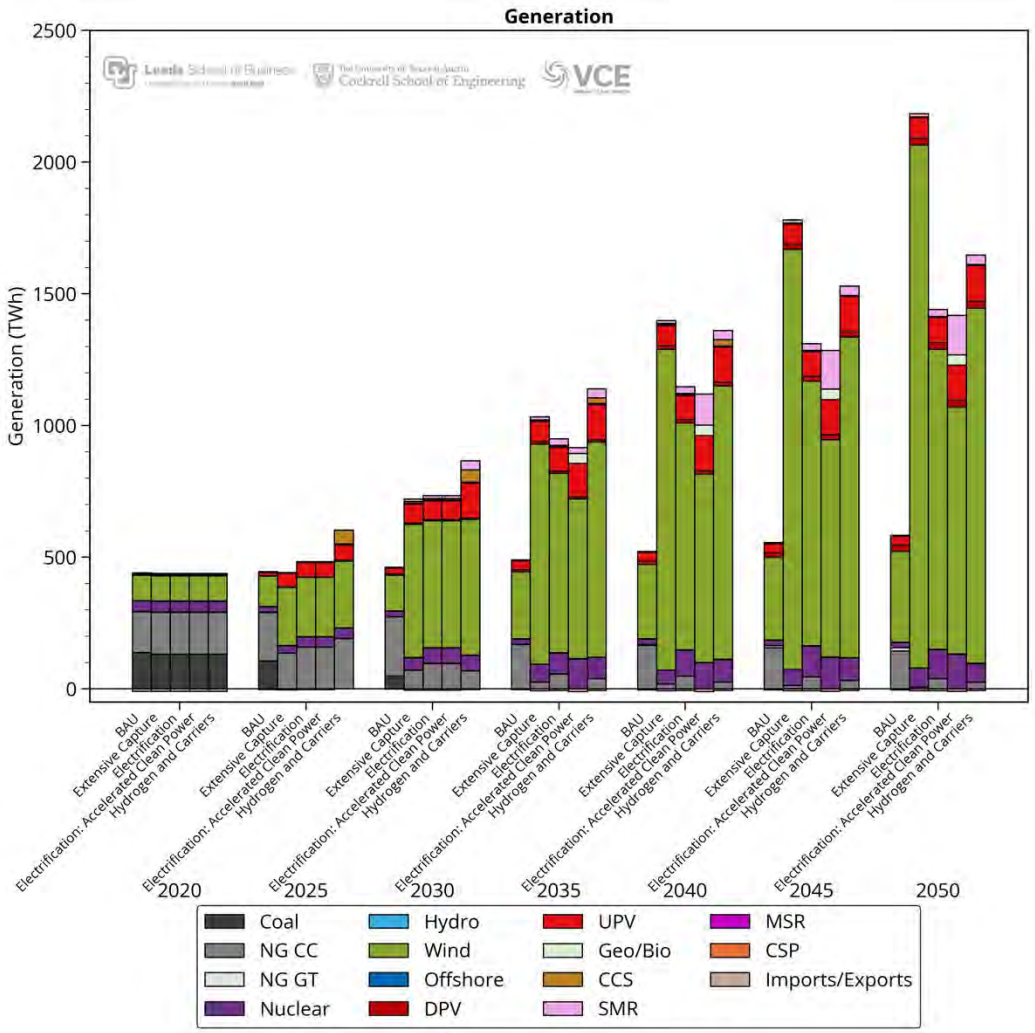

Figure 2.7: Breakdown of the evolution of generation sources for the scenarios modeled.

The daily dispatch of generation in the Texas grid in the "BAU" and "Hydrogen and Carriers" scenarios can be seen from Figs 2.8 and 2.9. Figure 2.8 shows the daily dispatch of generation over Texas in 2020. In 2020, the nuclear generation is operated as "base load" generator as all the nuclear costs are fixed costs that do not change based on capacity factor. Hence, nuclear is run at maximum possible capacity factor (taking into account periods of scheduled maintenance) to minimize cost per kWh generated. Coal generation is used slightly more in winter to meet demand due to the lower ambient temperatures resulting in lower heat-rates and thus lower cost of operation. In the shoulder season (spring) the coal generation reduces markedly because of wind generation being high. The same is true in fall, however, it is natural gas only that reduces output.

In summer, NGCC is the dominant generator used to meet load due to its lower heat-rates compared to coal, resulting in it being the more economic option in summer. Wind generation makes up 19% of the total generation used to meet load. The NGCT generation is hardly used and dispatched in only a few periods in spring and a few days towards the end of the year. The reason for this is that the NGCC generation, along with wind, is able to meet the changes in load.

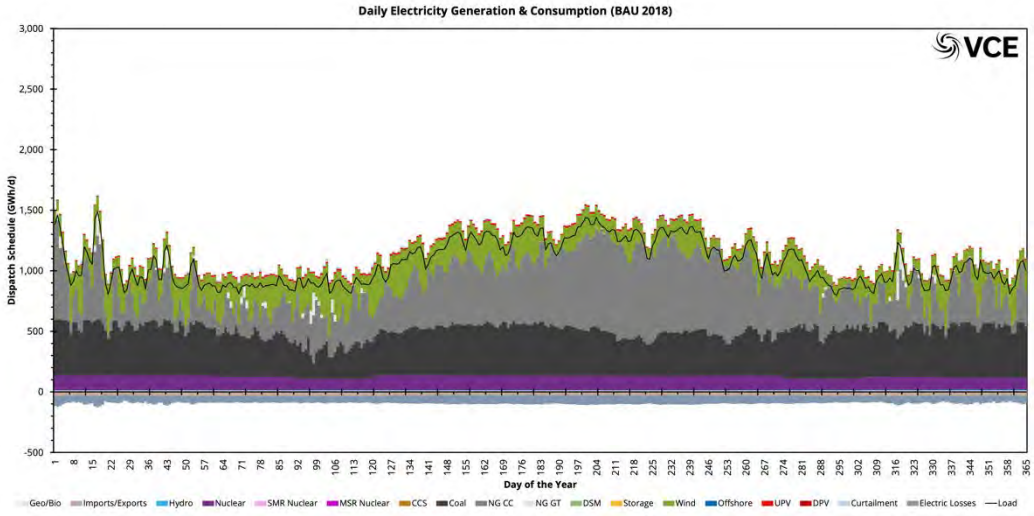

Figure 2.8: The daily generation aggregated over Texas in 2020.

The daily dispatch of energy over Texas in 2050 for the "BAU" and "Hydrogen and Carriers" scenarios is shown in Fig. 2.9. The large load driven by DAC and novel fuel creation in the "Hydrogen and Carriers" is apparent. As seen in Fig. 2.9, wind is dispatched daily and makes up most of the generation almost every day in both scenarios. Curtailment is higher in the winter periods and almost zero during the summer in the "BAU" scenario. There is almost zero curtailment in the "Hydrogen and Carriers" scenario as hydrogen production, DAC and synthetic fuels production ramps up during periods of low demand to use the excess generation. The DAC, hydrogen and other synthetic fuel production is ramped down during periods of low wind generation (typically daytime) and during periods of high system strain. Thus, the "Hydrogen and Carriers" scenario has significant flexible load to ensure the grid is stable during periods of high demand. We note that the synthetic fuel production and DAC facilities are constrained by strict ramp rates and production quotas to ensure economic and practical viability of the assets. The grid operation is similar in the electrification scenarios, however, with less demand flexibility, as those scenarios do not produce synthetic fuels and use less hydrogen to meet industrial demand. WIS:dom-P ensures that there is a 7% load following reserve at each time period while meeting the NERC specified PRM for Texas (ERCOT value applied to the whole of Texas).

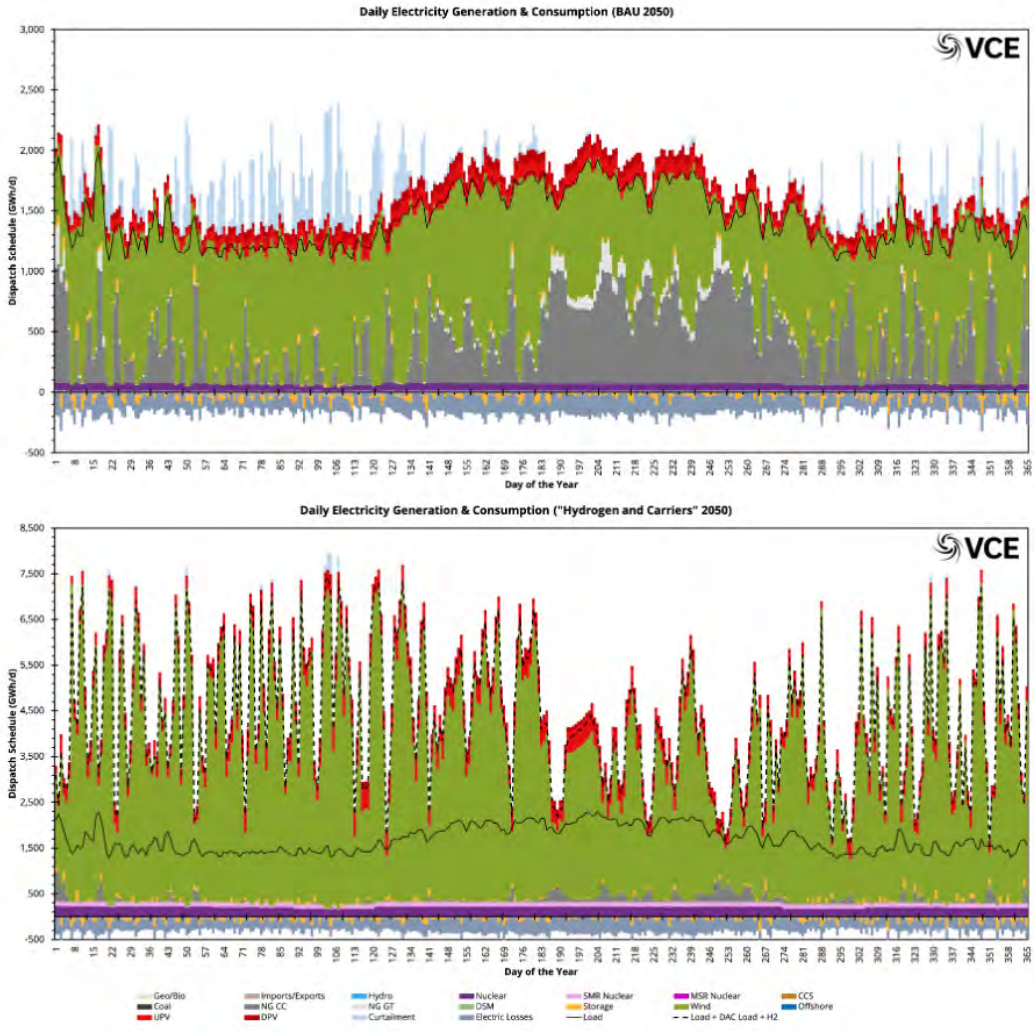

Figure 2.9: The daily generation aggregated over Texas in 2050 for the "BAU" scenario (top) and the "Hydrogen and Carriers" scenarios (bottom).

It is seen in Fig 2.9 (bottom panel) that even with huge amounts of flexibility and overcapacity of wind in the "Hydrogen and Carriers" scenario, there are time periods where the supply of electricity barely covers the inflexible demands (and natural gas with storage is dispatched over those periods). These periods are only able to be supplied because of the flexibility enabled via DACs for consumption of wind and excess GHG emissions from the natural gas power plants. As such, the need for dense clean generation capacity (nuclear, EGS, biomass, etc.) is minimized.

Figure 2.10 shows the period with the highest system strain on the grid in Texas in 2050 for the "BAU" scenario (top panel) and the "Hydrogen and Carriers" scenario (bottom panel). The system strain is defined as the product of thermal generation utilization rate, missing fraction of VRE generation and the load factor. Therefore, the system strain is highest when thermal generation utilization is at its maximum, VRE generation is at its minimum and load is at its highest. The period of highest system strain in Texas occurs in the first week of January.

On the evening of January 3rd, as seen in Fig. 2.10, the wind generation does not show up and as a result WIS:dom-P dispatches storage and NGCT to meet the demand peak that occurs in the evening period in the "BAU" scenario. During this period, both NGCC and NGCT are dispatched at their full available capacity along with storage. In the "Hydrogen and Carriers" scenario, as the wind generation ramps down, the flexible demand, which includes DAC, hydrogen and synthetic fuel production all ramp down. Even in this scenario, it still needs to deploy some NGCC generation along with storage to ensure demand is met. Therefore, some dispatchable generation (for example storage) will always be needed on the grid as demand flexibility alone cannot help overcome all periods of high system strain. This example shows that by accounting for the variability of VRE generation in the PRM calculations (discussed in Section 2.6), demand can be met reliably even in high strain periods in a high VRE penetration system.

We note that WIS:dom-P models the natural gas system along with the electricity grid (and new novel chemical production and infrastructure). The model ensures that fuel is available to the generators and heating customers at all times. If the model determines a lack of supply for any reason the model must determine the best path forward: more natural gas infrastructure, different heating equipment, different generation mix. These all compete within WIS:dom-P to produce the most economic outcome whilst ensuring reliability and robustness. These co-optimization efforts help minimize the possibility of the Winter Storm Uri event happening again in Texas.[12]

[12] https://www.vibrantcleanenergy.com/wp-content/uploads/2021/03/VCE-ERCOT-StormUri.pdf

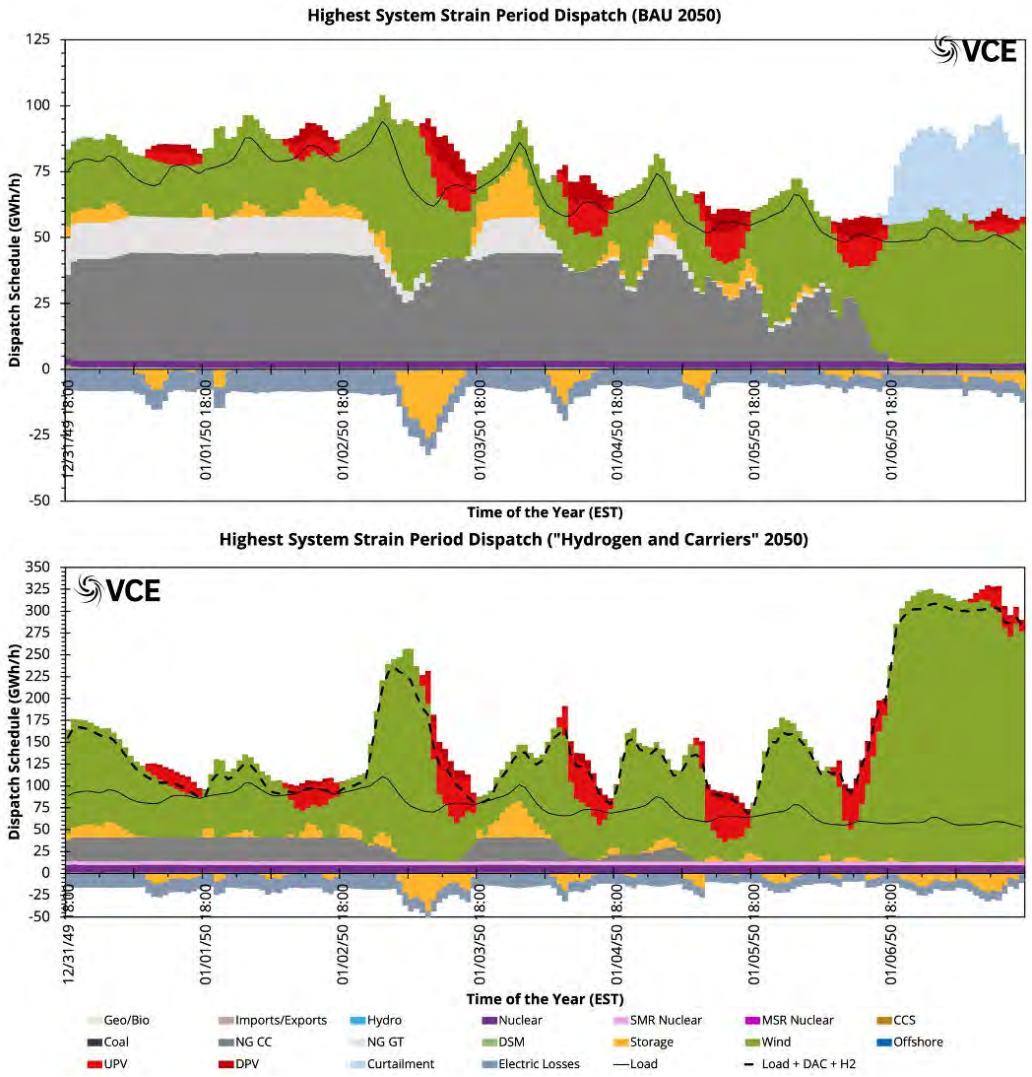

Figure 2.10: The most difficult week to supply demand in Texas in 2050. "BAU" scenario (top) and "Hydrogen and Carriers" scenario (bottom).

Storage plays an important role as dispatchable generation with NGCT coming online only during periods of very high system strain in order to keep the cost of operating the grid low. Fig. 2.11 shows the storage behavior as a function of system strain. Storage only charges during periods of lower system strain and discharges over a range of strain values to assist other generators in meeting load. In the "BAU" scenario, storage only charges when the system strain is lower than 60% and discharges at higher capacity factors during periods of high system strain. Similar storage behavior is observed in the decarbonization scenarios as well.

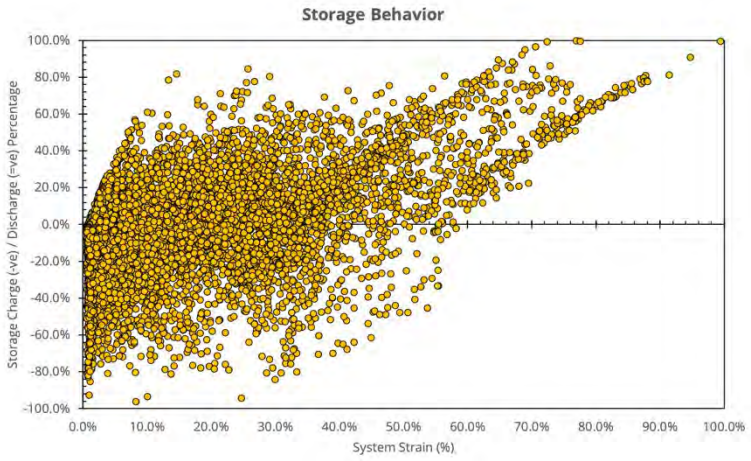

Figure 2.11: Storage behavior as a function of the strain metric over Texas in 2050.

Apart from storage, the marginal price of energy also responds to the system strain. Figure 2.12 shows the diurnal and seasonal trends in system strain and corresponding marginal price for the "BAU" scenario (top) and "Hydrogen and Carriers" scenario (bottom panel). As seen from Fig. 2.12 (top-left panel and bottom-left panel) the marginal price is sensitive to system strain and increases as system strain increases. The marginal price of energy is higher in summer compared with winter as the system strain is higher in summer compared with winter. In winter, the system strain is relatively flat with minor increases during the evening periods. In addition, marginal prices in both summer and winter are found to be lower in the "Hydrogen and Carriers" scenario compared with the "BAU" scenario due to the higher VRE penetration. Similar trends are observed in the other decarbonization scenarios, where diurnal trends in marginal prices correlate with system strain and are lower compared with the "BAU" scenario.

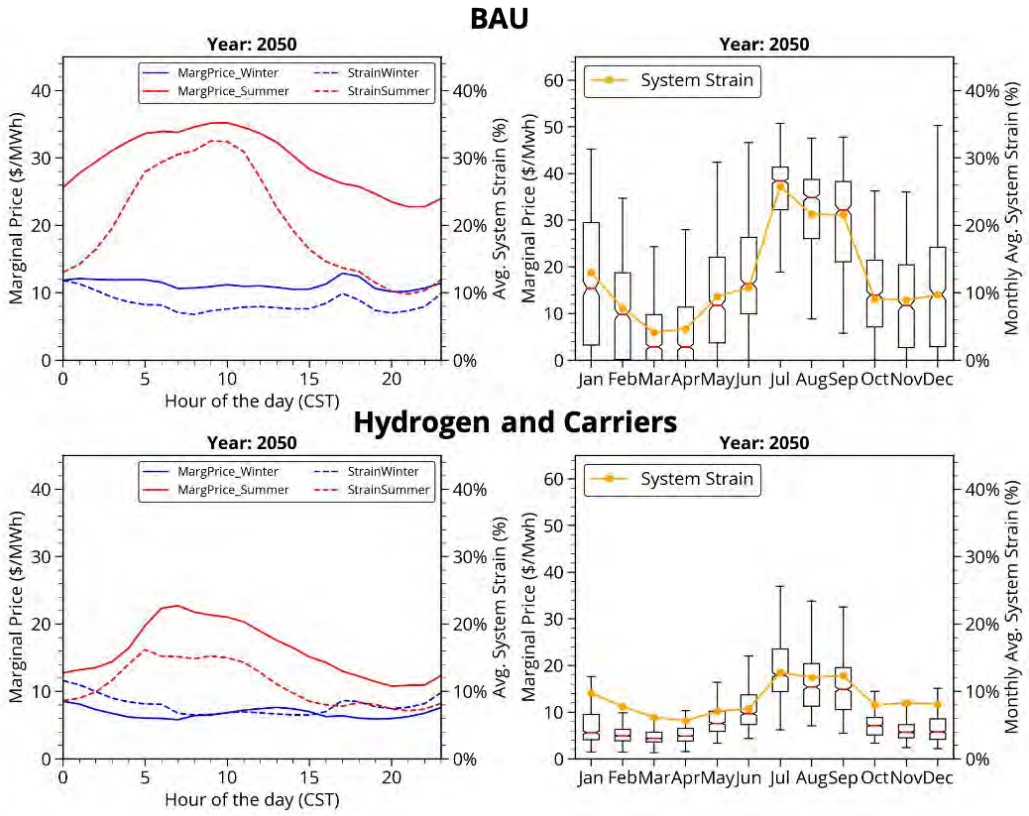

Figure 2.12: The diurnal marginal price and system strain (left) and the seasonal trend in marginal price and system strain (right) for the "BAU" scenario (top panels) and "Hydrogen and Carriers" scenario (bottom panels).

The system strain is lowest during the spring period and highest in the summer in Texas as seen from Fig. 2.12 (right panels). As a result, the median marginal prices are also the lowest in the spring and highest in the summer. In the "BAU" scenario, marginal price is seen to have the highest volatility in the winter months as the electrical system is dominated by VRE generation during these months and due to inflexible nature of the loads in the "BAU" scenario, there are periods of high marginal prices when demand peaks during periods of lower VRE generation. The February 2021 Winter Storm Uri highlighted an extreme version of this in Texas.[13] The marginal price volatility is found to be lower in the summer in the "BAU" scenario as demand is higher, better correlated with VRE generation and more thermal generation is dispatched during the summer months which keep the prices more stable.

In the "Hydrogen and Carriers" scenario, marginal price volatility is very low (with low median marginal price) during the winter periods as electrification (along with demand for hydrogen and synthetic fuels) ensures there is higher load flexibility and better correlation with VRE generation. The price volatility increases in the summer periods as demand increases and requires deployment of dispatchable generation such as NGCC to help meet load which increases margin-

[13] https://www.vibrantcleanenergy.com/wp-content/uploads/2021/03/VCE-ERCOT-StormUri.pdf

al prices during those periods. However, median marginal prices remain lower than those in the "BAU" scenario.

As a result of the co-optimization of the distribution system with the utility-scale generation, the DERs work together to reduce the peak load seen by the utility-scale generation. Figure 2.13 shows the duration curve of the original load along with the duration curve of the DER modified load. As seen from Fig. 2.13, the peak load over Texas in the "BAU" scenario is reduced from 98.8 GW to 80.5 GW, a 18.5% reduction. The minimum load on the other hand, increases from 40.7 GW to 45.8 GW, a 12.5% increase. As a result, the DER modified load is flatter, resulting in not only a reduced peak load, but also a higher load factor (increased from 60% to 71%), which delivers more efficient use of the thermal generation on the utility grid, further reducing costs. Similar percentage reductions in peak load are observed in the decarbonization scenarios as well, showing that distribution system co-optimization helps save costs and increase efficiency with or without electrification and decarbonization.

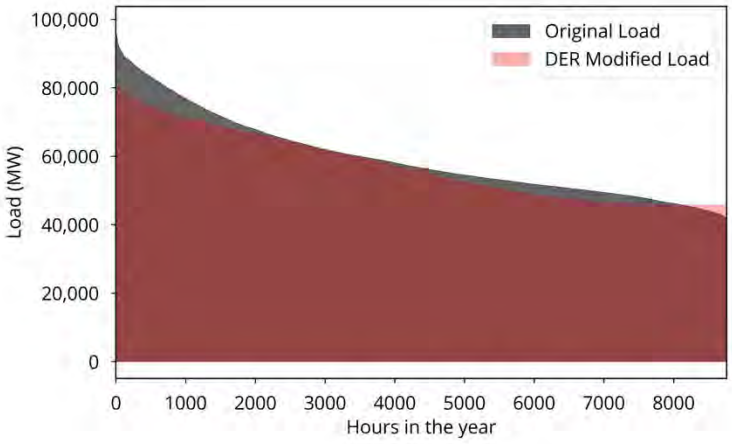

Figure 2.13: Duration curves of the original load and the DER modified load in 2050.

2.3.1 VRE Operation

The diurnal operation of VREs and storage demonstrate how WIS:dom-P takes advantage of the diurnal and seasonal characteristics of wind and solar to meet load. The operation characteristic of the VREs and storage was found to be very similar in all scenarios modeled and hence results from the "BAU" scenario are shown as representative examples. Figure 2.14 shows average diurnal capacity factors for wind, solar and storage in winter (top) and summer (bottom). As seen from Fig. 2.14, wind and solar generation complement one another both in the winter and summer seasons. The winter diurnal load is almost flat throughout the day with a couple of peaks in the early morning and afternoon periods. In winter, the wind generation meets the majority of the load during the nighttime and early morning hours while solar generation helps meet load during the day. Some storage is constantly discharging to smooth out the variability in the wind and solar generation with higher storage generation coinciding with the early morning load peak. Texas has

significant excess generation in the winter due to the higher wind capacity factors resulting in the excess energy being exported.

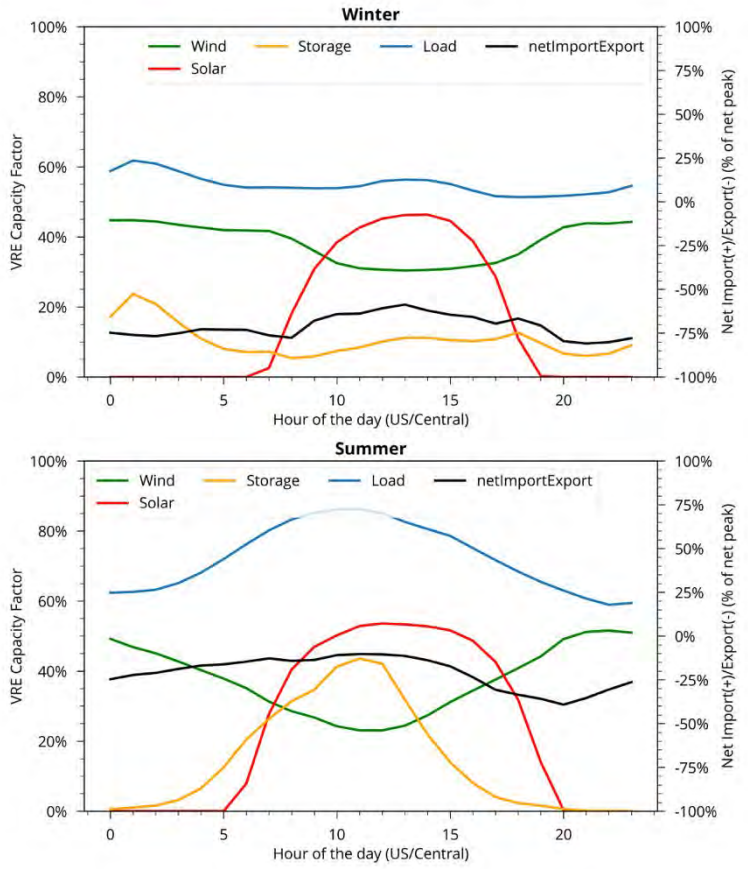

Figure 2.14: Diurnal VRE operation pattern observed in Texas in winter (top) and summer (bottom) in year 2050.

The shape of wind and solar generation in summer is significantly different from that in winter. Wind generation, in the summer, is seen to have a higher capacity factor during the nighttime compared to winter; it also has a lower capacity factor during the daytime compared to winter. Solar generation has a higher capacity factor in summer along with a broader period of peak generation due to the longer days. The load peaks in the morning period around noon local time just as the solar generation is also peaking. However, as Texas has much lower solar capacity installed, storage has to discharge along with solar to help meet the peak load in summer. The excess generation is lower in summer due to lower wind generation, especially during the daytime.

Storage installed on the utility-scale and distribution-scale exhibit different charge/discharge behavior over the course of the year. The charge/discharge behavior of storage on the utility grid and distribution grid is shown in Fig. 2.15. In winter, the distributed storage discharges in the early morning period coincide with the winter load peak and thus ensure that the utility-scale generation sees a lower load peak. The utility-scale storage charges during this time using any excess

wind generation. During the daytime, the distributed storage absorbs any excess distributed solar generation and thus prevents back-flow. The utility-scale storage on the other hand discharges to help wind generation meet load. The utility-scale storage starts charging again in the evening periods as wind generation picks up and there is excess generation.

The charge/discharge behavior of the utility and distributed storage are correlated with each other in summer. The storage on both grids charge during the early morning and evening periods as there is excess wind generation during this time. During the daytime, when load peaks in the summer and wind generation is at its lowest, solar generation is unable to meet all the load. Hence, both utility and distributed storage discharge to help meet the load during the daytime. This storage behavior in the summer is unique to Texas due to its wind dominated grid. In most regions of the CONUS, storage usually charges during the day as there is excess solar generation.

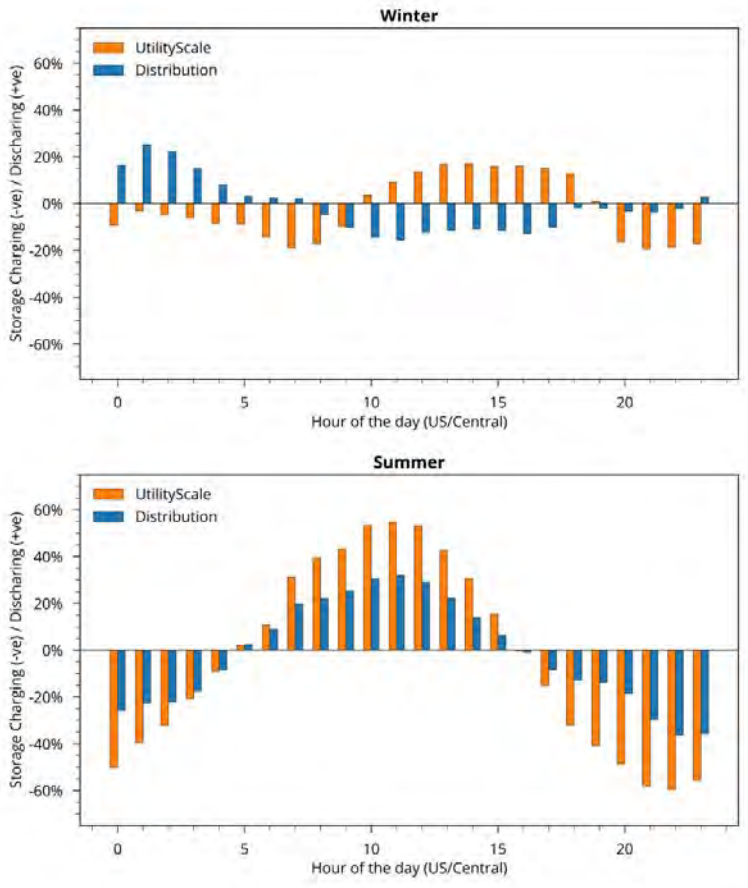

Figure 2.15: Behavior of utility scale and distribution scale storage installed in Texas in winter (top) and summer (bottom) in the year 2050.

2.4 Emissions and Pollutants

The change in annual electricity sector carbon dioxide (CO_2) emissions with respect to 2018 emissions for all scenarios modeled is shown in Fig. 2.16. It is seen that electricity sector emissions steadily decrease over the investment periods as a result of replacing fossil fuel generation with VRE generation. The decline in emissions is rapid from 2020 to 2035 as all the coal generation along with some older NGCC and NGCT generation is retired. After 2035, the reduction in emissions is incremental as all the fossil fuel generation that can be economically retired is already gone. By 2050, the annual emissions in the "BAU" scenario are 75% lower compared with 2018 levels. In the "Extensive Capture" scenario, the annual electricity sector emissions are reduced by 98% by 2050 as WIS:dom-P attempts to reduce electricity sector emissions as much as possible to reduce the need for DAC to remove CO_2 from the atmosphere. The "Electrification" and "Hydrogen and Carriers" scenarios reduce their emissions by about 96% by 2050 and the "Electrification: Accelerated Clean Energy" scenario reduces annual emissions by 100% by 2035 due to the electricity sector decarbonization goal.

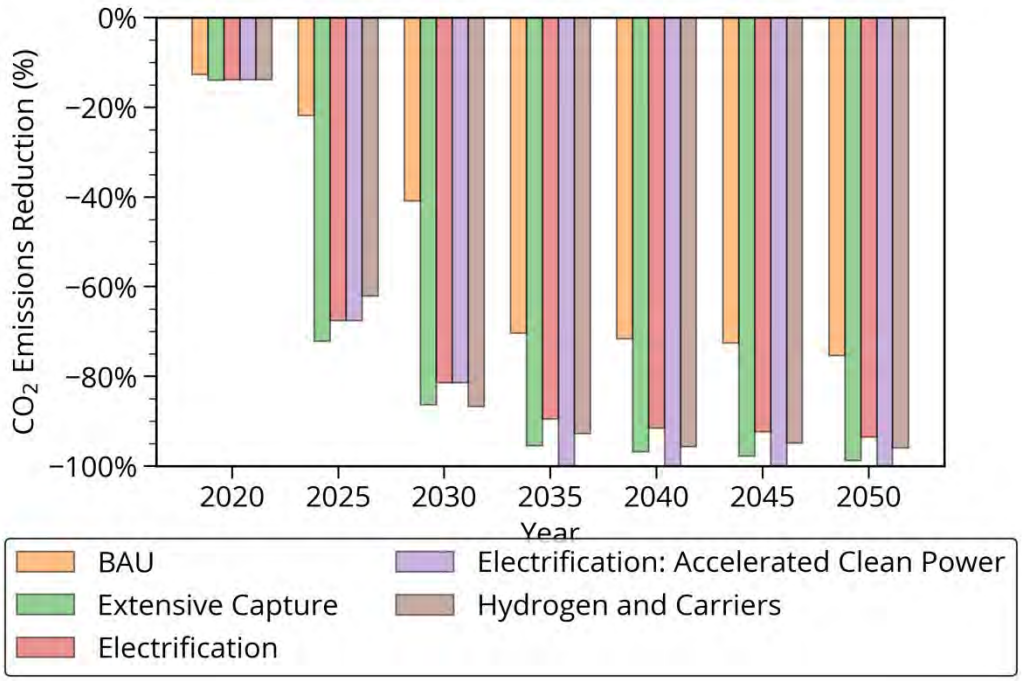

Figure 2.16: Percentage change in annual electricity sector emissions in Texas compared to 2018 levels.

The cumulative economy-wide CO_2 emissions in Texas for all the scenarios modeled is shown in Fig. 2.17. The "BAU" scenario, which does not aim to decarbonize or electrify the economy, has the highest cumulative CO_2 emissions, reaching 28,666 million metric tons (mmT) by 2050. The "Extensive Capture" scenario, which ensures the economy reaches net zero carbon emissions by 2050 by using DAC to remove CO_2 emissions from the electricity sector and the rest of the economy saves 13,016 mmT of emissions compared with the "BAU" scenario.

In the electrification scenarios ("Electrification" and "Electrification: Accelerated Clean Power"), the cumulative CO_2 emissions by 2050 are approximately the same and reduce economy-wide emissions by 2,495 mmT over the "Extensive Capture" scenario cumulatively by 2050. Therefore, electrification can help reduce CO_2 emissions faster and at a lower cost compared with not electrifying and removing emissions using DAC.

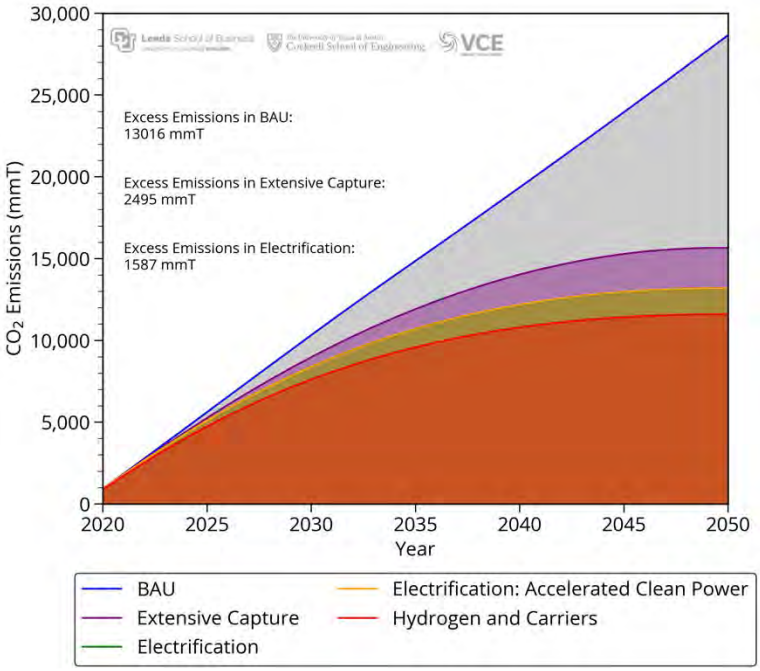

Figure 2.17: Cumulative economy-wide carbon dioxide emissions.

The "Hydrogen and Carriers" scenario results in the lowest cumulative economy-wide CO_2 emissions by 2050. The "Hydrogen and Carriers" scenario saves an additional 1,587 mmT of emissions over the electrification scenarios and 17,080 mmT over the "BAU" scenario. Therefore, electrification along with investing in synthetic fuels to replace traditional fuels results in the largest emission reductions with lower electricity retail rates compared with the "BAU" scenario. The "Hydrogen and Carriers" scenario also results in lowest disruption to existing infrastructure for all customers.

Apart from the CO_2 emission reductions, the scenarios modeled results in significant reductions in emissions of other criteria pollutants tracked by WIS:dom-P as shown in Fig. 2.18. The criteria pollutants emission reduction trends in the "Electrification" and "Hydrogen and Carriers" scenario are very similar and hence only the "Electrification" scenario is shown for brevity. In the "BAU" scenario, the SO_2 emissions decline from 2020 and drop to zero by 2035 as all the coal generation is retired, while in the decarbonization scenarios, the SO_2 emissions reduce to zero by 2025 due to the faster retirement of coal generation. Similarly, the PM_{10} and $PM_{2.5}$ emissions also drop to zero by 2035 due to the retirement of the coal generation in the "BAU" scenario and by 2025 in the decarbonization scenarios.

In the "BAU" scenario, the emissions of NOx drop significantly from 2020 to 2035 as a combined effect of retirement of coal and gas generation as well as reduced use of gas generation after 2035. The emissions of CH4 and volatile organic compounds (VOC) also reduce significantly by 2035 and remain constant afterwards due to retirement of coal generation and reduced use of gas generation. In the decarbonization scenarios, there is a faster drop in the NOx emissions due to faster retirement of coal and gas generation and minimal use of the remaining gas generation on the grid. The "Electrification: Accelerated Clean Power" is the only scenario where criteria air pollutants go to zero after 2035 as a result of the 100% decarbonization goal. The CH4 and VOC emissions include a 2% leakage rate from natural gas production.

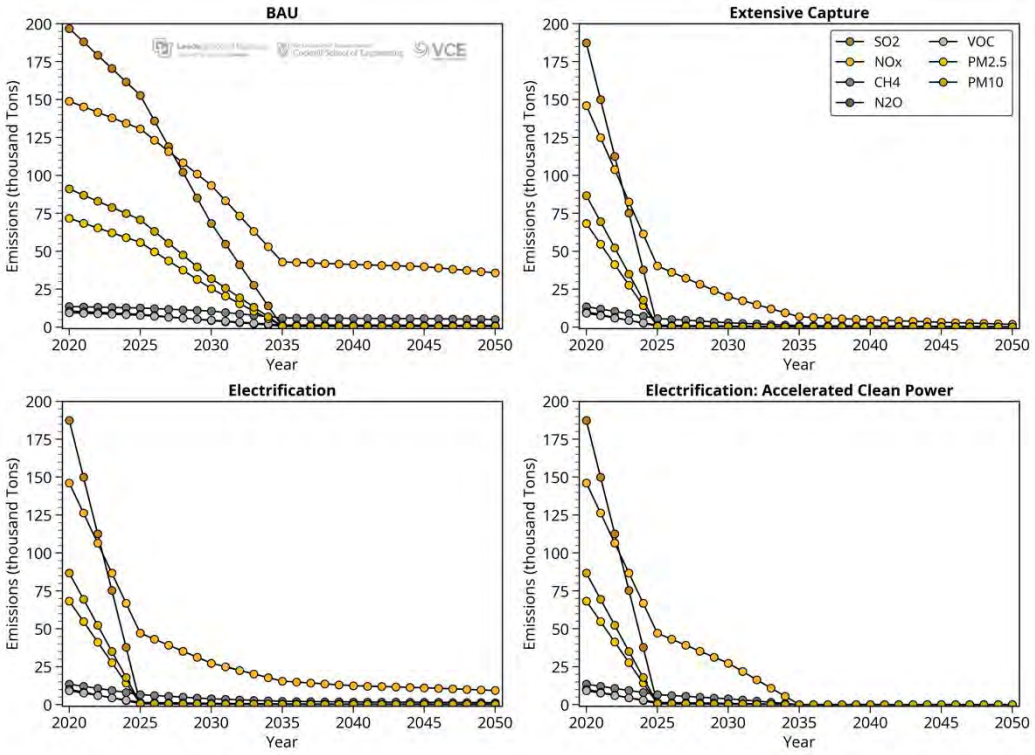

Figure 2.18: Emissions from other criteria pollutants tracked by WIS:dom-P.

2.5 Transmission Buildout

As discussed in Section 1.2, WIS:dom-P is initialized using the generation existing in 2018 along with the transmission topology. WIS:dom-P then determines the initial transmission required to meet load constrained by existing generators and existing transmission paths. As the model progresses through the investment periods, WIS:dom-P adds to the existing transmission as required for optimal capacity expansion and dispatch. All transmission added is modeled as new builds, therefore actual transmission costs can be lower than modeled if existing transmission pathways can be upgraded. The incremental inter-region transmission added over the investment periods in Texas for the scenarios modeled is shown in Fig. 2.19.

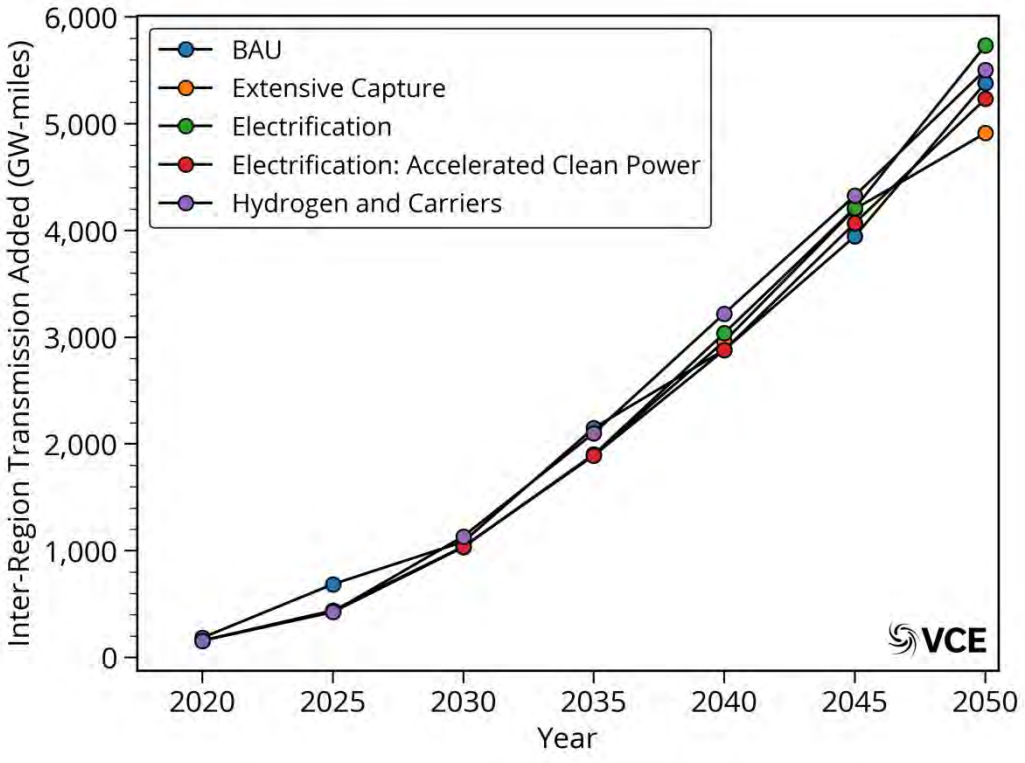

Figure 2.19: Incremental inter-region transmission added over the investment periods.

As seen from Fig. 2.19, inter-region transmission buildout in all scenarios follow a similar trend and there is only a 10% difference in total transmission added in all scenarios by 2050. The lowest inter-region transmission buildout occurs in the "Extensive Capture" scenario while the largest inter-region transmission buildout occurs in the "Electrification" scenario. Inter-region transmission buildout occurs from the High Plains region to the Northwest region and Metroplex region to bring the wind generation that is built in the Texas panhandle to the Northwest and Metroplex regions. Transmission is also built connecting the Gulf Coast, Central and Capital regions to bring power from the Capital and Central regions to the Gulf Coast where there is a large load center at Houston.

The in-region transmission built in Texas in the scenarios modeled is shown in Fig. 2.20. The "BAU" scenario adds the least amount of transmission adding 5,729 GW-miles of new transmission by 2050. The "Extensive Capture" scenario adds the highest amount of new transmission (32,974 GW-miles) as this scenario installs the most generation to power the DAC units. The "Hydrogen and Carriers" scenario adds the next highest amount of transmission at 23,233 GW-miles to connect new VRE generation added to the electrified load and hydrogen and synthetic fuel manufacturing facilities. The two electrification scenarios install approximately the same amount of transmission at 19,000 GW-miles as VRE generation is added to meet electrified loads as well as power DAC units installed to remove excess emissions.

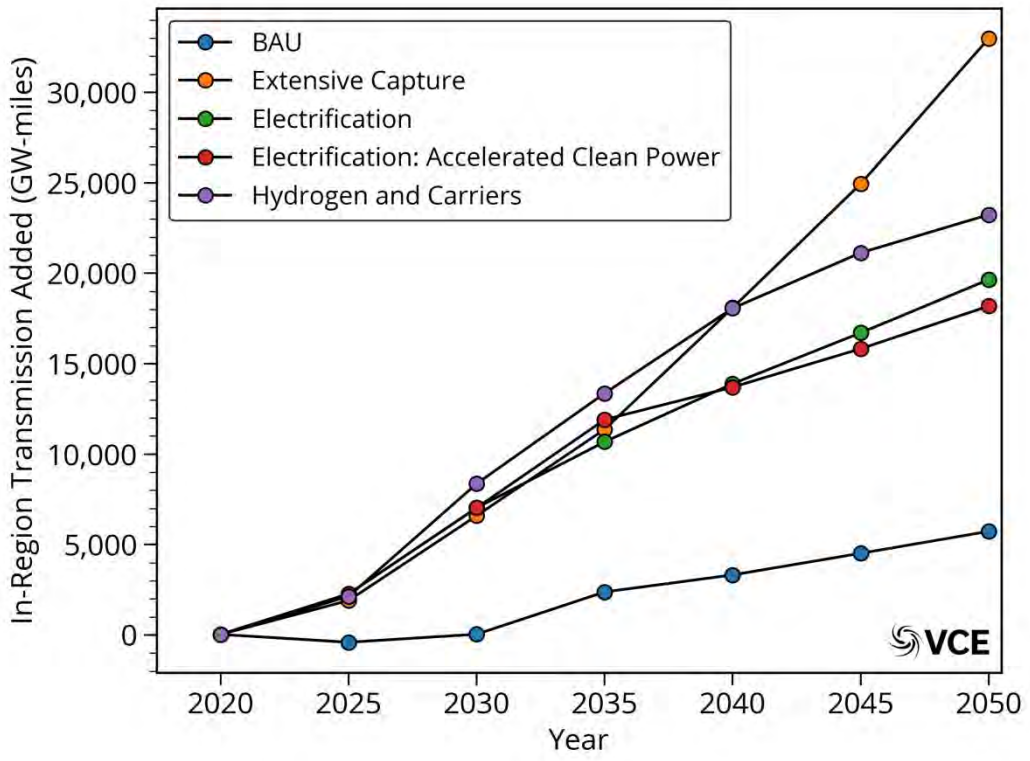

Figure 2.20: Incremental in-region transmission and spur lines added in Texas over the investment periods.

2.6 Reliability and Resource Adequacy

WIS:dom-P ensures reliability by making sure that the installed capacity in each investment period can meet demand along with a 7% load following reserve without fail at each time period (every hour for this study). Resource adequacy is ensured by meeting the North American Electric Reliability Council (NERC) specified unforced capacity (UCAP) Planning Reserve Margins (PRM) for each balancing area modeled. UCAP represents the capacity available at a given time taking into account the generator's forced outage rate. The modeled forced outage rates for thermal generators are given in Table 2.1.

WIS:dom-P models the reliability and resource adequacy as part of the capacity expansion process. As a result of including reliability and resource adequacy as part of the capacity expansion, WIS:dom-P ensures that at every timestep, the sum of expected generation from VREs and the unforced capacity for thermal units is greater than the load plus the PRM for the balancing region in question, while ensuring that there is enough generation at each timestep to meet load plus an additional 7% load following reserve. Thus, in addition to choosing sites with best capacity factors and correlation to load, WIS:dom-P also has to consider the impact on the grid when the generation from VREs is low or non-existent. As a result, WIS:dom-P ensures that even for periods of low or zero VRE generation, the PRM requirements are met for each balancing region. This overcomes limitations of traditional methods that assume a single (or seasonal) capacity value

for VRE generators. More details on how the model handles reliability and resource adequacy is described in WIS:dom-P technical documentation Section 3.14).[14]

Table 2.1: Unforced capacity fractions for thermal generators

Generator	Coal	NGCC	NGCT	Nuclear	Hydro	Geo	CCS	SMR	MSR
UCAP	87.7%	86%	85.3%	90.3%	89.5%	89.1%	86%	95%	95%

In order to express reliability using the traditional reliability metrics, the WIS:dom-P software outputs can be post-processed to determine these values. One of the commonly used reliability metrics is the Equivalent Load Carrying Capacity (ELCC). ELCC is determined by calculating the additional load that the system can carry due to the addition of a VRE generator while maintaining the same loss of load probability as before the VRE generator was added. Figure 2.21 shows the ELCC of wind, solar and storage over the investment periods for the "BAU" scenario. In 2020, solar has an ELCC of 100% due to only small levels of solar deployed on the Texas grid. As more solar is added over the investment periods, the ELCC of solar reduces steadily, except for a peak in 2035 as a result of increased load and fossil fuel generation retirements. The ELCC of solar settles at 27% by 2050.

Wind generation starts with a high ELCC of approximately 90% in 2020. The ELCC of wind falls in 2025 before rising again in 2030 due to the fossil fuel generation retirements that are replaced by wind generation. The ELCC of wind then continues to decline, settling at 50% in 2050. Storage starts out with lower ELCC values compared with wind or solar at 45% in 2020. However, as the Texas grid transforms from being fossil fuel dominated to VRE dominated by 2035, the ELCC of storage starts to increase and reaches 100% after 2035 since storage is the main dispatchable generation used by WIS:dom-P to meet load.

[14] https://vibrantcleanenergy.com/wp-content/uploads/2020/08/WISdomP-Model_Description(August2020).pdf

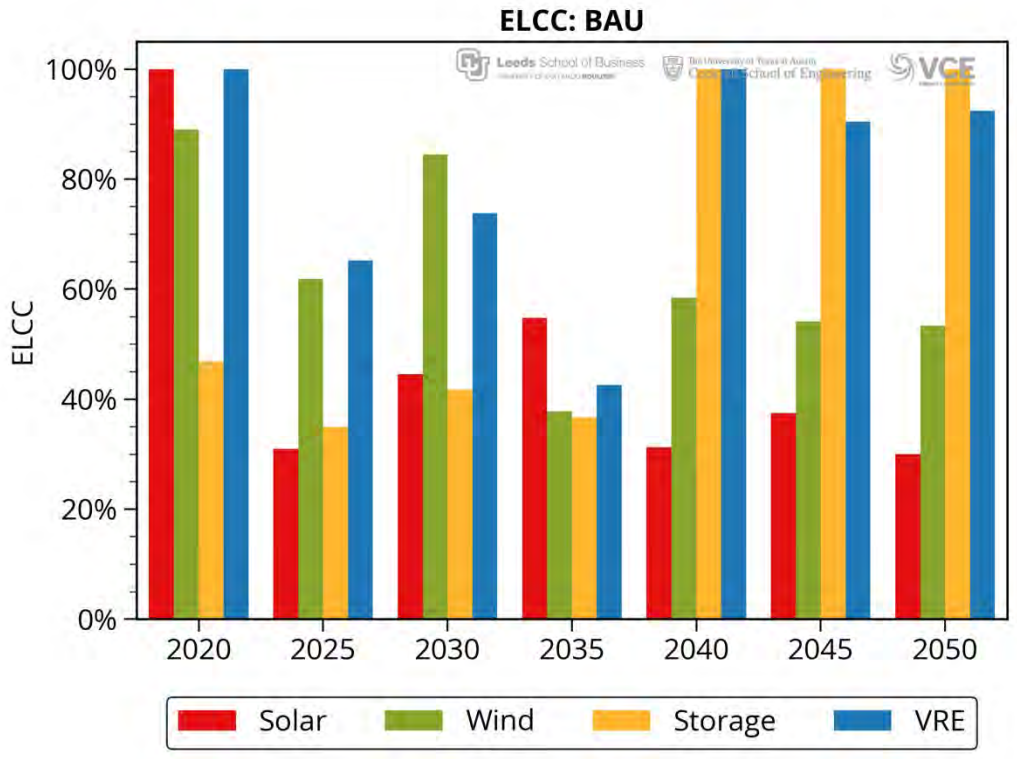

Figure 2.21: ELCC of wind, solar, storage and combined VRE system for the "BAU" scenario.

The ELCC of the VRE generation in the "Extensive Capture" and the "Hydrogen and Carriers" scenarios is shown in Fig. 2.22. The ELCC values in the two electrification scenarios are similar to that of the "Hydrogen and Carriers" scenario. In the "Extensive Capture" scenario, the ELCC of wind and solar initially reduces in 2025 and then rises to 100% by 2035 as the DAC units deployed make full use of all the wind and solar generation installed. In the "Hydrogen and Carriers" scenario, the ELCC of wind and solar hit 100% similar to the "Extensive Capture" scenario as the DAC units start to get installed. However, after 2035, only the wind remains at 100% while the solar ELCC drops as more solar generation is installed to meet electrified load. By 2050, the ELCC of wind generation also drops due to the large wind generation deployed to meet the electrified load in 2050.

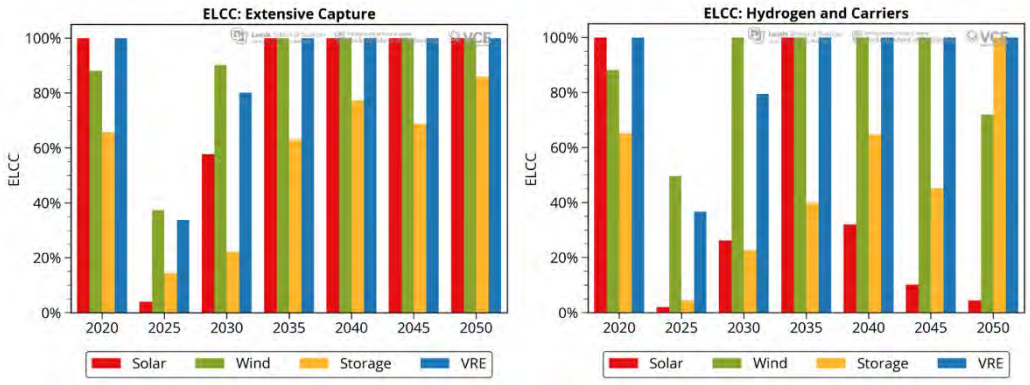

Figure 2.22: ELCC of wind, solar, storage and combined VRE system for the "Extensive Capture" (left) and "Hydrogen and Carriers" (right) scenario.

Another method to estimate capacity value is based on the role the VRE generation plays in meeting load during periods of highest demand. The capacity value is calculated as the reduction in net load during periods of peak demand as a fraction of installed VRE capacity. Figure 2.23 shows the capacity value calculated for the VRE generators during periods of peak demand. The capacity value of solar starts at 55% in 2020 and reduces slightly as more solar is added to the grid. However, the solar capacity value is seen to remain fairly constant from 2030 onwards as solar plays an important role in meeting daytime peak loads that occur in summer.

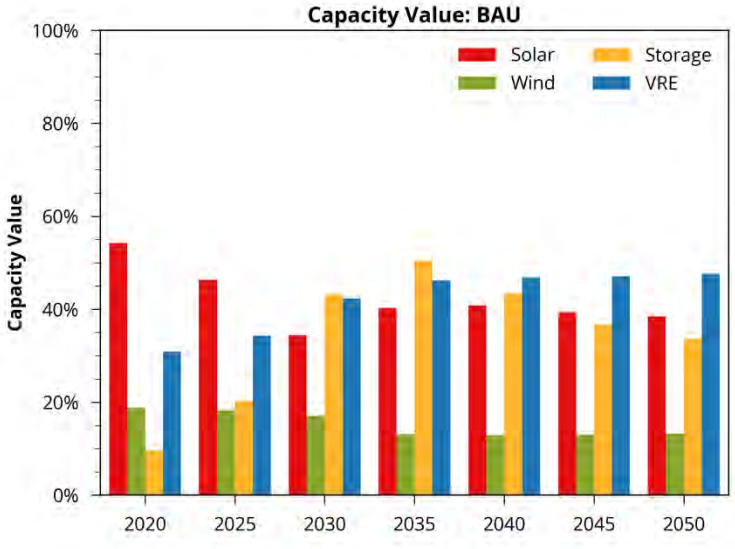

Figure 2.23: Capacity value of VREs calculated based on contribution during periods of peak demand.

The capacity value of wind calculated at periods of peak demand, starts at 19% in 2020. As more wind generation is added to the grid, the capacity value of wind reduces to 15% by 2030 where it remains constant until 2050. Wind has a lower capacity value compared to solar as its generation is lower during the peak load hours in summer and in winter it needs storage to help meet load during peak load hours.

The storage capacity value starts at 10% in 2020 and steadily increases reaching a peak of 50% in 2035 as a large amount of fossil fuel generation is retired resulting in storage becoming an important source of dispatchable generation. The capacity value of storage reduces slightly after 2035 reaching 35% in 2050 as WIS:dom-P installs more DPV generation to help meet summer peak loads.

The capacity value for the "Extensive Capture" and "Hydrogen and Carriers" scenarios is shown in Fig. 2.24. The capacity values of wind and solar show almost opposite trends in these scenarios compared to the "BAU" scenario and the capacity value of wind increases over the investment periods while the capacity value of solar reduces. The reason for this is that the decarbonization scenarios have large flexible loads such as DAC in the "Extensive Capture" scenario and combination of DAC, hydrogen production and synthetic fuel production in the "Hydrogen and Carriers" scenario. These loads operate at their highest when the VRE generation is at its highest as the marginal prices are at their lowest which coincides well with the wind generation. As a result, the wind generation shows a higher capacity value while the solar generation shows a lower capacity value when calculated using this method.

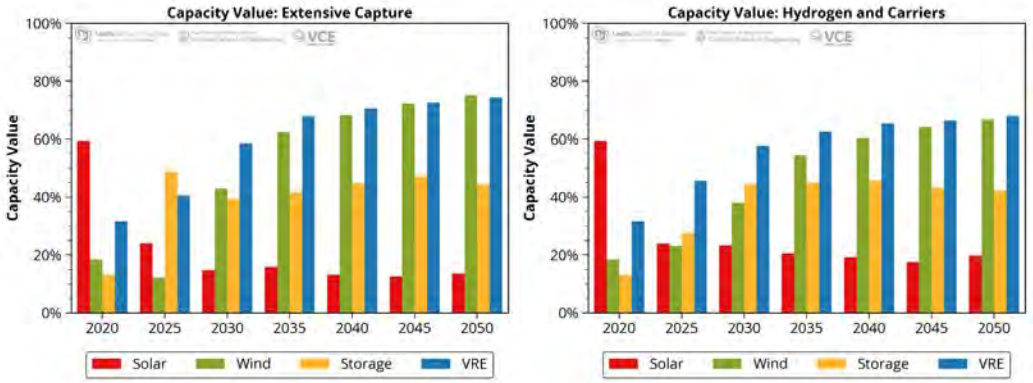

Figure 2.24: Capacity value of VREs calculated based on contribution during periods of peak demand for the "Extensive Capture" scenario (left) and "Hydrogen and Carriers" scenario (right)

VRE generation shows seasonal trends as discussed in previous sections and therefore their capacity value is also expected to show seasonal characteristics. Figure 2.25 shows the monthly average daily capacity value of the VRE generators calculated at the daily peak load timestep. The solar capacity value peaks during the summer due to the higher solar generation during this time of the year. However, the solar capacity value never exceeds the wind capacity value in summer as although solar generation is higher in summer, the wind generation plays a more important role in meeting load due to the timing of the peak load which occurs in the morning period.

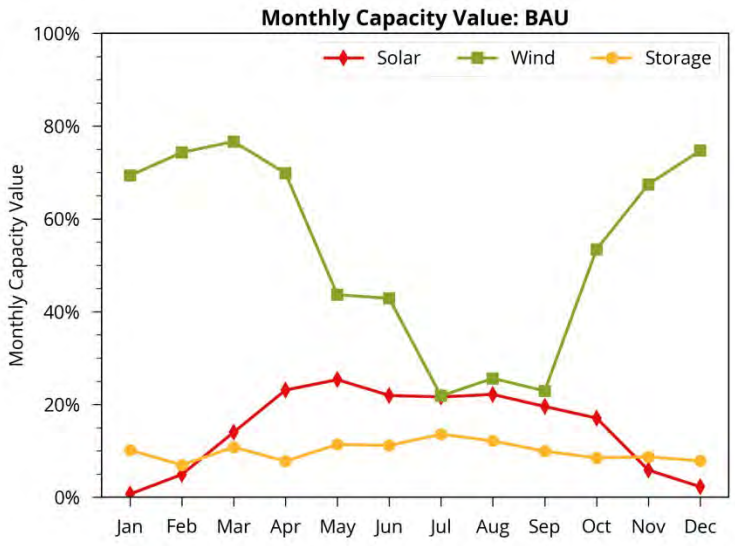

Figure 2.25: Monthly average capacity values in 2050 for Texas.

Wind monthly capacity value is higher in the winter as wind generation is higher in the winter and better correlated with wind peak loads. While wind generation is lower in the summer, it still plays a more dominant role during the peak load hours in summer and hence maintains a higher capacity value compared to solar. Storage has a near constant capacity value of between 10% - 15% over the course of the year as some storage is always dispatched during periods of peak load throughout the year.

The monthly capacity values for the "Extensive Capture" and "Hydrogen and Carriers" scenarios are shown in Fig. 2.26. As seen from Fig. 2.26, wind generation has an almost 100% capacity value in all the decarbonization scenarios over the year by 2050. The reason for this is that in the decarbonization scenarios, the load from the DAC units in the "Extensive Capture" scenario and load from a combination of DAC units, hydrogen production and synthetic fuel production is the largest load and is at its highest when the wind production is at its highest. Hence, the monthly capacity value of wind remains high throughout the year, while the capacity value of solar and storage are low as their generation is lower during this time of the day.

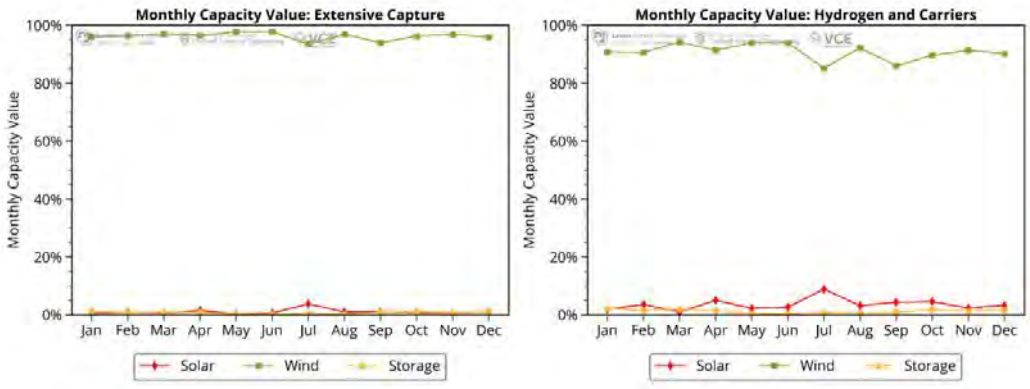

Figure 2.26: Monthly average capacity values in 2050 in the "Extensive Capture" scenario (left) and "Hydrogen and Carriers" scenario (right).

2.7 Siting of Generators (3-km)

WIS:dom-P uses weather datasets spanning multiple years at 3-km spatial resolution and 5-min temporal over the contiguous United States. WIS:dom-P performs an optimal siting of generators on the 3-km HRRR model grid. The existing generator layout reduced to a 3-km resolution along with the transmission paths above 115 kV is shown in Fig. 2.27. The grid is largely composed of fossil fuel generation in 2018 along with some wind and solar generation. Most of the wind generation is located in the Texas panhandle due to the higher capacity factors in that region. In addition, wind generation is also located along the gulf coast to take advantage of the diurnal sea-breeze that results in higher wind generation during the evening periods that coincides with load peaks.

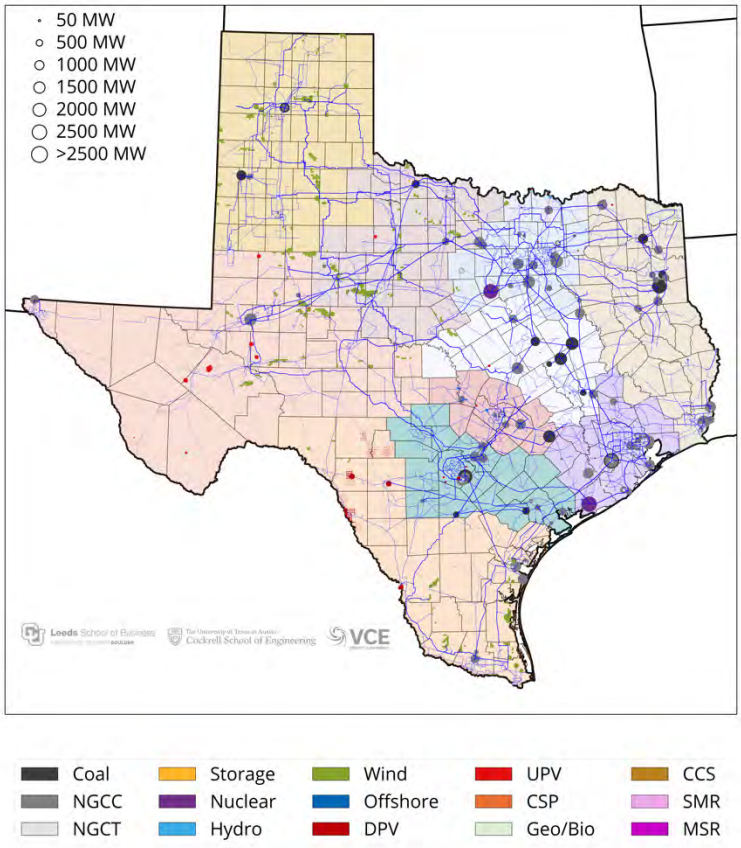

Figure 2.27: Installed generation layout in 2018 at 3-km resolution along with transmission paths above 115 kV.

Figure 2.28 shows the 3-km siting of the generation in 2050 in Texas for the a) "BAU", b) "Extensive Capture", c) "Electrification" and d) "Electrification: Accelerated Clean Power" scenarios. In all scenarios, the Texas grid is transformed from being fossil fuel dominated to VRE dominated. New wind capacity is prominent and wind generation is spread throughout the state to take advantage of the geographic diversity, which results in a more complementary generation profile in addition to generating more energy near the load centers. Significant wind is deployed consistently to the Texas panhandle, central Texas and the gulf coast as these regions have high wind capacity factors. Wind also gets deployed in the Northwest and West regions to take advantage of diverse generation profiles. Further, significant DPV is deployed in the Metroplex and Gulf Coast region as these regions have large load centers (Dallas and Houston respectively) and, thus, the DPV generation helps alleviate transmission congestion that routinely occurs in moving energy to these regions. It is apparent in Fig. 2.28, that "Extensive Capture" builds the most capacity by 2050 and relies heavily on wind to support the DACS demand. The general locations of the VRE technologies in the "Extensive Capture" scenario versus "BAU" are similar. In "Extensive Capture", more storage is built for firm generation over natural gas and shows up nearer the population centers of Houston, Austin and Dallas. Advanced nuclear power plants are built in the southeast portion of Texas.

The "Electrification" pathway has more generation installed than the "BAU" with more wind and solar across the state. Solar, in this case, favors the San Antonio, Austin and Houston areas since advanced nuclear is added nearer to Dallas. Both nuclear and advanced SMR nuclear are deployed more with the model choosing a new nuclear site near Dallas and the rest mainly being favored around the Gulf Coast region in this scenario. The "Electrification: Accelerated Clean Power" sees the most amount of solar built out of all the pathways discussed since other VRE technologies cannot be built fast enough for the aggressive 2035 decarbonization goal. As such, less wind is built in this scenario compared with the "Electrification". Increased amounts of nuclear and advanced nuclear technologies are also observed around Houston and Dallas. An SMR unit replaces a natural gas CC unit near El Paso. Enhanced geothermal is also built in southeast Texas to help reach the 2035 decarbonization goal. This provides dispatchable, clean generation to complement the large number of renewables facilities being built in this scenario.

All scenarios in Fig. 2.28 had the capability to install the Direct Air Capture except the counter-factual "BAU". This technology is currently in research and could be installed almost anywhere. Spatially, more DACs are assigned to counties with more generation. With this, DACs and wind are often co-located in future years. This is also true from a dispatch perspective where DACs electric load is used as a balance against the variability of the wind generation. VCE used the current oil and gas well infrastructure as a place to install these technologies starting at the center of a county and building out. The capacity at each well is capped according to the size requirements of DACs facilities. Where oil wells are sparse within a county, capacity will be split between well locations available and the capacity will be shown as larger than the space requirements. This is prominent in certain counties of the High Plains economic region.

The "Extensive Capture" scenario sees the most DACs installed across Texas. This signifies the amount of DACS needed to remove enough carbon dioxide for the state to be net-zero by 2050. The rest of the economy is not constrained to any emissions requirements and thus can operate as usual. DACs will be there to clean all carbon dioxide up. Far less DACs are observed in the "Electrification" and "Electrification: Accelerated Clean Power" scenarios. DACs installations are most prominent in the High Plains, Northwest, Central and Metroplex economic regions. This generally aligns with the deployment of wind.

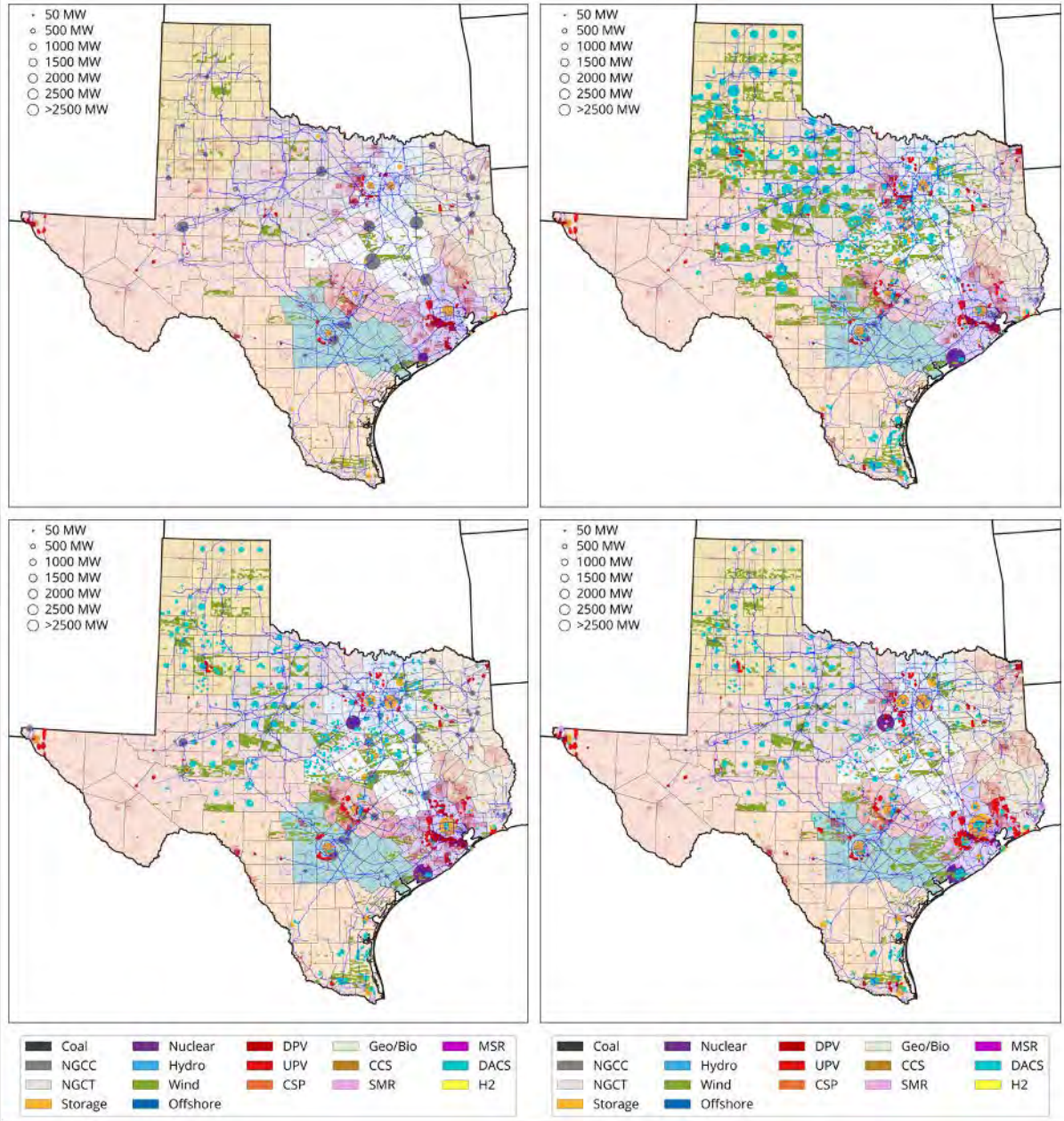

Figure 2.28: Installed generation layout in 2050 for the a) "BAU", b) "Extensive Capture", c) "Electrification" and d) "Electrification: Accelerated Clean Power" scenarios at 3-km resolution along with transmission paths above 115 kV. No more than 1.2% of any county land is covered by wind turbines.

In the "BAU" scenario, as a result of co-optimization of the distribution system, the grid is composed of almost equal parts of utility-scale solar and distribution-scale solar PV. For the other three scenarios, DPV remains similar in 2050 capacity buildout to the "BAU" scenario and UPV throttles to support the increased economy-wide load and emissions reduction. In the "Electrification: Accelerated Clean Power" pathway, the amount of UPV installed is almost four times higher than the "BAU" as the aggressive emissions goals have to be met and solar is used

to do so. In all scenarios, almost all the DPV generation is concentrated in the load centers such as Dallas, Fort Worth, Houston, Austin and San Antonio with small installations in smaller cities such as Lubbock. The UPV generation on the other hand is located outside of these high population regions due to lack of space.

The "Hydrogen and Carriers" scenario in 2050 is shown in Fig. 2.29. Hydrogen electrolyzers are sited to locations that have water since that is fundamentally needed for production of this fuel. Where possible, this technology will spatially align with retired thermal units (Coal, Natural Gas GT and Nuclear) within each respective county. The max capacity of the electrolyzers was also determined by the size requirements of the system. The Panhandle region has the most Hydrogen development by 2050. Wind fills out in similar ways in this scenario as does the solar around the larger city centers.

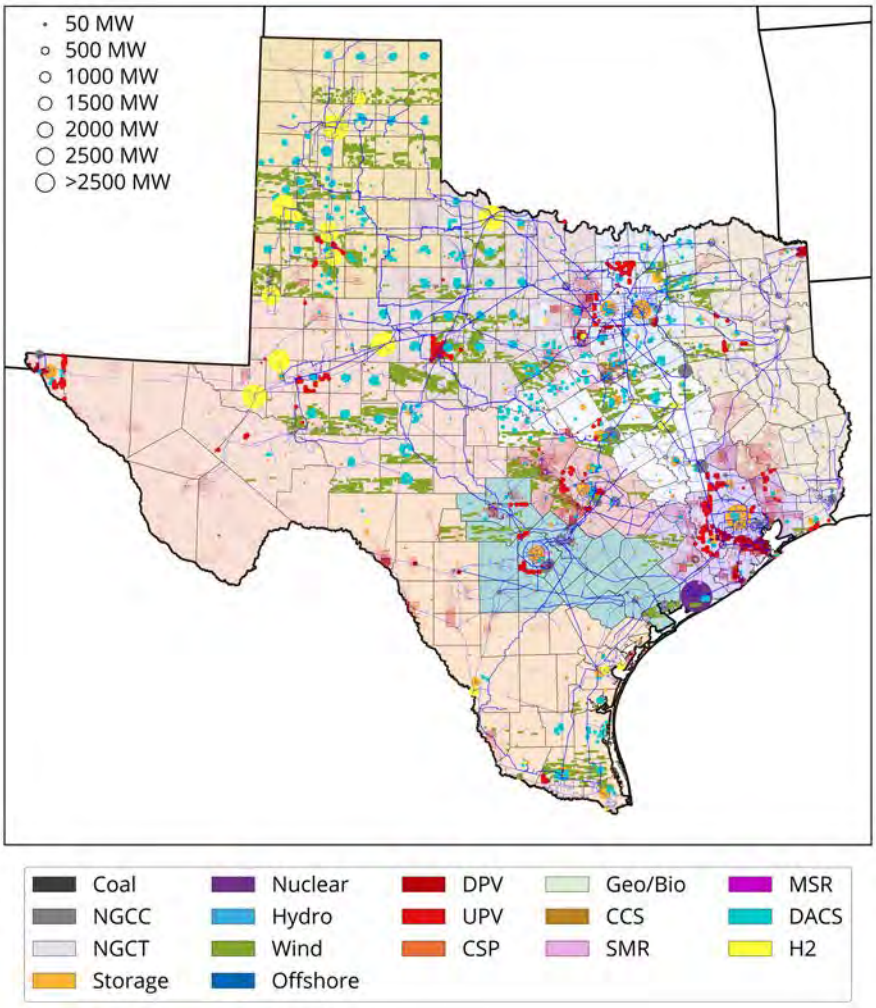

Figure 2.29: Installed generation layout in 2050 for the "Hydrogen and Carriers" scenario at 3-km resolution along with transmission paths above 115 kV. No more than 1.2% of any county land is covered by wind turbines. No more than 1.2% of any county land is covered by wind turbines.

Figure 2.30 shows the spatial potential layout for production of novel fuel technologies from the "Hydrogen and Carriers" scenario. These are co-located with Hydrogen facilities as Hydrogen is the base for all novel chemical fuel production. These can be produced for electricity production, stored or used in further iterations of novel chemical fuel production. The peak production values are charted.

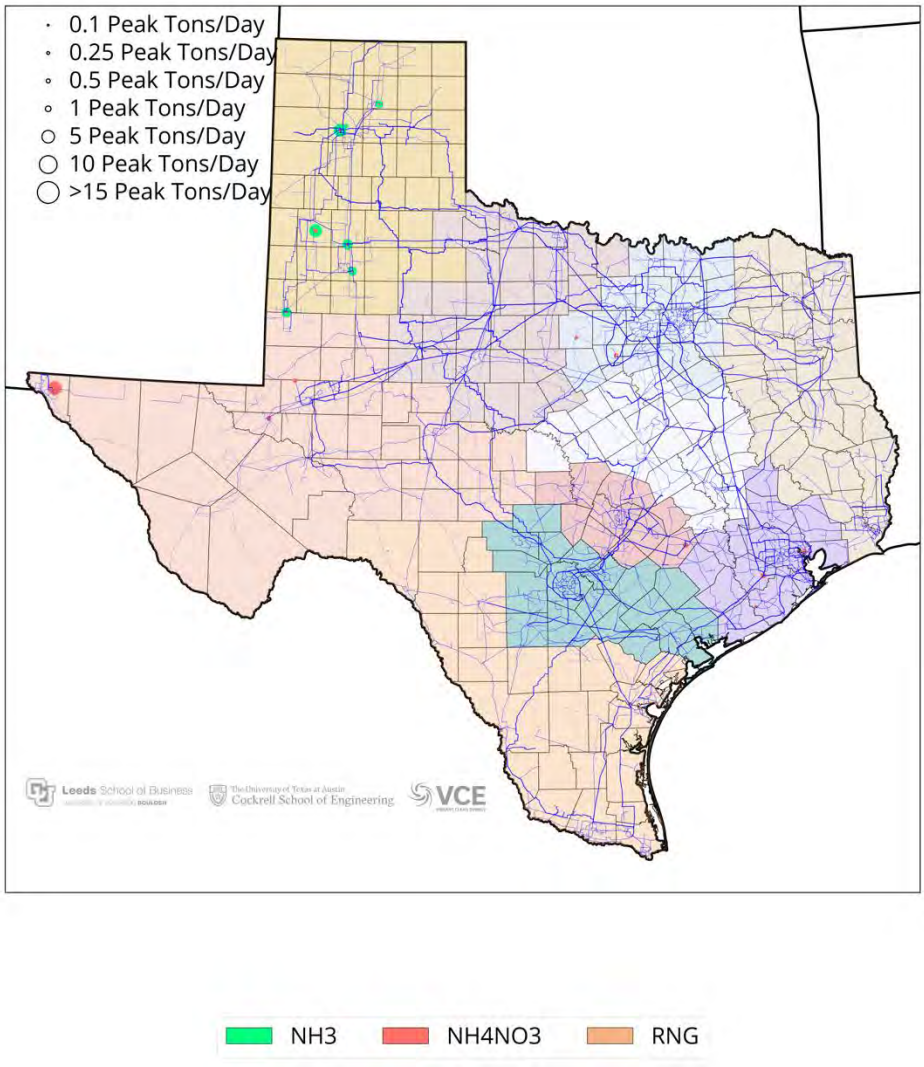

Figure 2.30: Novel fuel production layout in 2050 for the "Hydrogen and Carriers" scenario at 3-km resolution along with transmission paths above 115 kV.

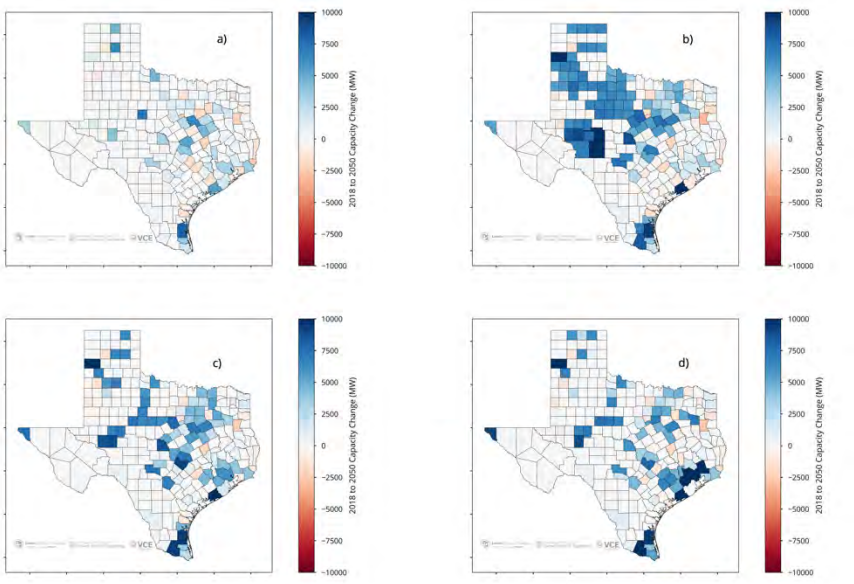

Figure 2.31: Total installed capacity change from 2018 to 2050 by county for the a) "BAU", b) "Extensive Capture", c) "Electrification" and d) "Electrification: Accelerated Clean Power". This does not include DACs or Hydrogen, only conventional and advanced generators.

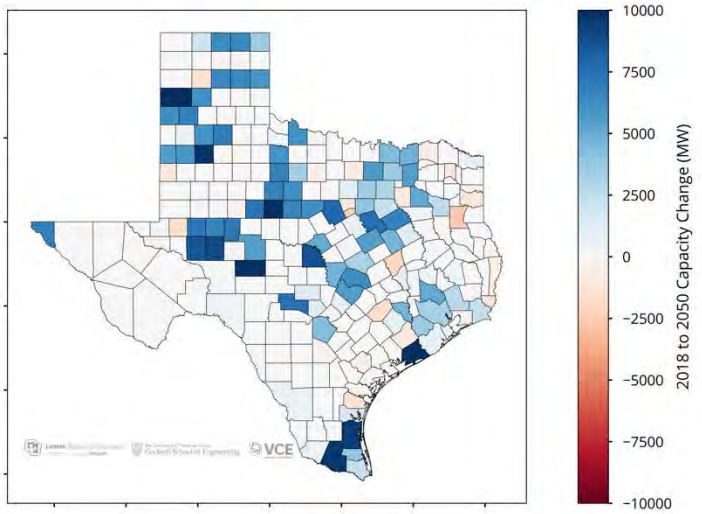

Figure 2.32: Total installed capacity change from 2018 to 2050 by county for the "Hydrogen and Carriers" scenario. This does not include DACs or Hydrogen, only conventional and advanced generators.

Figure 2.31 shows the total installed capacity difference by county between the first and last investment period considered (2018 and 2050, respectively). Figure 2.32 shows this for the

"Hydrogen and Carriers" scenario. Blue shades show counties that saw increased generator capacity. Shades of red show counties that saw decreased capacity by the end of the model runs. All pathways observe more counties with increased capacity than counties with decreased capacity. The spatial spread of increased capacity is mostly due to wind and solar technologies. Many counties, regardless of the scenario, observe an increase in generation. These counties are often encompassing or neighboring larger population centers where wind and solar can be built nearby. Examples of this are Carson County east of Amarillo, El Paso County in the west, Kennedy, Willacy and Cameron County in the southern tip of Texas and several counties surrounding Austin, Dallas and Houston. Often larger thermal plants are replaced with other technologies so the net capacity change is still positive even with plant retirements. Further, counties which saw a consistent decrease in capacity was due to the reduction of thermal generation in those regions. Examples of this are Amarillo County, Rusk County east of Dallas and Orange County along the southeastern border. However, neighboring areas to these counties often observed increased capacity.

When making the siting decisions the model takes into account several criteria to determine the optimal siting for the generators. In addition to taking into account expected generation and distance from the load, the model ensures that generation is not sited in unsuitable locations. The criteria used to filter out unsuitable locations for VRE generation are discussed in Section 3.2. In addition, the model has to ensure that it does not exceed the technical potential of each grid 3-km grid cell. The technical potential for the various VRE technologies in each grid cell is determined by taking into account several factors such as population, land cover, terrain slope etc. Finally, each technology is limited by the maximum packing density allowed to ensure that the generators do not hamper performance of other generators in the grid cell such as through wakes for wind turbines and excessive shading for solar panels. The details on these metrics and the available technical potential for the CONUS are discussed in greater detail in Section 3.2.

3 VCE Datasets & WIS:dom-P Inputs

3.1 Generator Input Dataset

VCE processed the Energy Information Administration annual data from 2018 to create the baseline input generator dataset for this study. From this dataset, information for Texas was obtained. The entire state of Texas includes 132.7 GW of installed capacity. WIS:dom has the ability to solve over such scales at 5-minute resolution for several years chronologically.

The WIS:dom-P generator input datasets are built upon the publicly available EIA 860 and EIA 923 data. The 2018 data is what was available for this study. VCE carries out several steps to align and aggregate technology types to the 3-km model grid space that matches the National Oceanic and Atmospheric Administration (NOAA) High-Resolution Rapid Refresh (HRRR). In the process, year-on-year changes were analyzed. Across the United States, general trends show (for fossil fuels) coal capacities falling with natural gas combined cycle growing. Wind, solar and storage plants are on the rise as well. The trend continues in the data throughout 2019 based upon the recently released EIA 860 annual data for that year.

Below, we outline the VCE process to prepare the generator input datasets:

1. Data is merged, aligned, and concatenated between the EIA 860 and EIA 923 data.

2. Initial quality control is applied to the data to ensure accuracy between datasets.

3. Align the location of the generators to the nearest 3-km HRRR cell. Care is taken to ensure the correct grid cell is chosen within state boundaries and water sites.

4. Aggregation of the generator types within each 3-km cell; e.g., multiple generators of the same fuel type are summed for capacity and capacity-weighted averaged are applied to operational parameters.

5. Further spatial verification is performed to ensure the output aligns with the original data.

6. Final model input format produced. A county level average of all generator types is also created.

VCE coordinates with the Catalyst Cooperative (https://catalyst.coop/), a company with the goal to help the energy research community by processing major publicly available sources into a format that is organized and stream-lined to use. This assists our processes and will allow it to become more rapid and frequent for these input datasets.

1	Coal
2	Natural Gas Combined Cycle
3	Natural Gas Combustion Turbine
4	Storage
5	Nuclear
6	Hydroelectric
7	Onshore Wind
8	Offshore Wind
9	Residential Solar
10	Utility-scale Solar
11	Concentrated Solar Power
12	Geothermal
13	Biomass
14	Other Natural Gas
15	Other Generation
16	Natural Gas - CCS
17	Pumped Hydro Storage
18	Small Modular Reactors
19	Molten Salts

Figure 3.1: The VCE input generator technology bins.

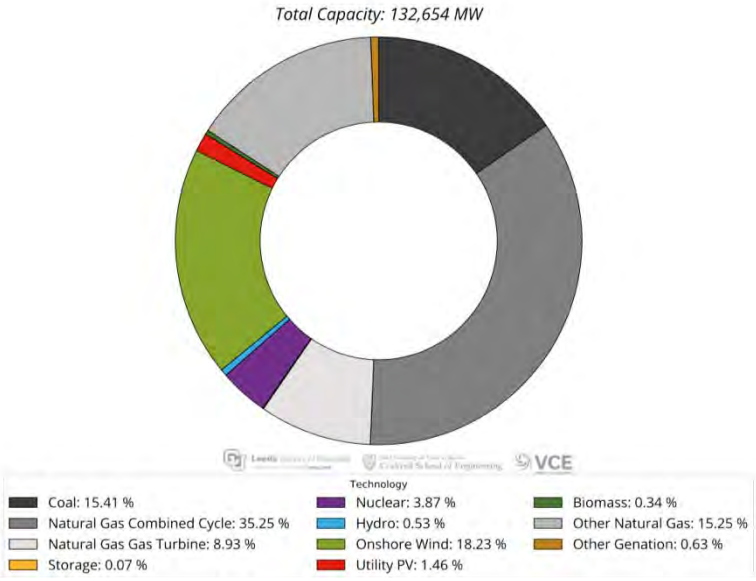

Figure 3.2: WIS:dom estimated installed capacity for Texas. The total capacity modeled for this region is 132.7 GW.

Figure 3.1 displays the generation technology types that are standard within the WIS:dom-P modeling. Figure 3.2 shows the installed capacities over the entire Texas footprint. Natural gas is the dominant technology across the state. Onshore wind capacity follows second behind natural gas, making up almost a fifth of the installed capacity. Coal is the third largest technology by installed capacity. A small amount of nuclear energy exists in Texas. Variable Renewable Energy (VRE) capacities for solar and hydro are relatively low. For comparison, the same chart is shown in Fig. 3.3 for all the installed capacity across the contiguous US. Note that across the contiguous US, the share of thermal generation is similar to that in Texas. There is also more coal and nuclear

in exchange for natural gas in Fig. 3.3 compared with Fig. 3.2. Further, solar and hydro VRE has more representation in the wider US than it does in Texas.

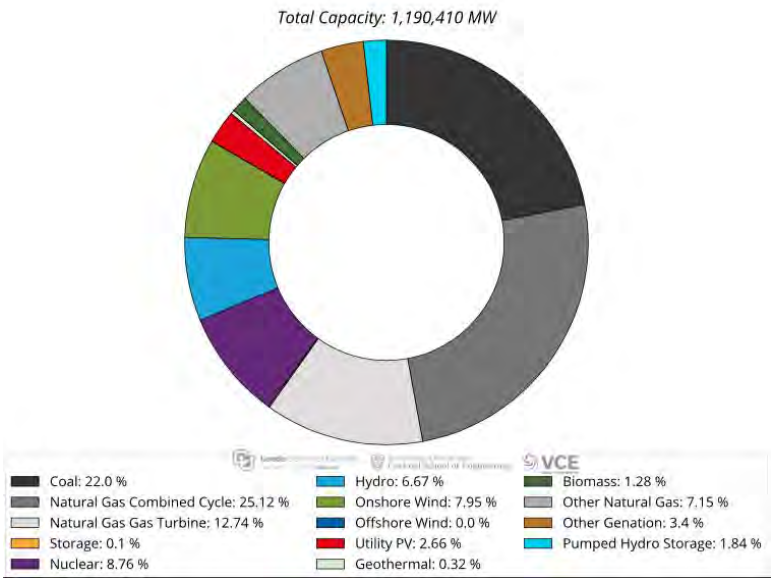

Figure 3.3: WIS:dom estimated capacity share for the contiguous United States. The total capacity modeled is 1,190 GW.

For this study, Texas was divided and modeled as economic regions.[15] This aligned WIS:dom-P output with ingest needed for REMI model runs. Two sets of regions were combined to create a total of ten economic regions that would be modeled for this study. Both Upper East and Southeast, as well as Upper Rio Grande and West regions were merged. Figure 3.4 shows the 2018 technology capacity stacked totals for each modeled economic region within Texas. Natural gas technologies have a presence in all economic regions, though it shows up the least in the Northwest region. Coal shows up most in the Central region. Nuclear power is installed in the Gulf Coast and Metroplex areas within the eastern half of the state. The Upper Rio Grande and West combined region has the highest amount of solar capacity. This makes sense as solar capacities are generally higher closer to the Desert Southwest of the United States. Hydro technology has the most presence in the Capital region where there are many waterways utilized to the west and northwest of Austin. The Northwest region holds the largest amount of installed wind capacity. However, the High Plains, South and Upper Rio Grande/West area come in close behind.

[15] https://comptroller.texas.gov/economy/economic-data/regions/2020/

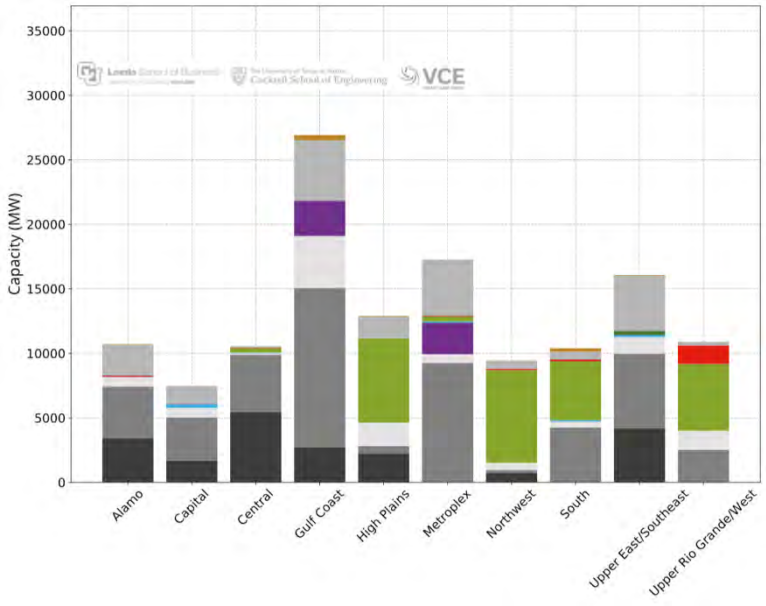

Figure 3.4: WIS:dom stacked capacity for the Texas economic regions used for this study. The Upper East and Southeast regions were grouped together, as were the Upper Rio Grande and West areas.

Figure 3.5 shows the technology layout spatially across Texas. Large natural gas plants are very prominent around the bigger metropolitan cities such as Houston, Austin and Dallas. Several coal plants are installed around the east central portion of Texas. In particular, a higher concentration of coal is noted between Waco, College Station and Crockett, Texas. Wind is the dominant technology of the Panhandle and northwestern Texas. Large solar installations are more common in southwest Texas. Many smaller utility-scale solar plants are also installed nearer the major population centers of Houston, San Antonio and north of Dallas. Hydro is most dense along the Colorado river to the northwest of Austin and along the Guadalupe River east of San Antonio.

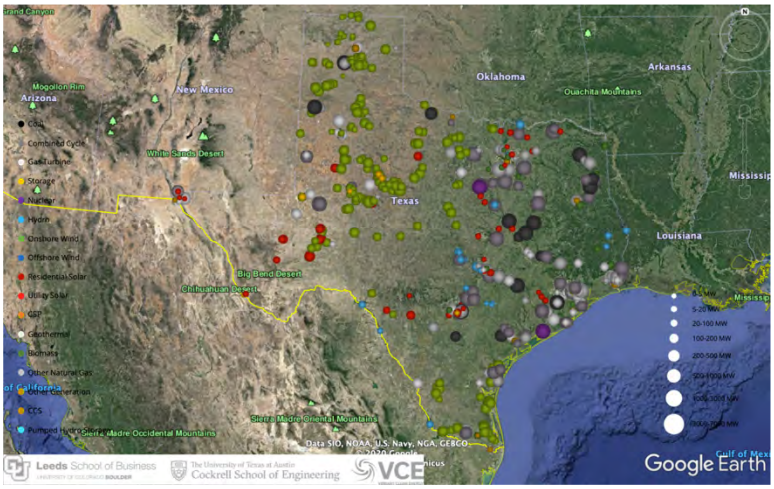

Figure 3.5: WIS:dom estimated location of various technologies for Texas.

3.2 Renewable Siting Potential Dataset

VCE performs an extensive screening procedure to determine the siting potential of new generators across the contiguous US. This ensures that the WIS:dom model has constraints on where it can build new generation. First, USGS land cover information is utilized as a base within each 3 km grid cell to determine what is there (Fig. 3.6 top left panel). The siting constraint information for onshore wind, offshore wind, utility-scale solar PV and distributed solar PV is displayed in the remaining three panels of Fig. 3.6. There is a zoomed view of Texas in Fig 3.7.

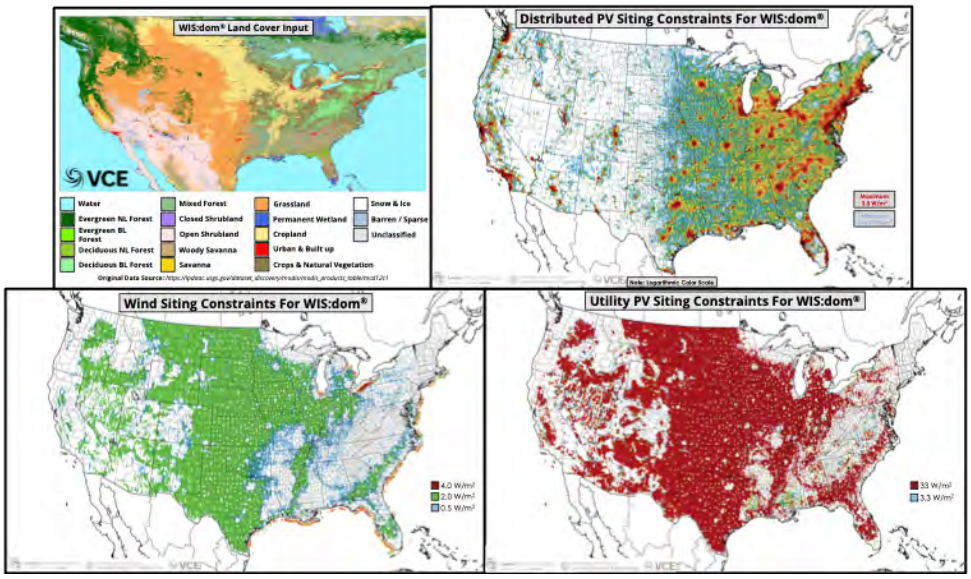

Figure 3.6: WIS:dom land cover (top left), distributed solar PV siting bounds (top right), utility-scale wind bounds (bottom right) and utility-scale solar PV (bottom right).

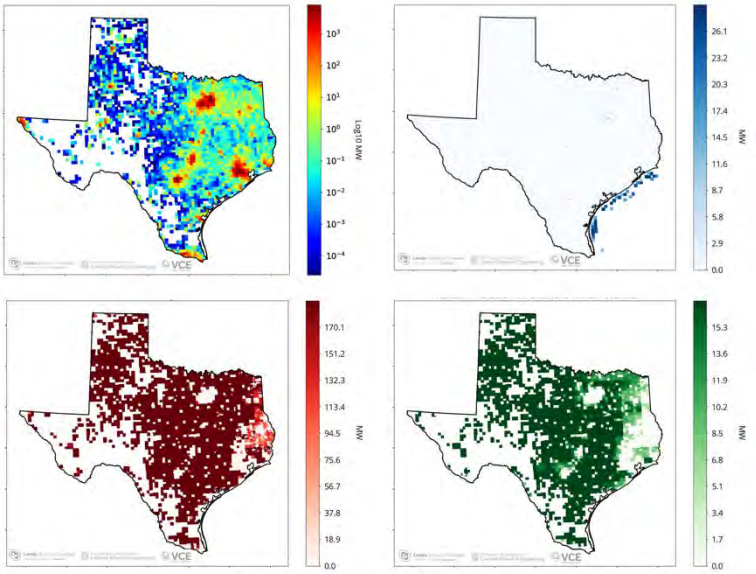

Figure 3.7: WIS:dom Rooftop Potential (top left), Offshore Wind Potential (top right), Utility-scale Solar Potential (bottom left) and Onshore Wind Potential (bottom right) in MW. The Distributed Solar Potential is converted to a Logarithmic Base 10 scale due to the ranges of value for that parameter. This is a closer look at Texas.

The first screening algorithm follows these steps:

1. Remove all sites that are not in appropriate land-use categories.
2. Remove all sites that have protected species.
3. Remove all protected lands; such as national parks, forests, etc.
4. Compute the slope, direction and soil type to determine its applicability to VRE installations.
5. Determine the land cost multipliers based on ownership type.
6. Remove military and other government regions that are prohibited.
7. Avoid radar zones and shipping lanes.
8. Avoid migration pathways of birds and other species.

The above, along with the knowledge of what is already built within a HRRR cell from the Generator Input data provides WIS:dom with a view of where it can technically build certain generators as well as certain technologies. Figure 3.6 also shows the siting constraints for wind, utility-scale solar PV and distributed solar PV.

For wind, utility-scale solar PV, distributed solar PV, and electric storage the available space is converted into capacity (MW & MWh) by assuming a density of the technologies. This is particularly important for wind and solar PV because of wake effects and shading effects, respectively. The maximum density of wind turbines within a model grid cell was restricted to no more than one per km^2 (< 4 MW / km^2). Solar PV was restricted to a maximum installed capacity of 33 MW per km^2. For storage, it is assumed that for a 4-hour battery the density is 250 MW / km^2. For all thermal generation, the density assumed for new build is 500 MW / km^2. Thus, for a 3-km grid cell the resulting maximum capacities (in the CONUS) are:

- Wind – 36 MW;
- Utility Solar PV – 297 MW;
- Distributed solar PV – 68 MW;
- Storage (4-hr) – 2,250 MW or 9,000 MWh;
- Thermal generators – 4,500 MW.

These densities and values also ensure that WIS:dom does not overbuild in a single grid cell because the combined space is constrained, as these numbers are maxima assuming only that technology exists.

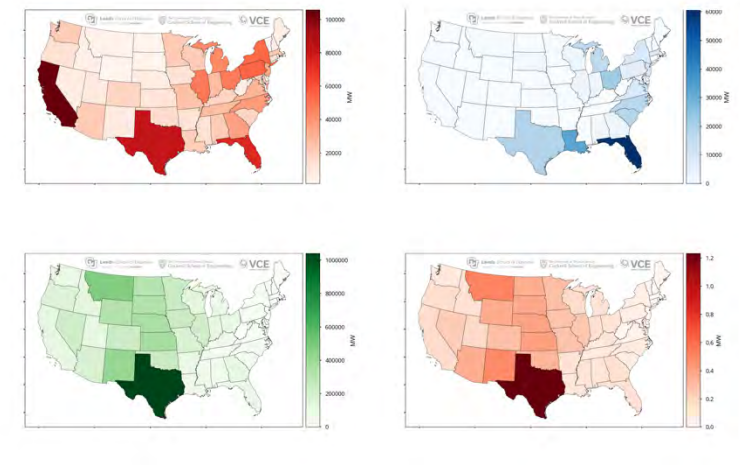

Figure 3.8: WIS:dom Total Sum Potential by state for Rooftop (top left), Offshore Wind (top right), Utility-scale Solar (bottom right) and Onshore Wind (bottom right) in MW.

The above (Fig. 3.8) shows the state sum of the land use potential for each variable resource across the United States. In onshore wind, distributed solar and utility solar, Texas has some of the highest potential in the country with its size and good weather resources. Offshore wind is also available with access to the Gulf Coast. Distributed solar potential is high in Texas with many large metropolitan areas available for rooftop setup. The onshore wind potential dwarfs the offshore wind potential for Texas. This speaks more to the amount of land and good onshore wind resources Texas has available. That said, offshore wind can still bring a considerable amount of capacity and support to the Texas grid. The amount of utility solar potential is the highest among

the VRE technologies considered. This strongly speaks to the ability of Texas to utilize the advantages of solar in addition to wind.

3.3 Standard Inputs

There is a standard suite of input data for the WIS:dom-P model that sets the stage for several base assumptions about the energy grid and generator technologies. This includes:

- Generator cost data (capital, fixed, variable, fuel);
- Generator lifetime terms;
- Standard generator heat rates;
- Transmission/Substation costs;
- Legislature in the energy sector:
- Renewable portfolio standards;
- Clean energy mandates;
- GHG emissions requirements;
- Storage and offshore mandates);
- PTC/ITC;
- Jobs for various technologies.

This is a list of the most commonly discussed standard inputs the model uses and are looked at in this document. The above list is not exclusive and much more information is ingested by WIS:dom-P to narrow down characteristics of various generation technologies. The list of standard files is continuously growing as the industry evolves. Additional inputs can be easily incorporated into WIS:dom-P. UT provided input and changes to several of these model parameters. This is discussed in detail below.

The standard inputs remain constant throughout the scenarios modeled for the study unless specifically requested to change. However, the standard inputs are changing within each scenario throughout each investment period modeled. The overnight capital, fixed O&M and variable O&M costs for each generator technology are based upon the NREL ATB values. The NREL values were chosen to be reputable values; are used by RTOs in their modeling; give high granularity and are updated frequently. The fuel costs are based from the EIA Annual Energy Outlook data, another source that is reputable and regularly updated. VCE provides fuel and capital costs multipliers by state to further tune the spatial layout of these standard cost inputs. Other standard inputs are a combination of VCE internal research and work with various partners in the industry.

These input assumptions are ingested into WIS:dom-P to provide insight and bounds to the optimization selections for each investment period. It offers the model a picture of what cost options are available to optimize.

The Low NREL ATB values from 2019 were used for capital, fixed and variable costs of all generator technologies.

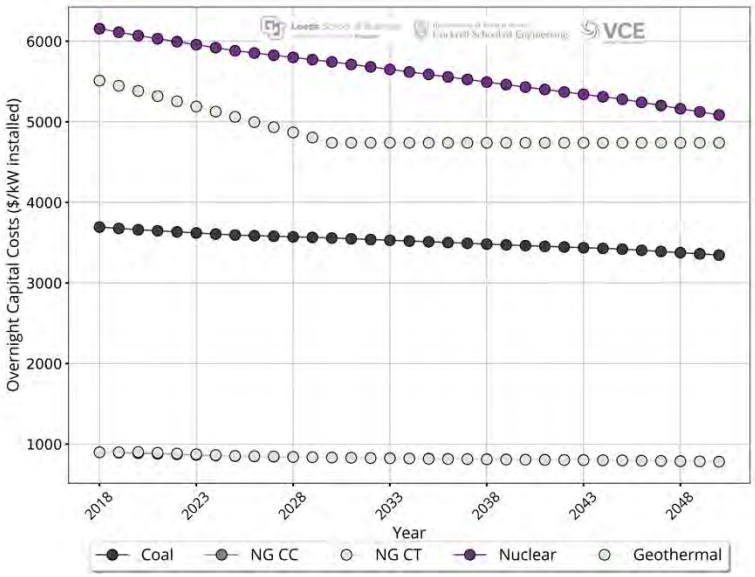

Figure 3.9: The overnight capital costs in real $/kW-installed for thermal power plants in WIS:dom-P. All costs are from NREL Low ATB 2019.

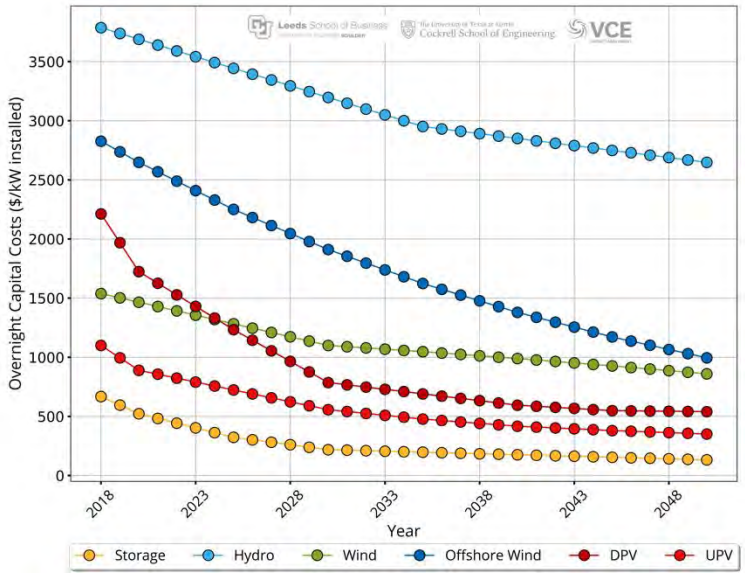

Figure 3.10: The overnight capital costs in real $/kW-installed for non-thermal power plants in WIS:dom-P. All costs are from NREL Low ATB 2019.

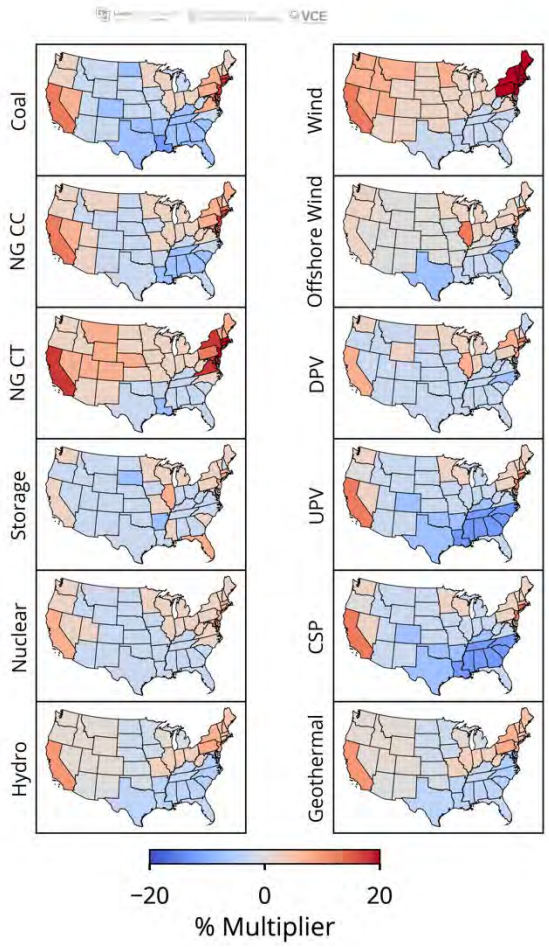

Figure 3.11: The WIS:dom-P Capital Cost Multiplier is shown by state for each technology across the US. Shades of red show where the capital cost is scaled higher by a given percentage. Cool shades show where technology capital costs in the model are scaled down by a given percentage.

Figure 3.11 shows that certain states and regions actually experience lower capital costs when building many technologies than the NREL ATB values. It is shown that Texas has lower capital costs for all generator technologies.

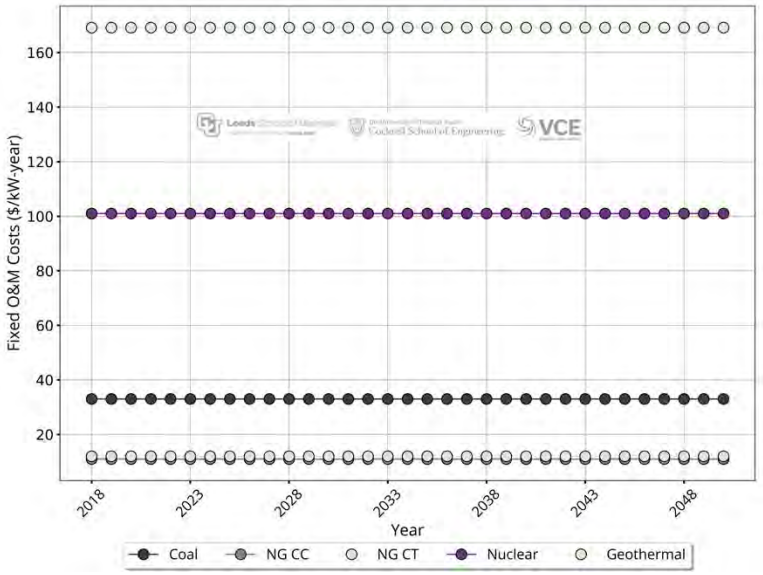

Figure 3.12: The fixed operations and maintenance (O&M) costs in real $/kW-yr for thermal power plants in WIS:dom-P. All fixed costs are from NREL Low ATB 2019.

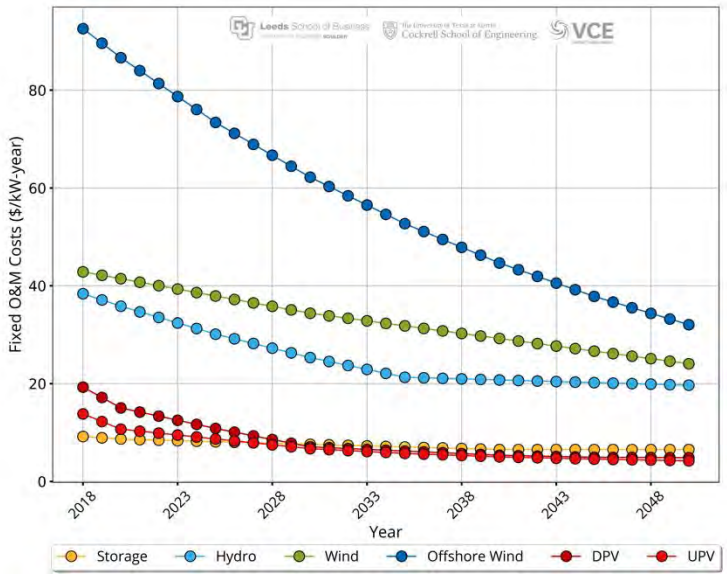

Figure 3.13: The fixed operations and maintenance (O&M) costs in real $/kW-yr for non-thermal power plants in WIS:dom-P. All fixed costs are from NREL Low ATB 2019, with the exception of storage costs, which were provided by Able Grid, Inc.

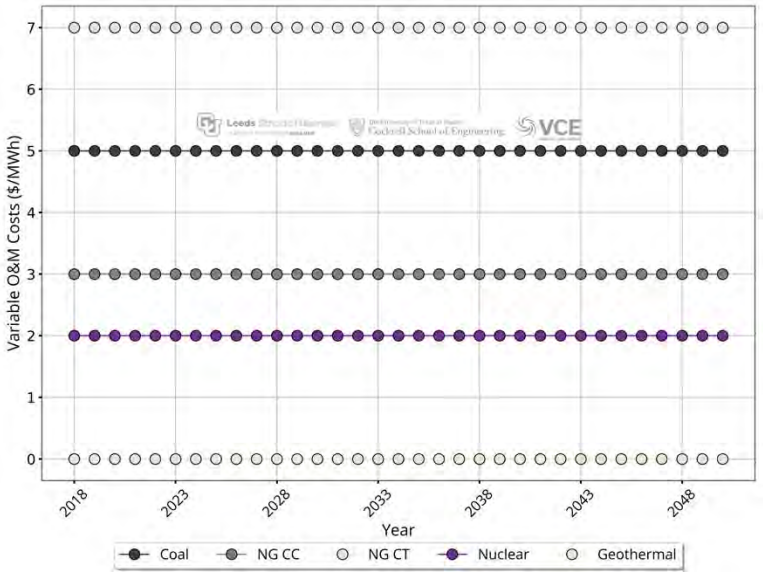

Figure 3.14: The non-fuel variable O&M costs for thermal generators in WIS:dom-P in real $/MWh. All variable costs are from NREL Low ATB 2019. The non-thermal units have zero variable O&M costs for renewables as those costs are combined into the fixed O&M costs.

Figure 3.15 shows the fuel costs of thermal technologies. These costs started from the 2019 EIA Annual Energy Outlook (AEO) model High Oil and Gas Supply Scenario. For this study, UT tuned the thermal fuel costs to Texas based on analysis of the various AEO fuel costs seen across Texas, regions within Texas and other southern states. WIS:dom-P input, by default, pulls the AEO fuel costs and NREL ATB values from the same year which was the case for this study.

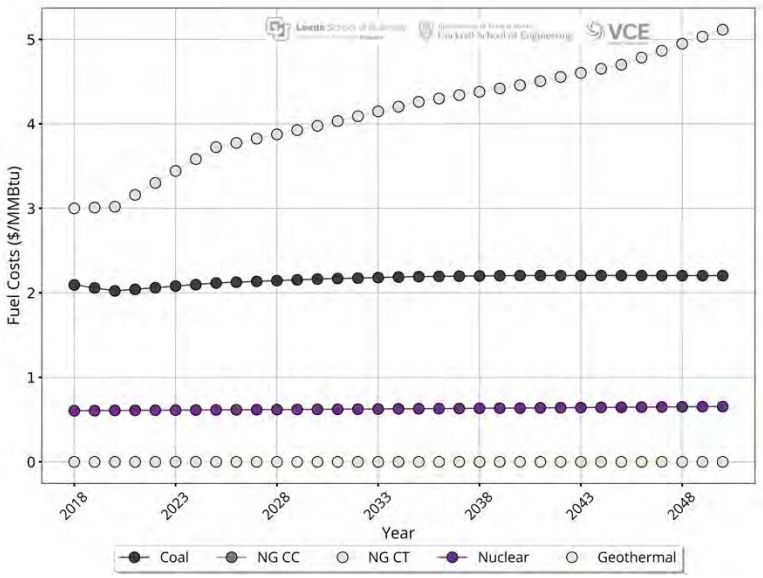

Figure 3.15: The fuel costs for thermal generators in WIS:dom-P in real $/MMBtu. All costs are from the 2019 EIA Annual Energy Outlook (High Oil and Gas Supply Scenario).

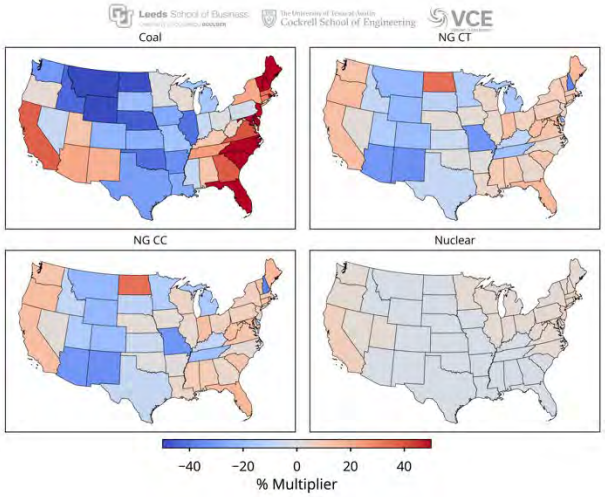

Figure 3.16: The WIS:dom-P Fuel Cost Multiplier is shown by state for each technology across the US. The color scale shows a percentage multiplier applied to standard fuel costs. Shades of red show where the fuel cost is scaled higher by a given percentage. Cool shades show where technology fuel costs in the model are scaled down a given percentage. Renewable fuels are not shown here as those fuel costs are the same no matter where the technology is and those fuel costs are null.

The previous Fig. 3.16 shows the spatial variations of fuel costs for thermal units (except geothermal since that cost is zero). Texas, in general, has a lower fuel cost for all types of thermal units considered.

Storage is one of the most discussed inputs. Storage can have highly variable cost input values depending on sources. It also is a heavy driver as to how the model handles renewables, transmission and future baseload. The following Fig. 3.17 shows the cost per kW ($/kw) versus the battery pack capital cost ($/kWh) from the 2019 NREL Low ATB costs for storage used in the scenarios for UT.

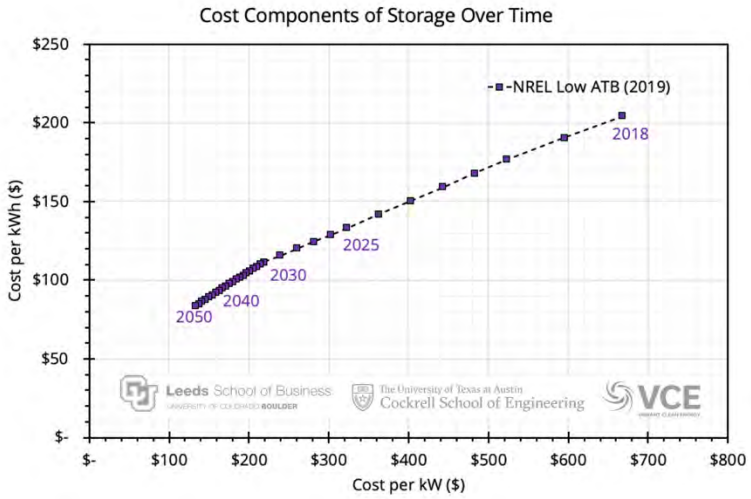

Figure 3.17: The Balance of System Capital Cost ($/kw) versus the Battery Pack Capital Cost ($/kWh). This is shown for the 2019 Low NREL ATB values in purple.

WIS:dom-P ingests generic heat rates for thermal technologies. These heat rates are internally calculated to provide a general idea of thermal technology performance. These heat rates are utilized for new thermal generation that is built over the investment periods. The heat rates for existing generation are tied to the data from the EIA 860 and EIA 923 data and are separate from the heat rates for new builds. UT provided updates to the heat rates used for new thermal generation within the model. What was normally used for heat rates in the 2050 investment period was applied to all investment periods. Ultimately, this lowered the heat rates of thermal generation both benefiting these technologies for earlier investment periods and aligning to values they observed in Texas. The heat rates used for this study can be seen in Fig. 3.18.

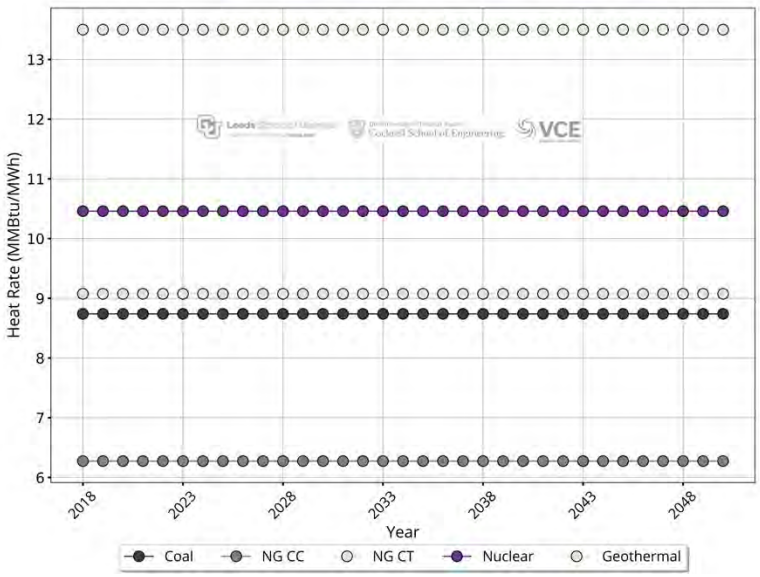

Figure 3.18: The generic heat rate for thermal generators in WIS:dom-P in MMBtu/MWh of electricity generated. Explicit heat rates for currently installed generators come into the model through the Input Generator Datasets and the EIA 860/923 data.

There are three typical advanced technologies that can be easily included in modeling scenarios. These include Natural Gas Carbon Capture Systems (CCS), Small Modular Reactors (SMR) and Molten Salt Reactors (MSR). Figure 3.18b shows the standard cost data for CCS and SMR technologies. The CCS costs are simply the costs from 2019 Low NREL ATB values. These costs reflect a natural gas plant with CCS, not the CCS unit alone. Variable costs for SMR units are rolled into other costs shown for this technology. The SMR cost values are created by VCE in conjunction with multiple industry partners. This study did not utilize the MSR advanced nuclear option.

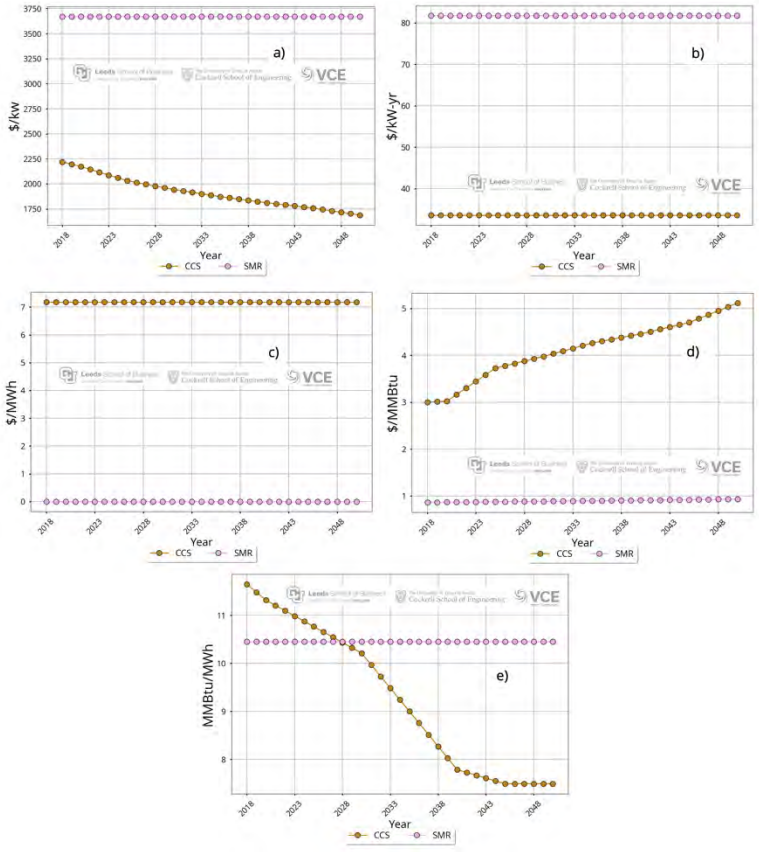

Figure 3.18b: The a) capital cost ($/kw), b) fixed cost ($/KW-yr), c) variable cost ($/MWh), d) fuel cost ($/MMBtu) and e) heat rate (MMBtu/MWh) for CCS and SMR technologies in WIS:dom-P. The variable costs for SMR plants are rolled into other costs shown here.

The CCS, SMR as well as Enhanced Geothermal Systems (EGS) were included in all scenarios except the "BAU" scenario. The MSR technology was determined by UT to be redundant to EGS and not deployed in this study. The EGS costs come from the 2019 Low NREL ATB values. They are shown in the costs of Fig. 3.9, Fig. 3.12, Fig. 3.14 and Fig. 3.15.

Direct Air Capture Systems (DACs) was a novel technology allowed to run in all scenarios apart from the "BAU". This technology captures carbon dioxide (CO_2) from the atmosphere using electrical demand from the grid. It is allowed to start showing up in the model by investment period 2025. This technology is utilized to both compete with other technologies as well as help sweep up emissions which supports decarbonization goals set within WIS:dom-P. The standard costs for this technology come from the Journal of Cleaner Production, Fasihi, et. al[16]. This technology is not yet in operation anywhere in the US. As such, there are no known improvements in technology that could equate to changes in cost going forward so values remain constant over all investment periods. The cost values from the source were amortized to $13.10/kg-peak CO_2 capital cost

[16] https://www.sciencedirect.com/science/article/pii/S0959652619307772

and \$0.2715/kW-yr fixed cost. A conversion efficiency of 1.785 MWh per metric ton of CO_2 was utilized. This efficiency includes additional electricity needed to pressurize the system.

The model allows for the storage of CO_2. This can be done through Deep Cycle Storage or Deep Storage. The former allows access to the stored CO_2 again for other uses if necessary whereas the latter does not. The model is allowed to optimally decide between these two storage methods.

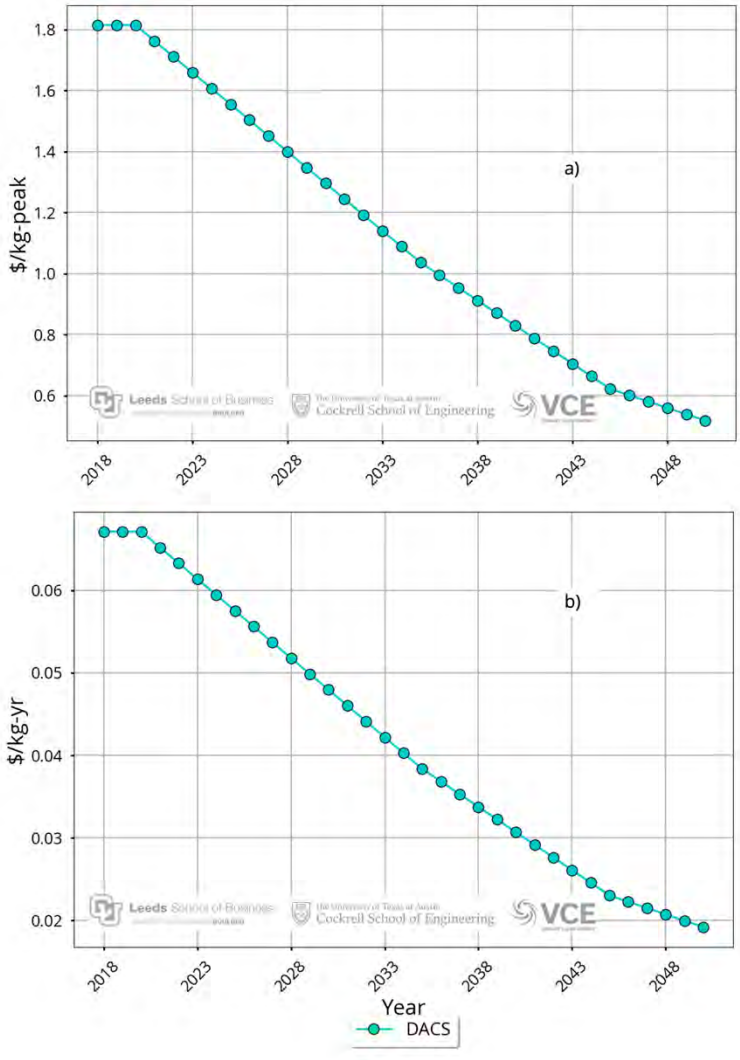

Figure 3.19: The a) capital cost (\$/kg-peak) and b) fixed cost (\$/kg-yr) for Cycle Storage and Deep Storage for CO_2 within WIS:dom-P.

The production of novel fuels and chemicals using electricity and feedstocks is modeled in WIS:dom-P in a compact form. For this study, this includes the use of Hydrogen, Ammonia and Methane. Hydrogen and Ammonia can both be produced from electricity and also be burned to create electricity within WIS:dom-P. The standard suite of Hydrogen costs was updated by

UT using the assumptions from an IEA "The Future of Hydrogen" report[17] and the "Hydrogen Pathways" NREL study.[18] UT vetted and confirmed the standard values VCE used for Ammonia, Ammonium Nitrate and Methane. Figure 3.20 shows these costs. Of the novel technologies used in this study, methane (CH4) is the only one which produces electricity during its production process. The conversion efficiency is thus negative.

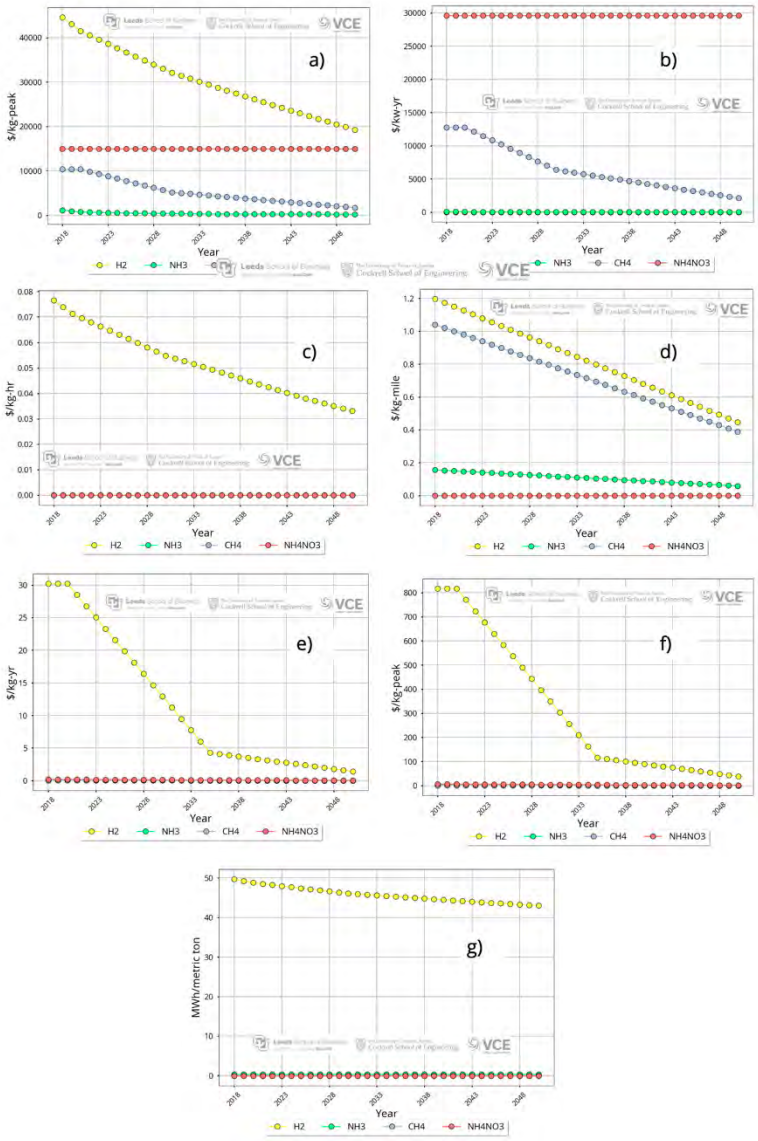

Figure 3.20: The a) capital cost ($/kg-peak), b) fixed cost ($/kw-yr), c) variable cost ($/kg-hr), d) transport cost ($/kg-mile), e) storage capital costs ($/kg-yr), f) storage capital costs ($/kg-peak) and g) conversion efficiency (MWh/metric ton) for the Hydrogen, Ammonia, Methane and Ammonium Nitrate technologies in WIS:dom-P.

[17] https://www.iea.org/reports/the-future-of-hydrogen
[18] https://www.nrel.gov/docs/fy14osti/60528.pdf

Figure 3.21 shows the inputs that limit facilities for the novel chemical technologies. Figure 3.22 shows the Hydrogen storage limits across the county. Texas has the second highest storage limit in the county.

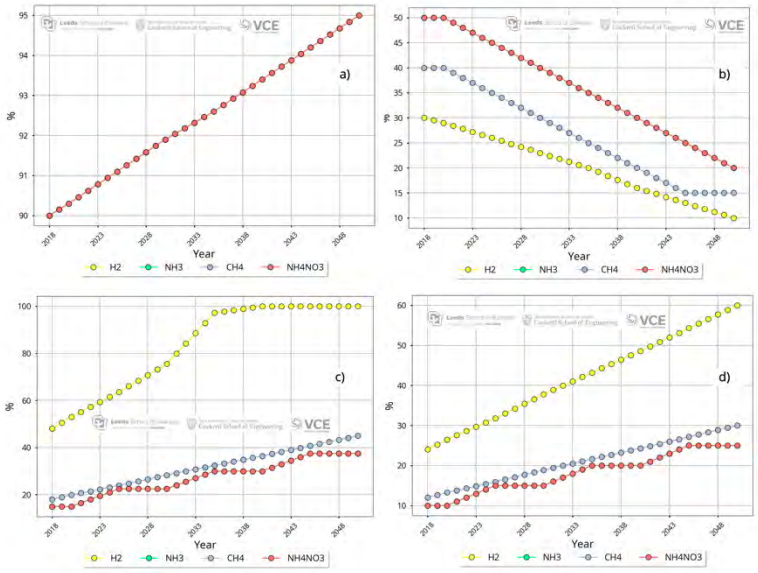

Figure 3.21: The a) maximum production, b) minimum production, c) ramp down capabilities and d) ramp up capabilities for the Hydrogen, Ammonia, Methane and Ammonium Nitrate technologies in WIS:dom-P all in percentage of facility capacity.

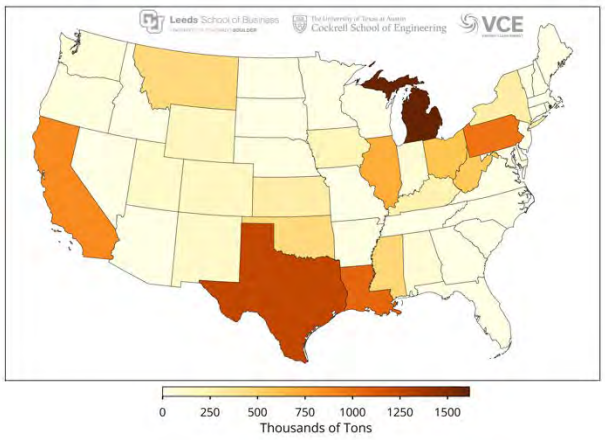

Figure 3.22: The total hydrogen storage limit by state in thousands of tons in WIS:dom-P.

In all scenarios, apart from the "BAU", Industrial CCS is allowed to compete in the WIS:dom-P model. In the "Hydrogen and Carriers" scenario, Conventional Ammonia and Renewable Natural Gas are allowed to compete against other technologies in WIS:dom-P. Figure 3.23 shows the information input into the model for these parameterized technologies that allow them to compete.

a)

Year	Industrial CCS Levelized Cost ($/tonne CO2)
2018	76.4
2020	75.9
2025	74.6
2030	73.3
2035	72
2040	70.7
2045	69.4
2050	68

b) c)

Year	Conventional NH3 Levelized Cost ($/kg)	Conventional NH3 Emissions Factor (tonne CO2e/tonne)
2018	0.431	2.642
2020	0.434	2.629
2025	0.532	2.595
2030	0.461	2.560
2035	0.462	2.526
2040	0.451	2.492
2045	0.455	2.458
2050	0.470	2.424

d) e) f)

Year	Renewable NG Levelized Cost ($/kg)	Renewable NG Combustion Emissions Factor (kg CO2e/kg)	Renewable NG Extraction Emissions Factor (kg CO2e/kg)
2018	0.207	2.650	1.120
2020	0.208	2.650	1.110
2025	0.255	2.650	1.090
2030	0.221	2.650	1.060
2035	0.222	2.650	1.040
2040	0.217	2.650	1.020
2045	0.218	2.650	0.997
2050	0.225	2.650	0.975

Figure 3.23: The a) levelized costs for Industrial CCS ($/tonne), b) levelized costs for Conventional Ammonia ($/kg), c) emissions factor for Conventional Ammonia (tonne CO_2e/tonne), d) levelized costs for Renewable Natural Gas ($/kg), e) combustion emissions factor for Renewable Natural Gas (kg CO_2e/kg) and f) extraction emissions factor for Renewable Natural Gas (kg CO_2e/kg). These parameterized technologies are allowed to additionally compete in WIS:dom-P within certain scenarios.

VCE uses the same real discount rate for all generator technologies including the Advanced and Novel technologies in the WIS:dom-P model. This value is 5.87%, which is applied with the book life of the technologies to provide the model with the amortized capital costs. The lifetime of the various technologies also impacts what/when the model optimally deploys generation as well as when it can retire units. The following Fig. 3.23 shows the standard economic lifetimes for the various technologies used within WIS:dom-P.

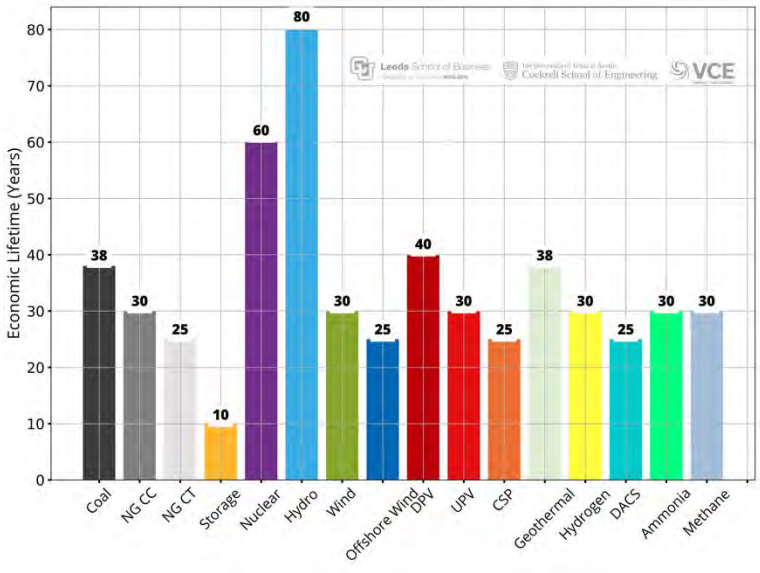

Figure 3.24: The economic lifetime for each generator type within WIS:dom-P in years. The economic lifetime means the time that the debt must be cleared from the units. The SMR technology has the same lifetime as conventional nuclear. Novel Chemical technologies including Hydrogen, Ammonia and Methane share the same lifetime.

Transmission plays a large part in the optimized decisions that the WIS:dom-P model executes. The decision to build renewable technologies can be affected by the standard inputs around transmission aspects. The HVAC capital costs (which includes substations) were updated by UT and derived from the CREZ transmission project in ERCOT[19]. UT expects these costs to be conservative for Texas because new transmission will generally be rural, not all transmission will be double circuit and improvements from the CREZ project are expected. These new costs were slightly less expensive than the typical VCE values. The VCE HVDC transmission costs were reviewed by UT, but were not changed. These AC and DC costs are plotted for multiple years over various distances in Fig. 3.25.

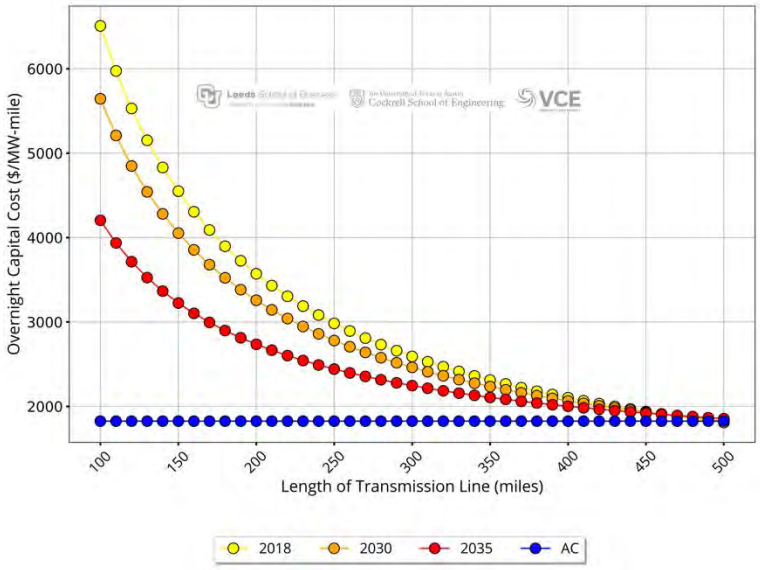

Figure 3.25: Shows the overnight capital cost of DC transmission in WIS:dom-P in real $/MW-mile installed over various distances. Costs are shown for 2018, 2030 and 2050. The overnight capital cost of AC transmission (including substations) is also shown in blue. This is the same cost no matter the investment period.

The economic lifetime, or rather, length of amortization, of the transmission assets in the model are 60 years for all investment periods.

VCE documents and researches the various state legislature and renewable energy goals by tracking Renewable Portfolio Standards, Clean Energy Mandates, Offshore Wind Mandates, Storage Mandates and GHG Emission Reduction Mandates. These are utilized to inform the WIS:dom-P model of what is expected and what goals are set. This provides the bounds and definitions of what the model is required to build as it optimizes systems of the future. Over 30 states have a renewable portfolio standard in place. Just over 10 states currently have a clean energy mandate. The northeast has become increasingly aggressive in setting offshore wind energy targets. Storage mandates have started to show up in recent years as well. The following images lay out the legislative goals by 2050. Texas did have a goal of 10,000 MW of installed renewable energy by

[19] https://www.texastribune.org/2013/10/14/7-billion-crez-project-nears-finish-aiding-wind-po/

2025. This has already been surpassed and, to-date, no other mandate has been put in place. The Production Tax Credit and the Investment Tax Credit for renewables is also shown below. This directly ties into the cost of renewables built in WIS:dom-P.

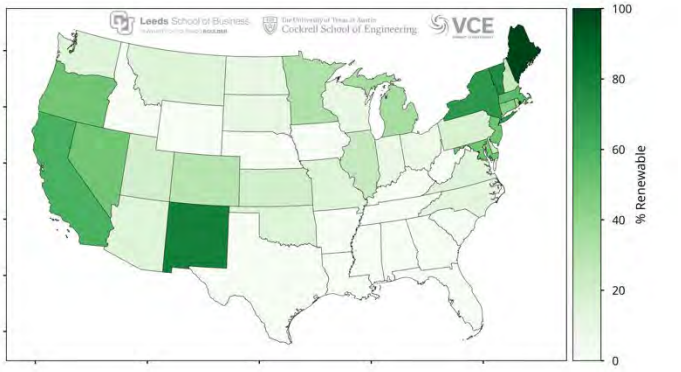

Figure 3.26: The Renewable Portfolio Standards percentage requirement of each state across the US by 2050.

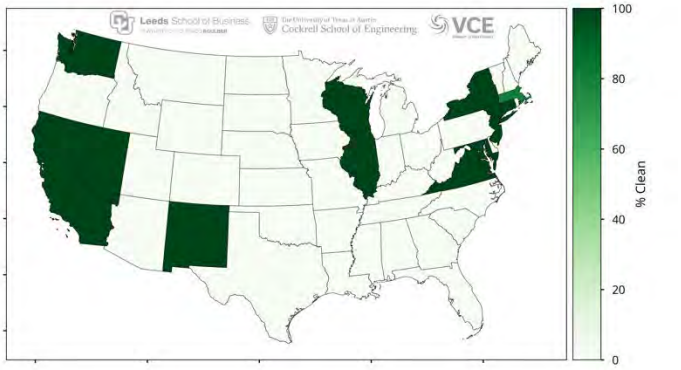

Figure 3.27: The Clean Energy Mandate percentage requirements of each state across the US by 2050.

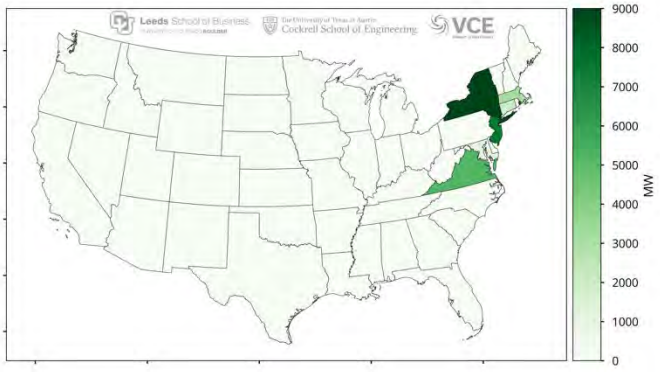

Figure 3.28: The Offshore Wind requirement in MW for each state across the US by 2050.

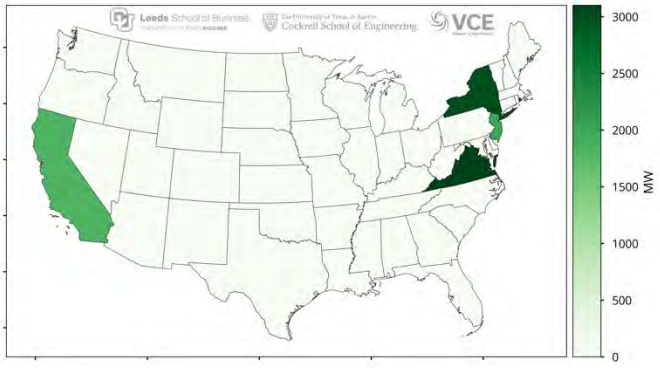

Figure 3.29: The Storage Mandates requirement in MW for each state across the US by 2050.

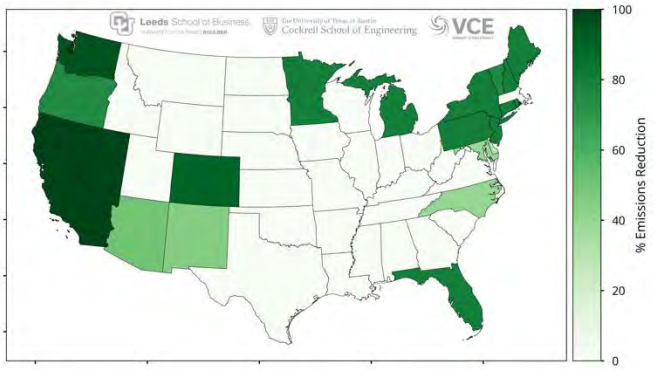

Figure 3.30: The GHG Emissions Reduction percentage requirement of each state across the US by 2050.

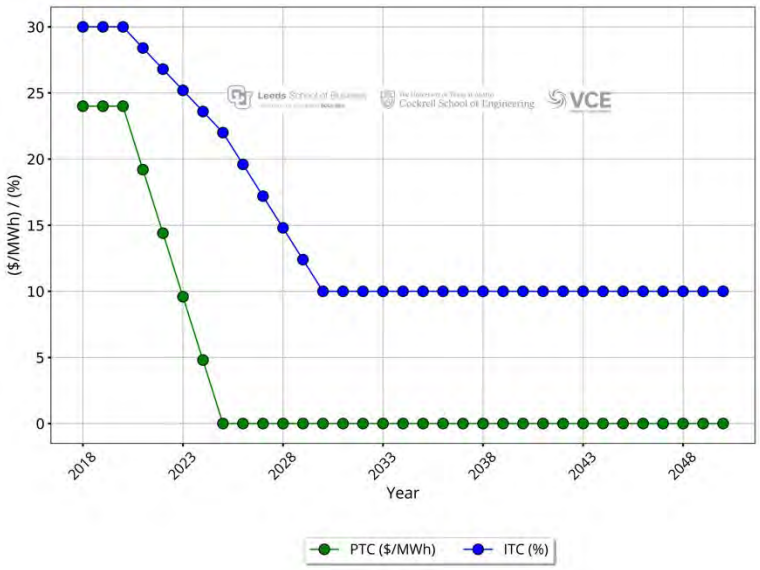

Figure 3.31: The Production Tax Credit subsidiary and the Investment Tax Credit. Note that for 2030 and beyond, the 10% ITC remaining is for utility scale projects only.

As of December 2020, new legislation was released that extends out the PTC and ITC. A new ITC incentive was also put in place for Offshore Wind development. Lastly, if more than 50% of a project is built on federal land, those projects are able to maintain a ten-year safe harbor for these federal incentives. This study was commenced before these changes went into effect and thus, the new incentive updates are not included in these scenarios.

VCE also performs work and analysis to represent job numbers that arise from various technologies and transmission across the US. These inputs set the stage for how many jobs become available depending on what is deployed during the various investment periods. This is an im-

portant metric for decision makers to know and understand as the energy industry evolves. VCE uses a combination of sources to derive these numbers including IMPLAN, JEDI and US Energy Job reports.

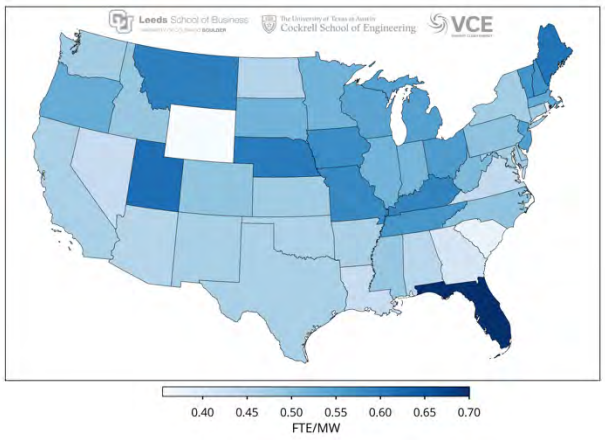

Figure 3.32: Employment per MW available from Coal.

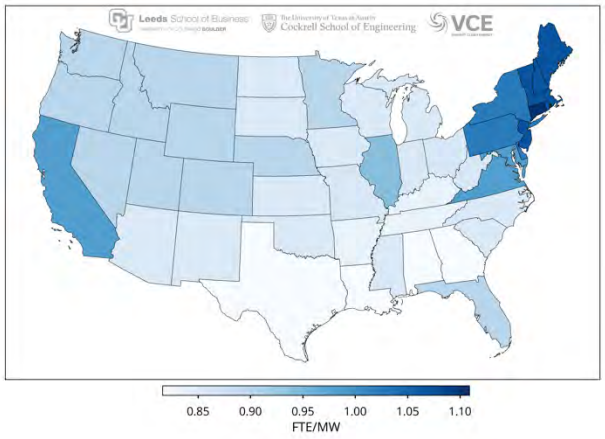

Figure 3.33: Employment per MW available from Distribution.

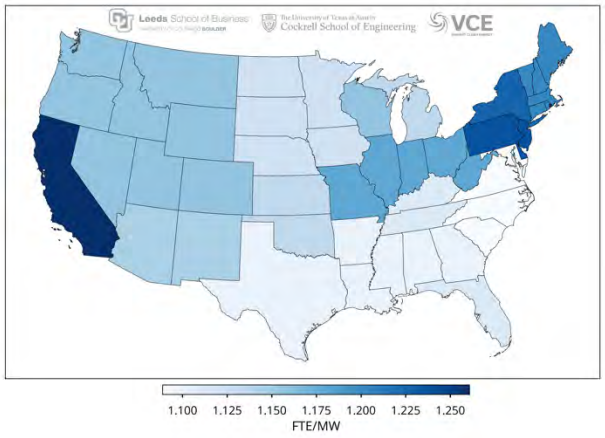

Figure 3.34: Employment per MW available from Geothermal and Biomass.

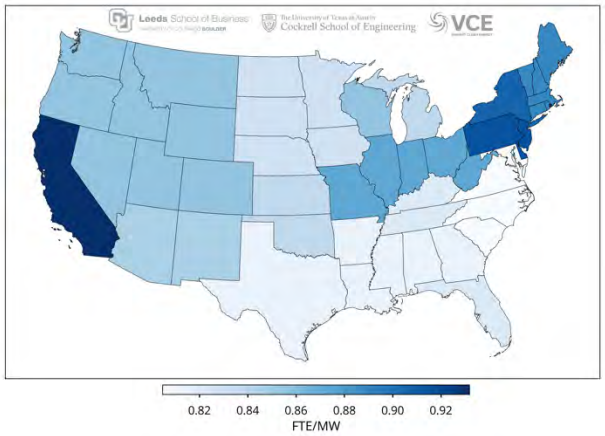

Figure 3.35: Employment per MW available from Hydro.

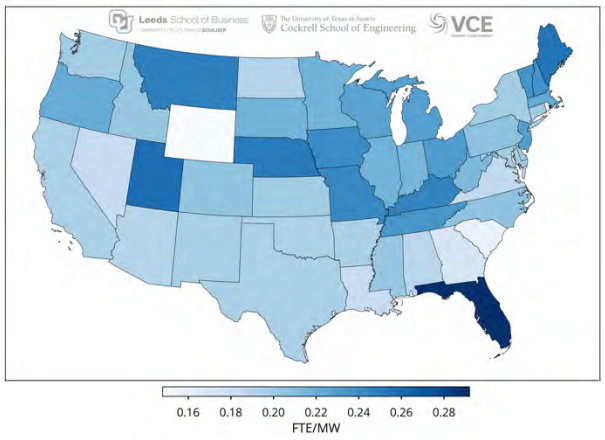

Figure 3.36: Employment per MW available from Natural Gas.

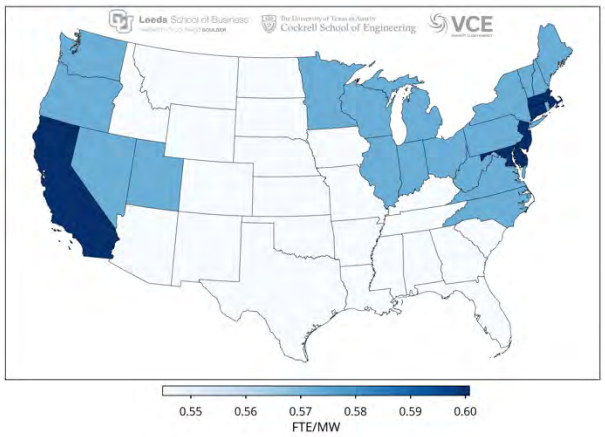

Figure 3.37: Employment per MW available from Nuclear.

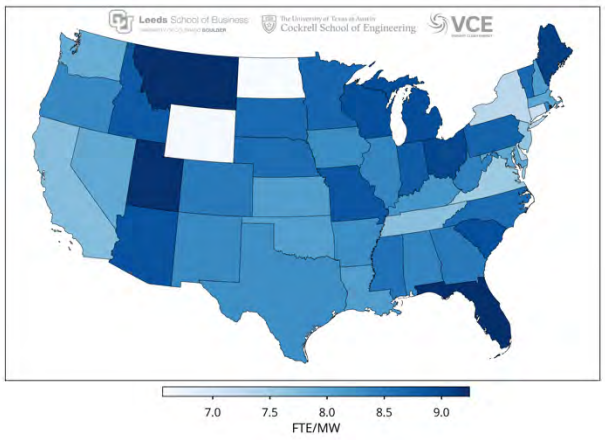

Figure 3.38a: Employment per MW available from Distributed Solar.

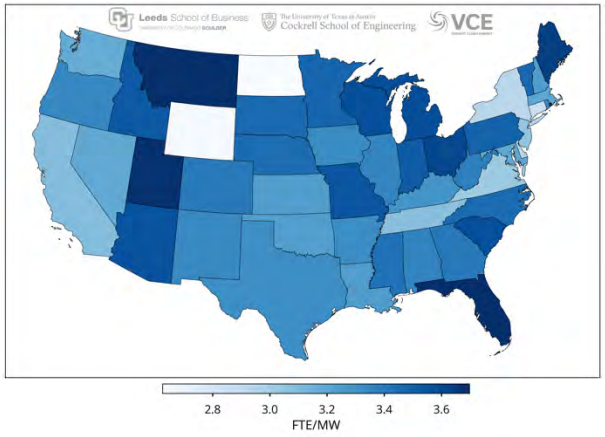

Figure 3.38b: Employment per MW available from Utility Solar.

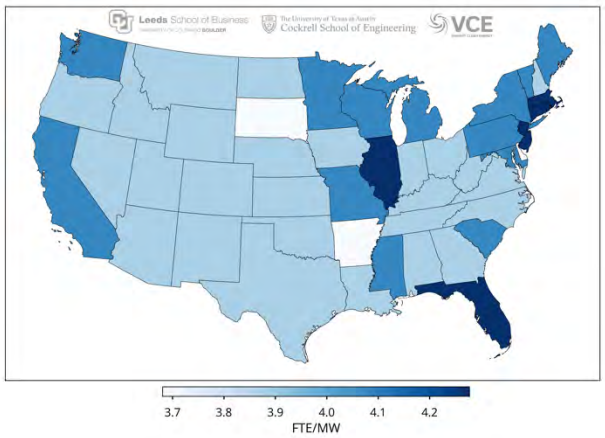

Figure 3.39: Employment per MW available from Storage MW.

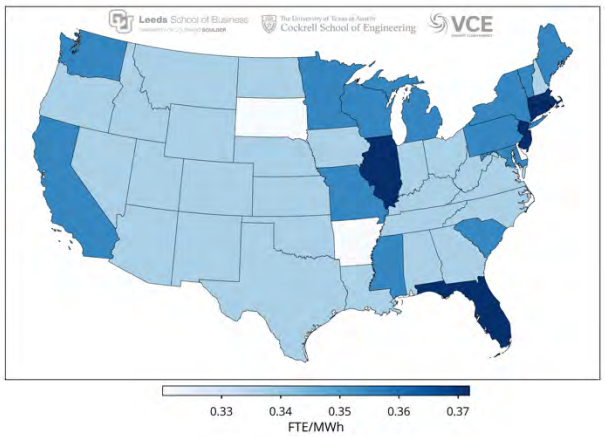

Figure 3.40: Employment per MWh available from Storage.

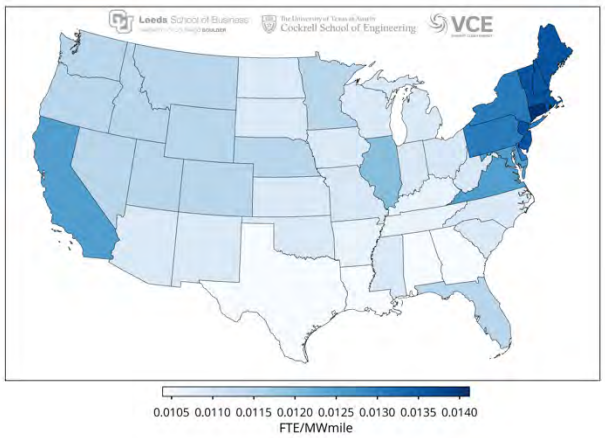

Figure 3.41: Employment per MW available from Transmission.

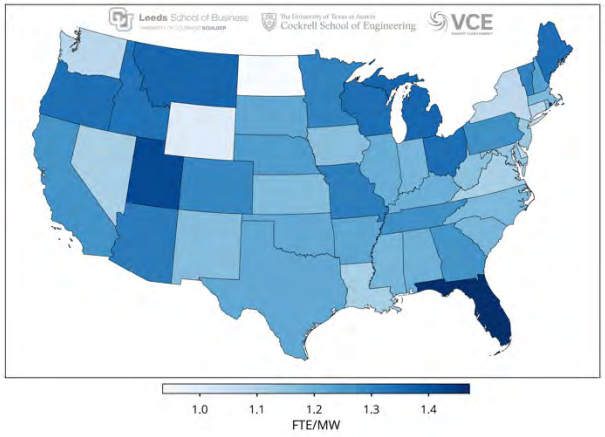

Figure 3.42: Employment per MW available from Wind.

3.4 Texas Weather Analysis

The present section will analyze the weather data specific to the state of Texas for this study. This section will provide some insight into how certain renewable sources are selected by the model. Figure 3.43a and Fig. 3.43b displays the average wind and solar capacity across this region by hour of the day. The wind is for the 100-meter (above ground) level. The solar technology is single axis tracking pitched to latitude tilt. The load is also displayed for comparison. The series are shown for the average of the entire year and then the summer (June, July, August) and winter (January, February, March) seasons. The weather year for 2018 is used as the basis for this analysis. Figure 3.43a shows a typical normalized load pattern. Figure 3.43b shows a normalized electrified economy load pattern for comparison.

Figure 3.43a and Fig. 3.43b shows the solar resource is both higher in peak and longer in duration during the summer, reaching around 60% capacity factor in those months for Texas. For wind, the reverse occurs where this resource drops during the summer and increases during the winter across the entire state. The stronger jet stream and weather patterns in winter are apparent. However, for Texas, that seasonal discrepancy is not large, in particular in the nighttime hours. Wind also exhibits a diurnal pattern where higher production is observed during the nighttime hours. This is a normal phenomenon for wind when the decoupling of the boundary layer near the surface at night allows for wind speeds to regularly increase due to less friction from the surface. Nighttime hours can see around 50% capacity factors from the wind resource on average for the whole year. It is easy to see the complementary temporal patterns in the wind and solar resources. The load in Fig. 3.38a for Texas shows a standard load pattern. The summer load dwarfs the winter months. For Fig. 3.43b, an electrified economy load pattern is plotted for Texas. The loads for each season flatten out across the day compared to a standard load pattern. Summer load does not reach as high a peak under electrification. A very early morning peak also develops shortly after the midnight hour.

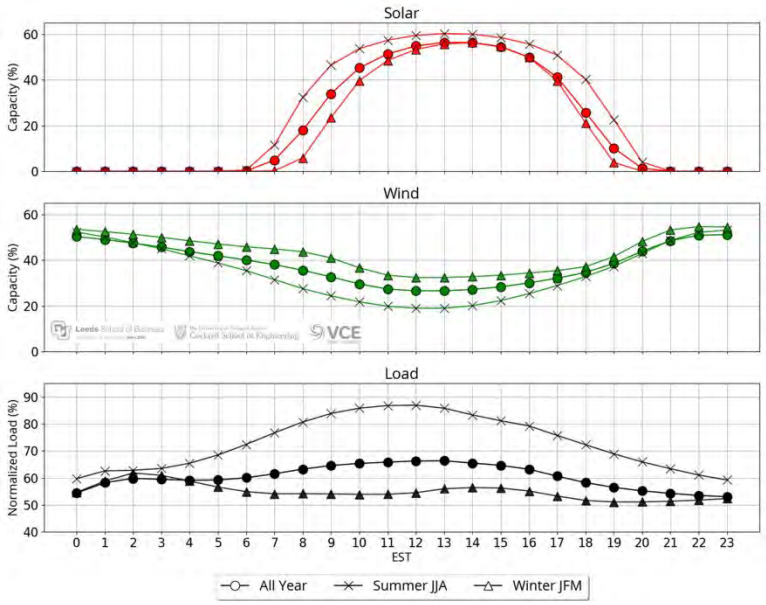

Figure 3.43a: The average solar (red) and wind (green) resource shown for the states in Texas alongside the corresponding load (black) by hour of the day (EST). The circles show the hourly averages for the entire 2018 year. The other two series look at the summer (JJA) and winter (JFM) months of 2018. This shows a normalized standard load pattern.

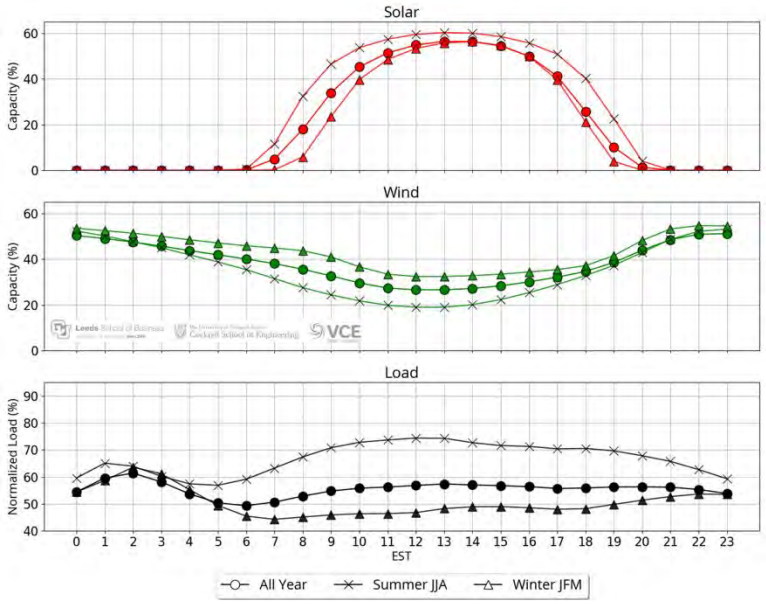

Figure 3.43b: The average solar (red) and wind (green) resource shown for the states in Texas alongside the corresponding load (black) by hour of the day (EST). The circles show the hourly averages for the entire 2018 year. The other two series look at the summer (JJA) and winter (JFM) months of 2018. This shows a normalized electrified economy load pattern.

The following Fig. 3.44a and Fig. 3.44b are similar to Fig. 3.43a and Fig. 3.43b; but displaying the three parameters (solar, wind or load) together, to identify how they change against each other for the whole year, summer and winter. Figure 3.39a shows a standard load scenario. Figure 3.44b displays an electrified economy load scenario. In Fig. 3.44a, it is clearer that the solar resource peaks near the load peak. In the yearly average, but especially in the summer months, the shapes of these two series align well, though slightly offset. The peak of the solar tends to occur on average a few hours in advance of the diurnal peak load (leading to large evening ramps, typically described in the "duck curve"). In winter, the shape of the wind resource is more correlated with the shape of the load. This observation along with the anti-correlated nature of wind and solar shows the viability of wind. In Fig. 3.44b, the load is from an electrified economy. It is apparent that the nighttime increases in wind capacity align better with the nighttime increase in load in this situation. This points to an increasing value of wind in an electrified economy. Solar still shows daytime value and alignment with daytime load peaking.

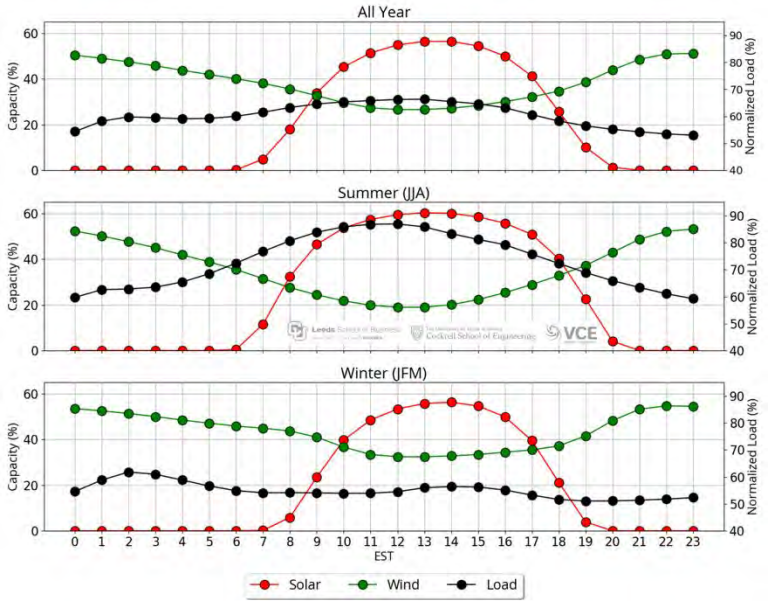

Figure 3.44a: The average solar (red) and wind (green) resource shown for the Texas states alongside the corresponding load (black) by hour of the day (EST). This is shown in seasonal groupings now; the entire 2018 year, the summer (JJA) of 2018 and winter (JFM) of 2018. This shows a normalized standard load.

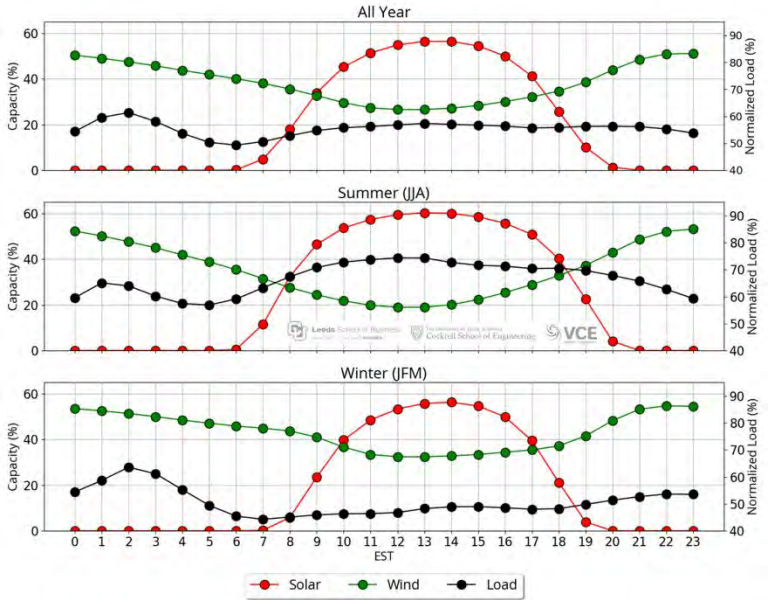

Figure 3.44b: The average solar (red) and wind (green) resource shown for the Texas states alongside the corresponding load (black) by hour of the day (EST). This is shown in seasonal groupings now; the entire 2018 year, the summer (JJA) of 2018 and winter (JFM) of 2018. This shows a normalized electrified economy load.

VCE investigated the wind and solar resources at different spatial granularities as well for the present analysis. Figure 3.45 and Fig. 3.46 shows the average annual wind and solar resourc-

es throughout the day for Texas. Note that offshore potential sites are available to Texas in the Gulf of Mexico. That data is included in the state wind resource average. Figure 3.47 and Fig 3.48 shows the average wind and solar resource for the 2018 weather year by state for the United States. This shows how Texas compares with the rest of the country. These four images combined show that Texas has some of the highest wind resources in the US, especially at night. This is particularly impressive given the geographic extent of the state. This state sits solidly in the central wind belt of the US and has the opportunity to take advantage of this. On the solar side, the desert southwest states dominate in resource magnitude. Albeit, with the large east-west extension of Texas, this state still finds itself among the upper echelon when it comes to solar.

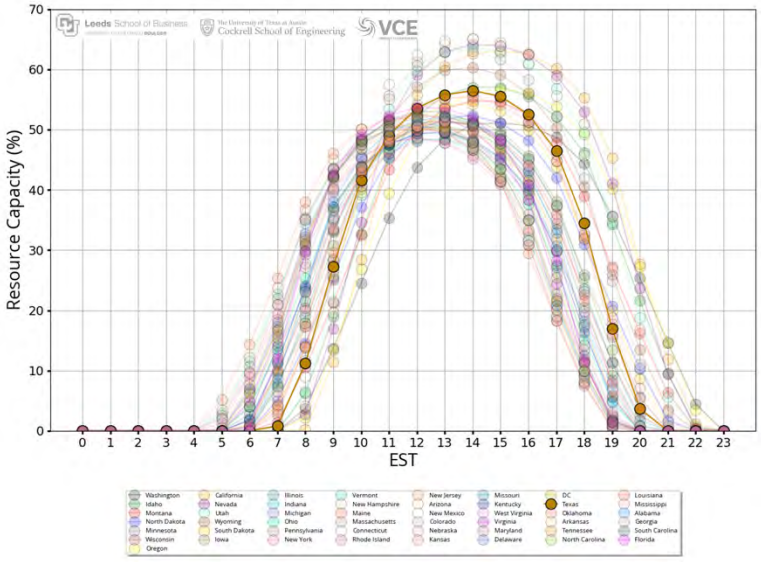

Figure 3.45: The 2018 average hourly solar resource capacity for all states. Texas is not opaque.

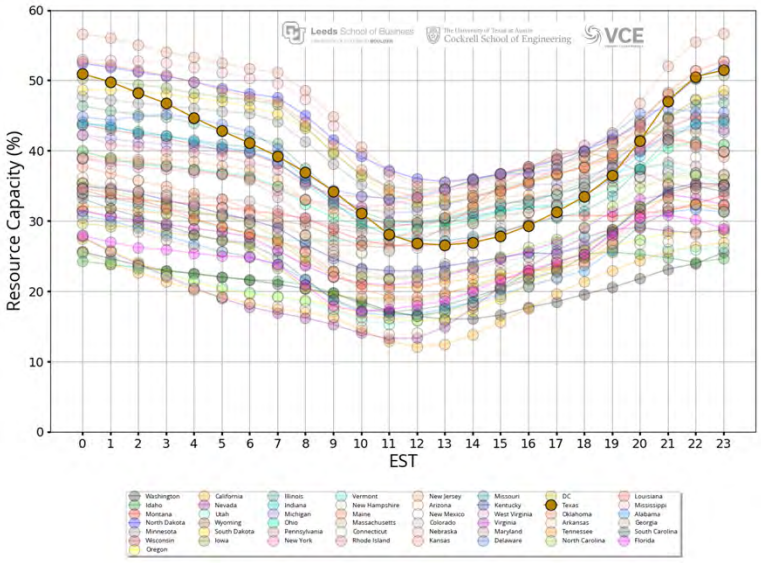

Figure 3.46: The 2018 average hourly wind resource capacity for all states. Texas is not opaque.

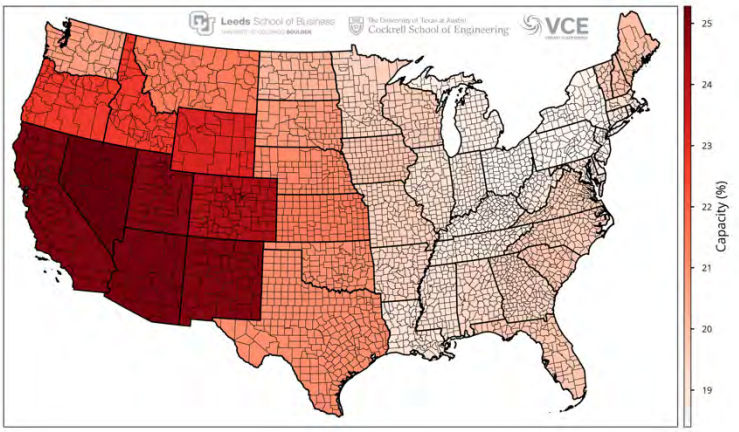

Figure 3.47: The average solar capacity factor (%) for 2018 by state in the US.

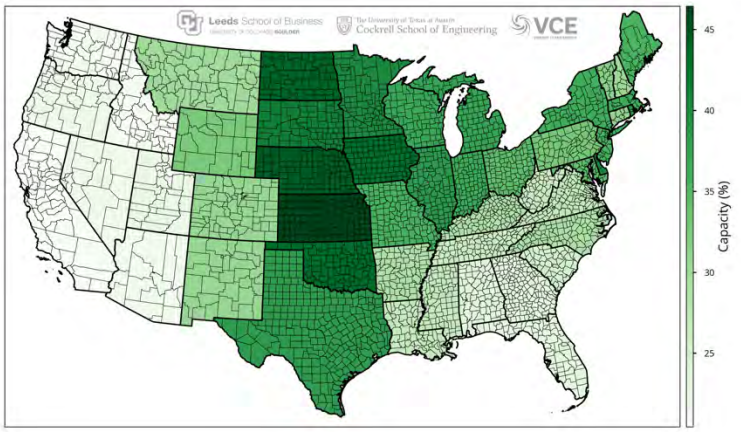

Figure 3.48: The average wind capacity factor (%) for 2018 by state in the US.

VCE utilizes the 3-km NOAA HRRR weather model as the raw inputs for the weather and power datasets. Figure 3.49 looks at the wind capacity resources at this granularity across Texas. The high resource in the Panhandle is pronounced. The west central and southern tip of Texas also shows good wind resources. In general, wind power capacity factors are lower along the eastern Texas state border. Higher wind is observed in smaller pockets in the southwest portion of the state. Figure 3.50 shows that the solar resource increased going from east to west in the state. The strongest solar is observed in the southwest portion of the state. It is clear from Fig. 3.49 and Fig. 3.50 that the wind resources are far more heterogeneous than the solar resource, but that Texas as a whole has very good resource quality in both.

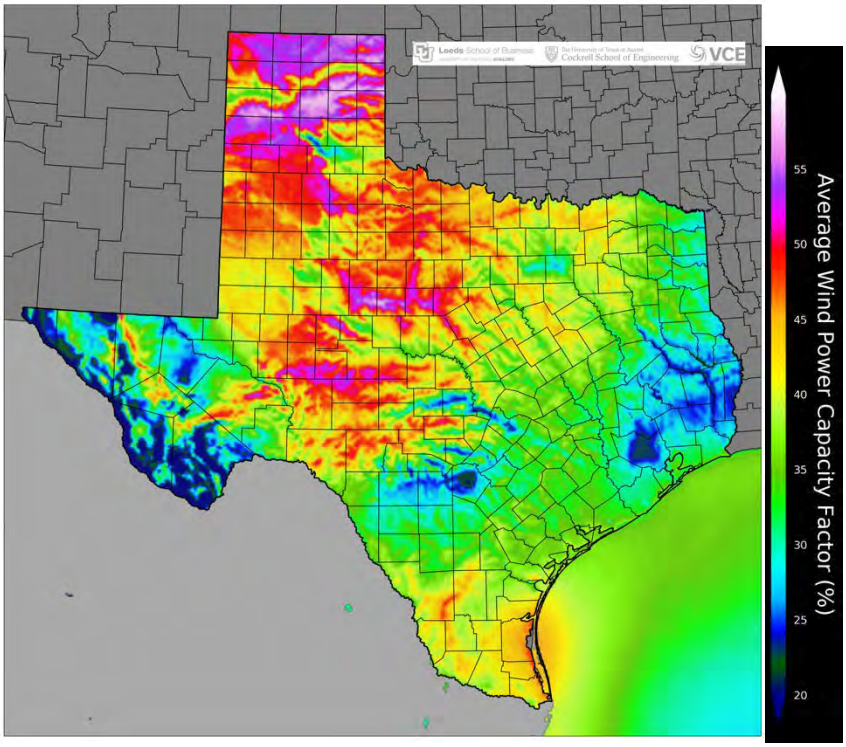

Figure 3.49: The 3-km 100-meter wind resource across Texas in 2018.

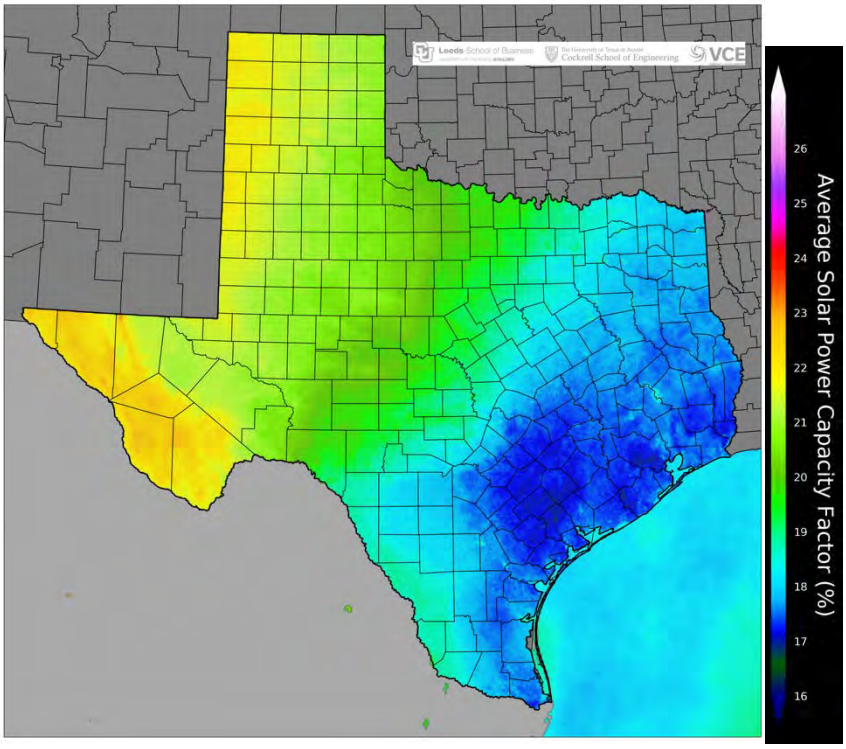

Figure 3.50: The 3-km latitude-tilted solar resource across Texas in 2018.

VCE analyzed a day of high wind during 2018 in Texas. Figure 3.51, reproduced from the NOAA weather archives, shows a surface weather analysis in April 2018. A springtime extra-tropical cyclone was centered over northern Kansas. The strong surface pressure gradients around this system brought strong southerly winds to all of Texas. Figure 3.52a shows a time series view of the wind and solar resources alongside a normalized standard load in Texas during this high wind event. Wind capacity factors in Texas reach almost 100% at their peak during this period for the entire state. Figure 3.52b shows the same weather data against a normalized electrified load. The very early morning demand spikes are apparent. Several times that week, those demand spikes align with nighttime increases in wind power capacity factors.

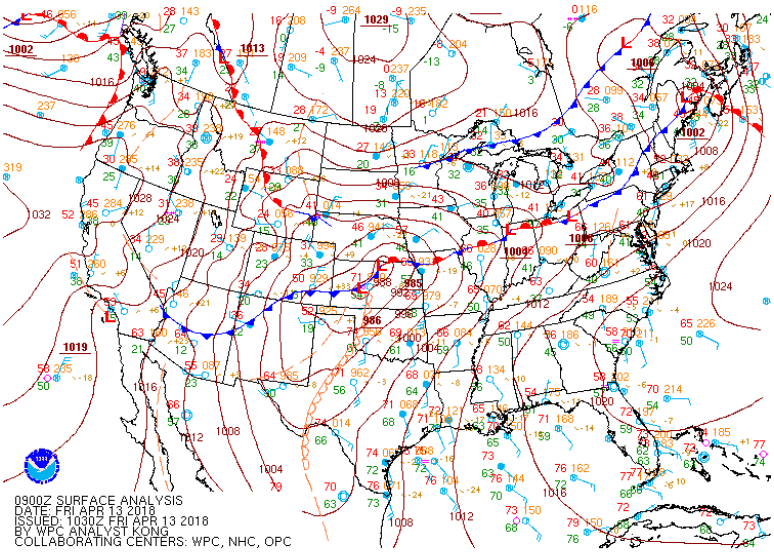

Figure 3.51: Surface Weather Analysis Plot from April 13th, 2018 at 09 UTC. This surface plot is provided from NOAA's Weather Prediction Center Archives (https://www.wpc.ncep.noaa.gov/archives/web_pages/sfc/sfc_archive.php).

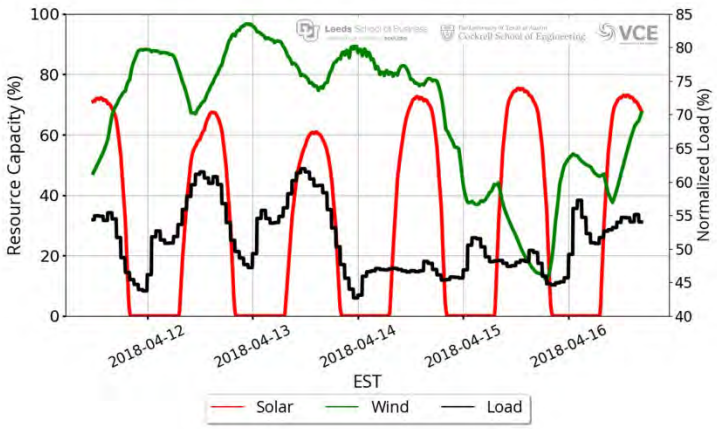

Figure 3.52a: A time series of the average solar (red) and wind (green) resources across Texas in April 2018. The standard load (black) is also plotted. This was one of the highest wind periods from 2018.

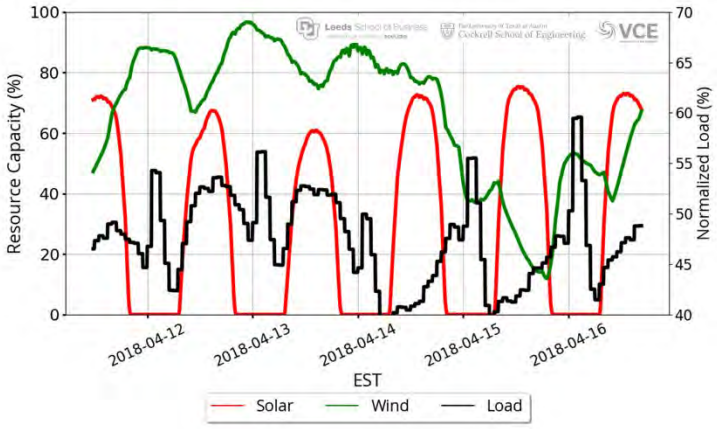

Figure 3.52b: A time series of the average solar (red) and wind (green) resources across Texas in April 2018. The electrified load (black) is also plotted. This was one of the highest wind periods from 2018.

The next figures (Fig. 3.53a and Fig. 3.53b) show a September week that had some of the lowest wind observed in 2018 for the state of Texas. A summer wind doldrum established itself for a few days. The diurnal nighttime increase in wind speed is still apparent and many times the wind reaches over 15% capacity as the sun is setting for the day.

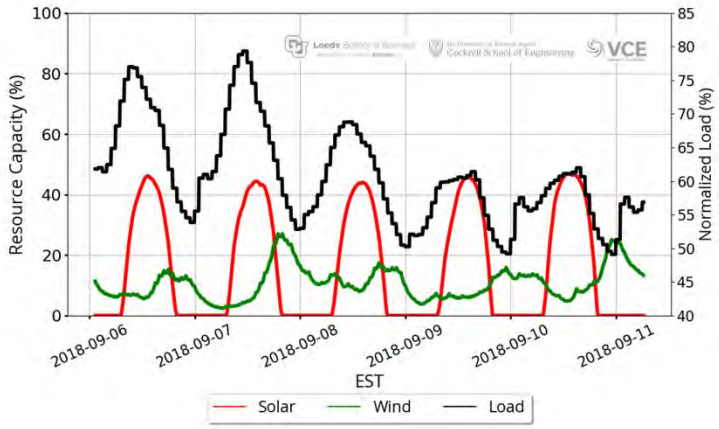

Figure 3.53a: A time series of the average solar (red) and wind (green) resources across Texas in September 2018. The standard load (black) is also plotted. This was one of the lowest wind periods from 2018.

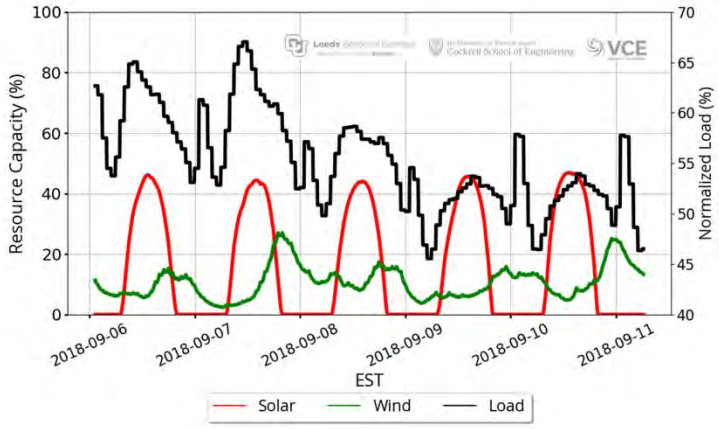

Figure 3.53b: A time series of the average solar (red) and wind (green) resources across Texas in September 2018. The electrified load (black) is also plotted. This was one of the lowest wind periods from 2018.